USDA Forest Service
U.S. DEPARTMENT OF AGRICULTURE

Rocky Mountain Research Station | RMRS-GTR-443 | December 2024

Remote Sensing of Forest Insect and Disease Outbreaks in the Western United States: Tree, Stand, and Landscape Responses and Technologies and Methods for Detection and Attribution

Jeffrey A. Hicke, Benjamin C. Bright, Ryan P. Hanavan, Andrew T. Hudak, Arjan J.H. Meddens, Abhinav Shrestha, Amanda T. Stahl



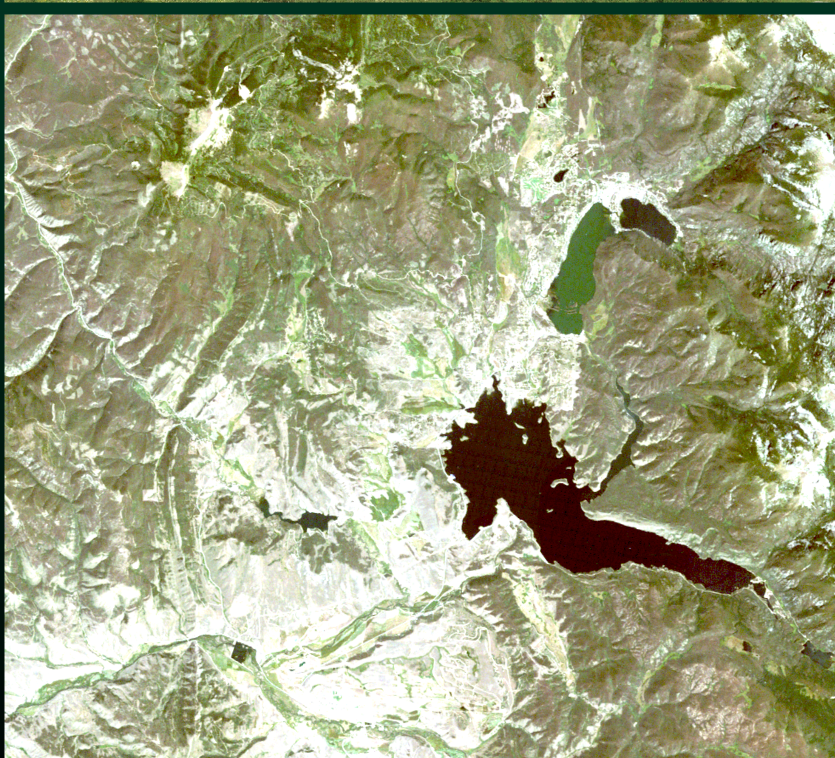


Hicke, Jeffrey A.; Bright, Benjamin C.; Hanavan, Ryan P.; Hudak, Andrew T.; Meddens, Arjan J.H.; Shrestha, Abhinav; Stahl, Amanda T. 2024. **Remote sensing of forest insect and disease outbreaks in the western United States: Tree, stand, and landscape responses and technologies and methods for detection and attribution.** RMRS-GTR-443. Fort Collins, CO: U.S. Department of Agriculture, Forest Service, Rocky Mountain Research Station. 92 p. https://doi.org/10.2737/RMRS-GTR-443

Abstract

Insects and diseases are significant disturbance agents in many forests. In some places, annual surveys by observers in aircraft are valuable resources, but can have significant issues that result in gaps. Using remotely sensed data is therefore attractive. Here we provide a review of this topic that is novel in several ways. We describe tree, stand, and landscape responses to insects and diseases, then link these responses to remote sensing technologies and methods for detection and attribution. We focus on insects and diseases that cause substantial damage and mortality to conifers in the western United States (excluding Alaska and Hawaii), but present information in a general way that allows for extension to other regions. Tree responses (e.g., color change) can vary but can be generalized within groups of host tree and disturbance agent associations. At stand and landscape levels, spatial and temporal characteristics of tree damage or mortality can differ substantially within and among agents. A variety of remote sensing technologies and methods are available for exploiting the host tree responses to detect and attribute damage and mortality. Important knowledge gaps exist that limit detection and monitoring, but recent rapid developments in technologies and methods show significant promise. Our review provides scientists and managers with information for advancing remote sensing capabilities related to forest insects and diseases.

Keywords: insects; diseases; review; western United States; detection; attribution

Cover: Clockwise from upper right: (a) Trees with different types and damage stages: fully red (killed), branch flagging, and top-kill and downed trees. Courtesy photo by A. Shrestha, RedCastle Resources. (b) Conifers killed by bark beetles in Washington State. Drone image courtesy of A. Stahl, Washington State University. (c) Red lodgepole pines killed by mountain pine beetle in central Colorado in 2009. Landsat imagery. (d) Red lodgepole pines killed by mountain pine beetle in Colorado. Courtesy image by J. Hicke, University of Idaho.

Authors

Jeffrey A. Hicke, Professor, Department of Earth and Spatial Sciences, University of Idaho, Moscow, Idaho

Benjamin C. Bright, Geographer, Rocky Mountain Research Station, U.S. Department of Agriculture, Forest Service, Moscow, Idaho

Ryan P. Hanavan, Remote Sensing Program Manager, Forest Health Assessment & Applied Sciences Team, U.S. Department of Agriculture, Forest Service, Missoula, Montana

Andrew T. Hudak, Research Forester, Rocky Mountain Research Station, U.S. Department of Agriculture, Forest Service, Idaho

Arjan J. H. Meddens, Assistant Professor, School of the Environment, Washington State University, Pullman, Washington

Abhinav Shrestha, Geospatial and Remote Sensing Specialist, Department of Earth and Spatial Sciences, University of Idaho, Moscow, Idaho

Amanda T. Stahl, Research Associate, School of the Environment, Washington State University, Pullman, Washington

Acknowledgments

We gratefully acknowledge funding support from the Western Wildland Environmental Threat Assessment Center (WWETAC) of the Forest Service, Agreement #22-JV-11261994-036, and the NASA Commercial Smallsat Data Scientific Analysis (CSDSA) Program Award, Agreement #80NSSC21K1155. We thank the time and effort of two reviewers, Michèle Slaton and Dustin Wittwer, whose comments improved the manuscript.

This page intentionally left blank.

Contents

1. Introduction

Insects and diseases can cause widespread and severe forest disturbances (Kautz et al. 2017) that affect ecosystem structure, function, and biodiversity (Hicke et al. 2012; Weed et al. 2013). In the western United States (and western Canada), outbreaks of multiple bark beetle and defoliator species, primarily mountain pine beetle (*Dendroctonus ponderosae* Hopkins) and western spruce budworm (*Choristoneura freemani*), have occurred over millions of hectares (ha) of forest in recent decades (Hicke et al. 2012, 2020; Williams and Birdsey 2003). Given that climate change will lead to more favorable conditions for many insects and pathogens (Bentz et al. 2010; Sturrock et al. 2011; Weed et al. 2013), the extent, severity, and duration of outbreaks of many of these biotic agents are likely to increase in the future.

Remote sensing has been employed for decades to detect and monitor tree damage or mortality from insects and diseases (e.g., Ahern 1988; Heller and Bega 1973; Radeloff et al. 1999; Rencz and Nemeth 1985; Vogelmann and Rock 1988). Although visual observations, such as aerial surveys, can be considered remote sensing, for the purpose of this report, we use the term “remote sensing” to mean observing with instruments, typically from unmanned aerial systems (UASs), airplanes, or satellites. We use “detection” to mean identification of a forest disturbance caused by an insect or disease and “attribution” to mean identifying the cause of detected disturbances.

Remote sensing of biotic disturbances is useful in multiple ways: (1) near-real-time monitoring of forests, (2) retrospective mapping and analysis, and (3) attributing forest disturbance among different agents. Near-real-time monitoring of forests for damage or mortality from biotic agents can aid forest monitoring and enable more rapid responses. Particularly useful are early detection efforts that identify incipient or pre-eruptive populations, which can lead to more informed and successful management responses.

In the United States, this monitoring is primarily accomplished via field visits or aerial surveys. Both have a long history and use, as well as drawbacks. The time, effort, and expense of field visits limit their spatial extent and frequency. Aerial surveys have been an invaluable resource, but not every forest location is surveyed every year or immediately after visible signs and symptoms appear, resulting in nonsystematic and inconsistent sampling. Safety concerns of flying exist related to weather conditions and COVID-19. Aerial surveys are subjective in nature; observations are influenced by flying conditions and surveyor experience, and changes in survey approaches have led to challenges in linking older surveys to newer surveys (Hicke et al. 2020).

Remote sensing has the potential to augment field visits and aerial surveys in several ways (although it also has drawbacks) (table 1). Remote sensing outputs are quantitative and repeatable estimates and can fill in spatial or temporal gaps in other types of surveys, such as occurred during the COVID-19 pandemic because of reductions in survey time (Hanavan et al. 2022) Products could be generated at specific (e.g., early or late in the growing season) and multiple times during the growing season and could provide early detection and progression of tree damage and guide field visit or aerial survey flight planning. Bark beetles attack host trees in late summer, and these trees change visually early the next summer. Annual survey flights that occur in mid- to late summer usually detect the effects of bark beetles one year after they attack. Thus, early or previsual detection (i.e., in the year of attack), as may be possible with remote sensing, will be particularly useful for monitoring and management. Finally, additional comparisons and/or integration of remote sensing and aerial survey products could improve methods and mapping and lead to more operational use of remote sensing.

Table 1—Advantages or benefits and disadvantages or drawbacks of remote sensing and aerial surveys.

Method	Advantages or benefits	Disadvantages or drawbacks
Aerial surveys	• Long time series • Many recorded attributes (host species, damage agent, severity, damage versus mortality) • Established protocols used for years • Likely higher accuracy of attribution to damage agent and host species than computer-based methods • Possibility of adjusting perspective and altitude to increase accuracy • Improved possibility to detect damage during atmospheric conditions adverse for satellite remote sensing	• Subjective observations potentially influenced by flying conditions, surveyor experience • Inclusion of undamaged trees within damage polygons • Incomplete spatial or temporal coverage • Safety risk • Challenges associated with changing approaches (switch from dasm to dmsm) • Can be affected by adverse atmospheric conditions

Remote sensing	• Quantitative measurement
	• Repeatable, automated algorithms
	• Large suite of available and potential instrumentation/platforms
	• Potential for wide and complete spatial extent
	• Time series capability, including intra-annual
	• Retrospective analysis can
	    • improve earlier estimates
	    • map historical damage if sensor data are available
	• Assess ecological impacts of damage (e.g., remaining live trees, carbon or water fluxes)
	• Measurements extend beyond the visible region of the electromagnetic spectrum to take advantage of different or increased signals in other regions
		• Historically, spatial resolution/temporal resolution tradeoff
		• Detection limited to substantial tree responses; more subtle tree responses (e.g., partial defoliation) are more challenging
		• Limited ability to attribute damage to agents
		• Extended time series are limited to coarser resolution imagery
		• Requires significant analyst training
		• Can require substantial data storage and processing capabilities
		• Can be affected by adverse atmospheric conditions

Second, remote sensing studies can provide retrospective mapping and analysis that can document or refine the extent and severity of damage or mortality (which may not have been evaluated by aerial surveys). The results of such studies can be used to improve understanding of the characteristics of outbreaks (e.g., Meddens and Hicke 2014), identify drivers (e.g., Senf et al. 2016), and assess ecosystem impacts, including changes to trees, stands, and ecosystem processes (e.g., Bright et al. 2013; Hanavan et al. 2015; Meng et al. 2018; Pontius et al. 2017).

Finally, in addition to detecting damage or mortality from insects and diseases and estimating severity (number of trees damaged or killed per area), remote sensing studies have potential for attributing forest disturbance among different agents. In addition to insects and diseases, forests are affected by fires, harvests, landslides, and storms. Such attribution has been demonstrated by recent studies (see review by Stahl et al. 2023); however, as we document below, few studies exist to date that separate damage caused by different insects and diseases despite their obvious utility in forest monitoring and management.

Multiple published studies have reviewed and synthesized existing literature to describe approaches that have been used to map and monitor insect and disease disturbances with remotely sensed data (Cotrozzi 2022; Hall et al. 2016; Huang et al. 2019; Lausch et al. 2016, 2017, 2018; Senf et al. 2017; Torres et al. 2019). These reviews address insect and disease disturbances and discuss published studies, though in varying levels of focus and detail. Our overall objective of this review is to augment and build upon these reviews in several novel ways:

We provide an organized framework starting with tree, stand, and landscape responses to forest insects and diseases, which we then link to remote sensing characteristics (fig. 1). Although the details of responses and characteristics are unique to each ecological setting, our approach provides a framework that can easily be adapted to fit future studies.

1. In addition to discussing detection, we review and synthesize studies that attribute forest disturbances to specific biotic agents.
2. We focus on insect and disease outbreaks that cause substantial damage or mortality in the coniferous forests of the western United States (excluding Hawaii and Alaska) with the intent to better inform forest managers in this region about remote sensing of these damage agents and the potential severities of particular events.
3. We describe examples of applications of different technologies and methods used to study insects and diseases, with an emphasis on studies from recent years.

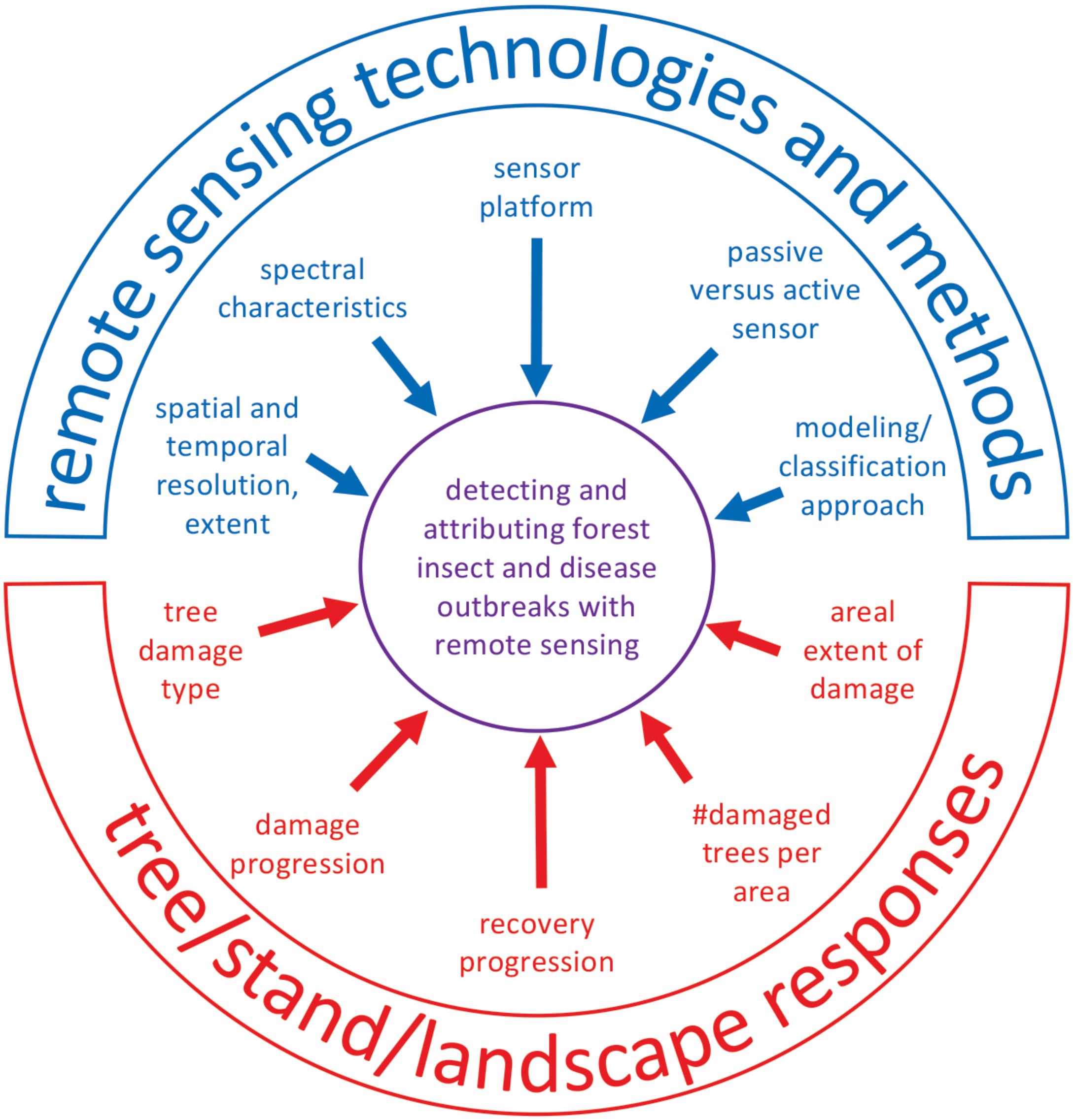

Figure 1—Tree, stand, and landscape responses to insects and diseases and technologies and methods for using remote sensing to detect or attribute these forest disturbances.

Our report is useful and timely for analysts and researchers wanting to apply or develop technologies and methods to monitor, map, and study forest insect outbreaks. The information we present is also helpful for end users and forest managers interested in learning more about the capabilities of remote sensing.

The report is organized as follows: We first address tree, stand, and landscape responses by describing the relevant biology and ecology of major forest insects and diseases. We then discuss characteristics of remote sensing technologies (sensors, platforms) and methods (e.g., processing, analysis, modeling, evaluation) applicable to forest insects and diseases. We provide examples of how remote sensing has been applied to mapping outbreaks of bark beetles, defoliators, sucking insects, and diseases. We discuss knowledge gaps and opportunities, identify potential priority investments, and make recommendations for future studies. We finish with a synthesis and conclusions.

2. Tree, Stand, and Landscape Responses to Forest Insects and Diseases

We compiled insect and disease characteristics and tree, stand, and landscape responses to biotic disturbance agents important in conifers of the western U.S. (excluding Hawaii and Alaska). Abiotic factors such as drought, fire, and flooding are not addressed. We focus on characteristics and responses of forest insects and diseases relevant to detection and attribution using remotely sensed data. We provide an extensive listing of these in table A.1 and summarize some specific, common agents by biotic and agent type in table 2. Citations for statements in this section below are included in tables 2 and A.1; we relied on published forest entomology reviews that summarize characteristics of individual agent-host associations. Guides describing aerial signatures of insect and disease damage produced for aerial surveyors, such as Ciesla 2006 and Ciesla et al. 2015, are excellent resources for remote sensing. These guides, however, focus on visual clues alone, as compared with other regions of the electromagnetic spectrum. Although this information is specific to the western U.S., analogous characteristics and responses to biotic agents occur in forests worldwide, and thus what we present can be applied more broadly.

Table 2—Advantages or benefits and disadvantages or drawbacks of remote sensing and aerial surveys.

Type of disturbance agent	Example insect or pathogen	Insect or disease characteristics	Tree, stand, and landscape responses	Example references
Bark beetles	• Mountain pine beetle (*Dendroctonus ponderosae*) • Spruce beetle (*D. rufipennis*) • Piñon ips beetle (*Ips confusus*)	• Hosts can be limited to one tree species or include multiple species (usually confined to one genus) • Feeds on phloem • Multiple generations per year to one generation every two years • Adult flight and host tree attack in early to late summer • Aggressive beetle species can kill trees at high populations; nonaggressive species kill trees when host compromised by other stressors such as drought • Older, larger trees and denser stands dominated by host species are more susceptible	• Trees killed by successful attacks • Progression of needle color after attack: green to red or yellow; evident visually in year following attack • Needlefall within 3-5 years following attack, resulting in gray tree • Tree mortality can be low or high severity, spatially diffuse or extensive • Outbreaks can occur rapidly for several years or more slowly for a decade	• Ciesla et al. (2015) • Hall et al. (2016) • Holsten et al. (1999) • Negrón and Wilson (2003) • Rocky Mountain Region, Forest Health Protection (2010)
Defoliators	• Douglas-fir tussock moth (*Orgyia pseudotsugata*) • Western spruce budworm (*Choristoneura freemani*)	• Hosts can be limited to one tree species or include multiple species • Feeds on needles • Feeds for 1-2 months in spring/early summer • One-year life cycle • Multilayer, dense stands are most susceptible	• Crown color change from webbed needles, defoliation, topkill • Tree growth reduced; tree mortality can occur with multiple years of severe defoliation • Outbreaks can occur rapidly (several years) or for several decades • Outbreaks can cause scattered or widespread damage	• Ciesla et al. (2015) • Fellin and Dewey (1986) • Hall et al. (2016) • Pederson et al. (2020)
Sucking insects	• Balsam woolly adelgid (*Adelges piceae*) • Spruce aphid (*Elatobium abietinum*)	• Hosts are conifers • Examples are invasive; first recorded in western U.S. in early 1900s • Multiple generations per year • Feeds by inserting mouthparts into needles, branches, twigs, buds • All sizes of trees attacked, but larger trees more susceptible	• Attacked trees show stunted growth, crown decline, flagging, fiddle-shape, top curl, gouting, yellow or brown needles, needle loss • Damage can continue for many years after initial infestation • Some species and cause host mortality after 2-3 years of heavy infestation • Symptoms of dying tree: foliage turns yellow, then deep red or brown • Infestation in a tree can last years • Diffuse or severe mortality can occur	• Ciesla (2006) • Hagle et al. (2003) • Oregon Department of Forestry (2017) • Ragenovich and Mitchell (2006)

Table 2 continued.

Type of disturbance agent	Example insect or pathogen	Insect or disease characteristics	Tree, stand, and landscape responses	Example references
Pathogens	• *Armillaria* spp. • *Heterobasidion annosum*	• Hosts: 100s of species of plants, including conifers • Attacks roots, stem, and/or needles	• Symptoms: crown thinning; needle color change to yellow then brown, branch dieback • On large trees, infection over multiple years can lead to tree mortality; on small trees, trees can die within a year • Can weaken trees, predisposing them to attack by other agents • Can kill weakened or healthy trees • Mortality is scattered throughout stand; can be extensive • Expanding centers of mortality, which contain older gray trees (or downed trees) in center, newly infected trees at periphery	• Ciesla (2006) • Schmitt et al. (2000) • Williams et al. (1986)

2.1 Bark Beetles

Biotic agents can be broadly categorized as those that kill trees to reproduce (bark beetles) and those that initially only damage trees but may kill trees through repeated, severe damage (defoliators, sucking insects, diseases). Most often, the bark beetle species covered in this report kill a tree as part of a successful attack. Most of these bark beetles belong to the genus *Dendroctonus*, which translates to "tree killers." Multiple species of bark beetles kill trees during epidemics and cause substantial tree mortality across the western U.S. (Hicke et al. 2020). Aggressive bark beetle species, such as mountain pine beetle and spruce beetle (*Dendroctonus rufipennis*), can kill healthy trees during outbreaks (Raffa and Berryman 1987; Rudinsky 1962; Weed et al. 2015).

Bark beetle populations often reach epidemic levels after other factors, including drought or other biotic agents, stress host trees and leave them susceptible to attack, or when blowdown events increase breeding material. For example, outbreaks of fir engraver (*Scolytus ventralis*) resulting in substantial tree mortality typically start from large-scale disturbance events such as blowdowns or repeated defoliation from western spruce budworm or Douglas-fir tussock moth (*Orgyia pseudotsugata*) (Ferrell 1986). Unlike other bark beetle species that kill substantial numbers of trees, fir engravers only require a small strip of cambium to successfully reproduce, potentially leading to only dead branches or top-kill (Randall 2012).

Adult bark beetles attack host trees by burrowing through the outer bark and excavating galleries in the phloem for feeding and egg-laying. Adults introduce a fungus into the host trees that penetrates the xylem, reducing water transport to needles. The seasonal timing of attacks varies by beetle species, ranging from late spring to late summer. Life cycles vary from multiple generations per year to 1–2 years per generation. Older, larger trees, and those in denser stands (which are more stressed because of competition for resources), are attacked first.

Trees killed by bark beetles progress through several stages relevant for detecting damage using remote sensing. Initially, "green-attack" trees exhibit no visual change, but experience a reduction in transpiration as the fungus vectored into the host by the beetle penetrates the xylem (Hubbard et al. 2023; Yamaoka et al. 1990). This reduction in water loss through needles causes an increase in leaf temperature (Heller 1968). The attacked tree progresses to the next stage in which needles lose their chlorophyll, desiccate, and turn from green to red or yellow (fig. 2). Pines typically turn red in this stage, with subtle color variations ranging from a deeper red in lodgepole pines (*Pinus contorta*) to a more orange-red in ponderosa pines (*Pinus ponderosa*). Spruces (*Picea* spp.) in the Rocky Mountains of the conterminous U.S. turn yellow or red, then grayish in this stage, whereas spruces in Alaska turn red (Holsten et al. 1999).

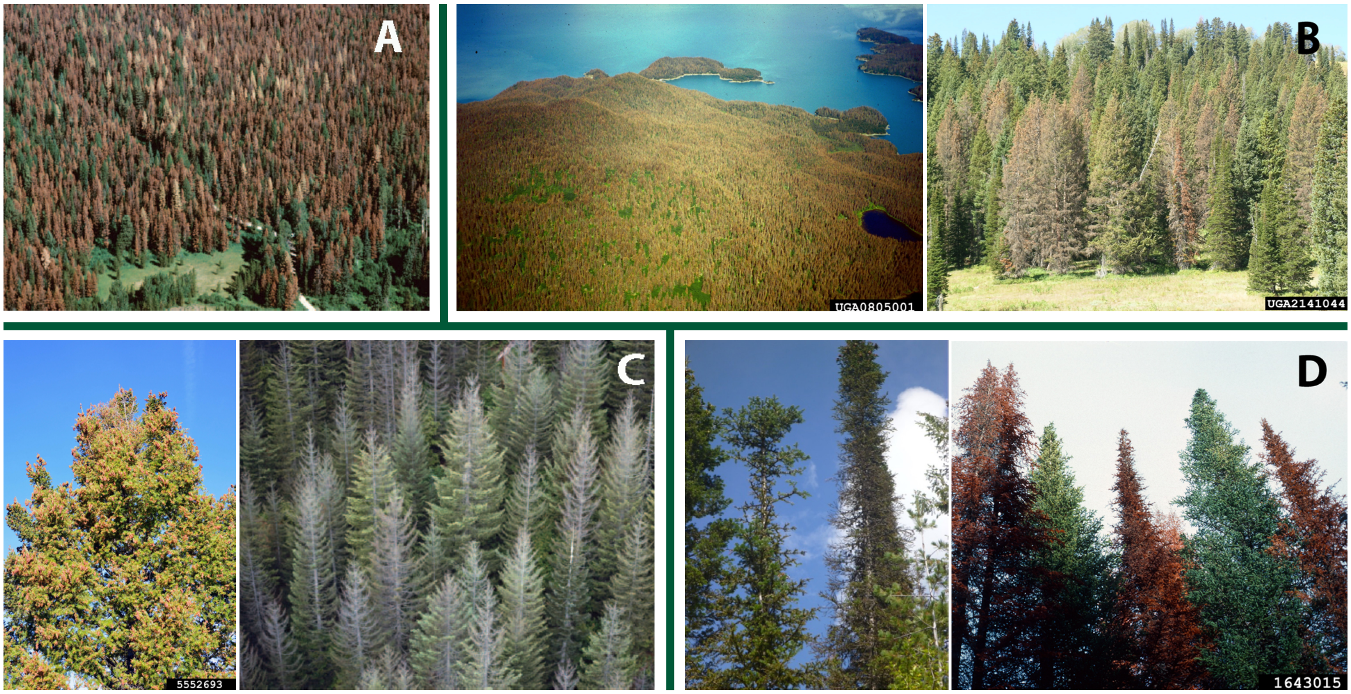

Figure 2—Tree responses vary among insects and diseases. (a) Colors of different host trees attacked by mountain pine beetle: redder trees are lodgepole pines and yellower trees are ponderosa pines. USDA Forest Service photo from Ciesla 2006. (b) Different colors of host trees attacked by spruce beetle. USDA Forest Service photos by left: Edward H. Holsten, from Bugwood.org and right: A. Steven Munson, from Bugwood.org. (c) Different colors of host trees affected by defoliation by western spruce budworm: current-year defoliation showing the reddish hue of damaged needles. Left: Courtesy photo by William M. Ciesla, Forest Health Management International, from Bugwood.org, and partial and nearly complete defoliation. Right: USDA Forest Service photo from Ciesla 2006. (d) Crown deformities (left) and tree mortality caused by balsam woolly adelgid (right). Left: USDA Forest Service photo by G. Davis. Right: USDA Forest Service photo by Coeur d'Alene Field Office, from Bugwood.org).

Variability exists in the time from needles turning red or yellow before falling from the killed trees. Needles fall more quickly from piñon pines killed by piñon ips (*Ips confusus*), which are capable of 2–6 generations per year (Furniss and Carolin 1977; Schultz and Bedard 1987). and therefore can attack hosts early in the growing season, thereby allowing needles to desiccate within the same year. In contrast, needlefall occurs 2–5 years after lodgepole pines are killed by mountain pine beetle (Wulder et al. 2009). After needlefall, killed trees become gray because the foliage is gone, leaving twigs, branches, and boles visible (equivalent to severe damage by defoliating insects). After 5–30 years, snags fall (Audley et al. 2021; Kearns et al. 2005; Latif et al. 2023; Rhoades et al. 2020; Schmid et al. 2009).

Within stands, mortality severity (number of trees killed or crown area of killed trees within an area) can range from low (a few killed trees scattered across a landscape) to high (70% or greater) (Cole and Amman 1980; Hicke et al. 2016; Meddens and Hicke 2014) (fig. 3). Aerial surveys of the western U.S. and Canada indicate that most locations experience low-severity tree mortality (in terms of crown area of killed trees) from bark beetles (Hicke et al. 2016; Meddens et al. 2012). The presence of mortality can last 1–10 years or more, both within a stand and over a larger outbreak area, depending on beetle/host association, beetle populations, and climate conditions (Cole and Amman

1980; Hicke et al. 2020; Meddens and Hicke 2014). Annual rates of mortality within stands can exceed 30-40% (Cole and Amman 1980; Meddens and Hicke 2014) (fig. 3). More rapid and shorter duration mortality within stands can occur with high beetle populations (e.g., severe mountain pine beetle outbreaks) or severe drought conditions that drive outbreaks (e.g., piñon ips). Widespread tree mortality occurs when the climate is suitable for beetle population growth and maintenance and in landscapes that have an abundance of susceptible trees, such as host species of large, old, and/or stressed trees.

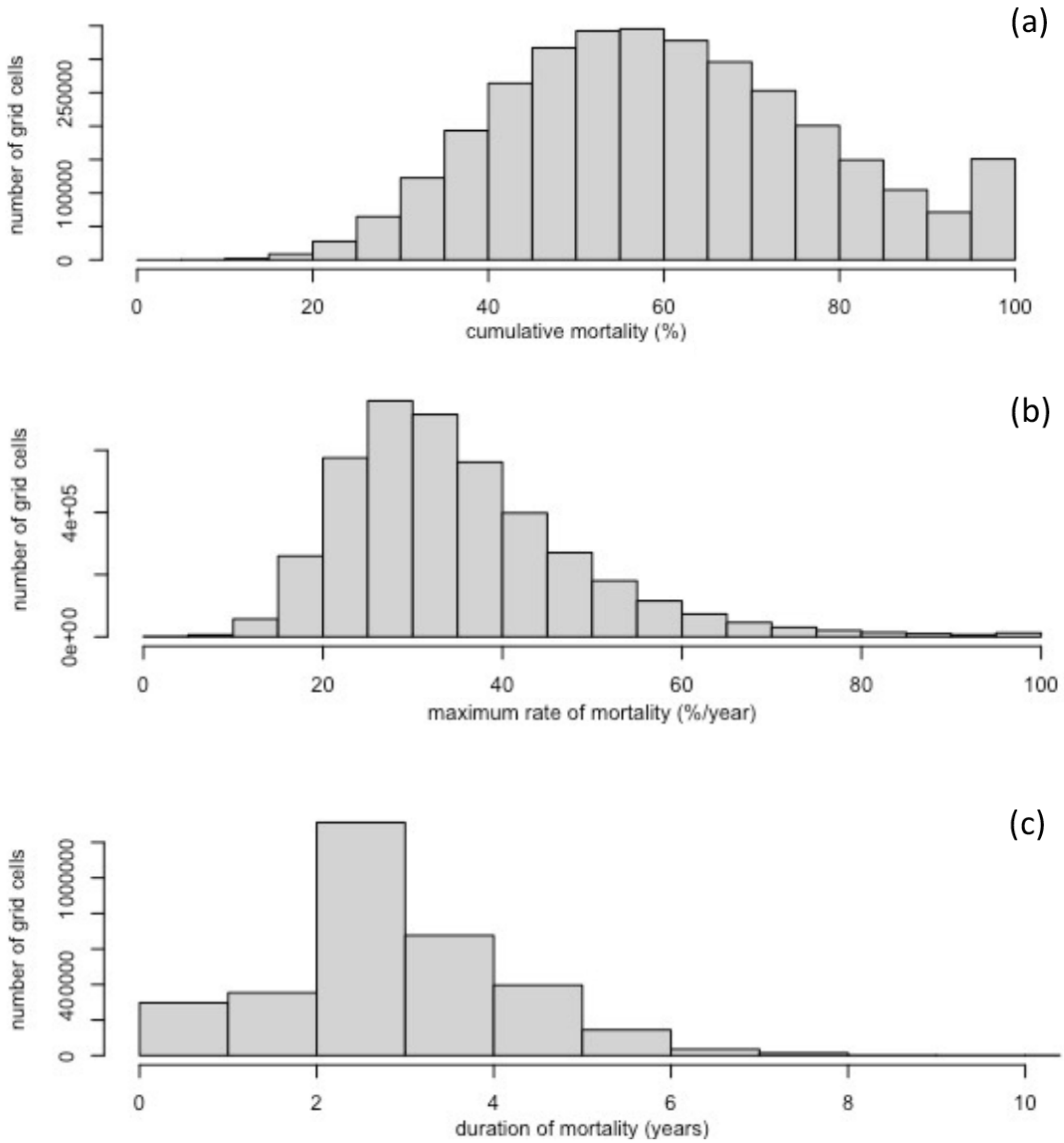

Figure 3A-C—Insect outbreaks are variable in severity, outbreak duration and rate, and recovery time. Histograms of (a) cumulative mortality (%); (b) maximum year-to-year mortality rate (%/year); and (c) duration of outbreak (years) for an outbreak of mountain pine beetle in Colorado, 2002-2011 (Meddens and Hicke 2014).

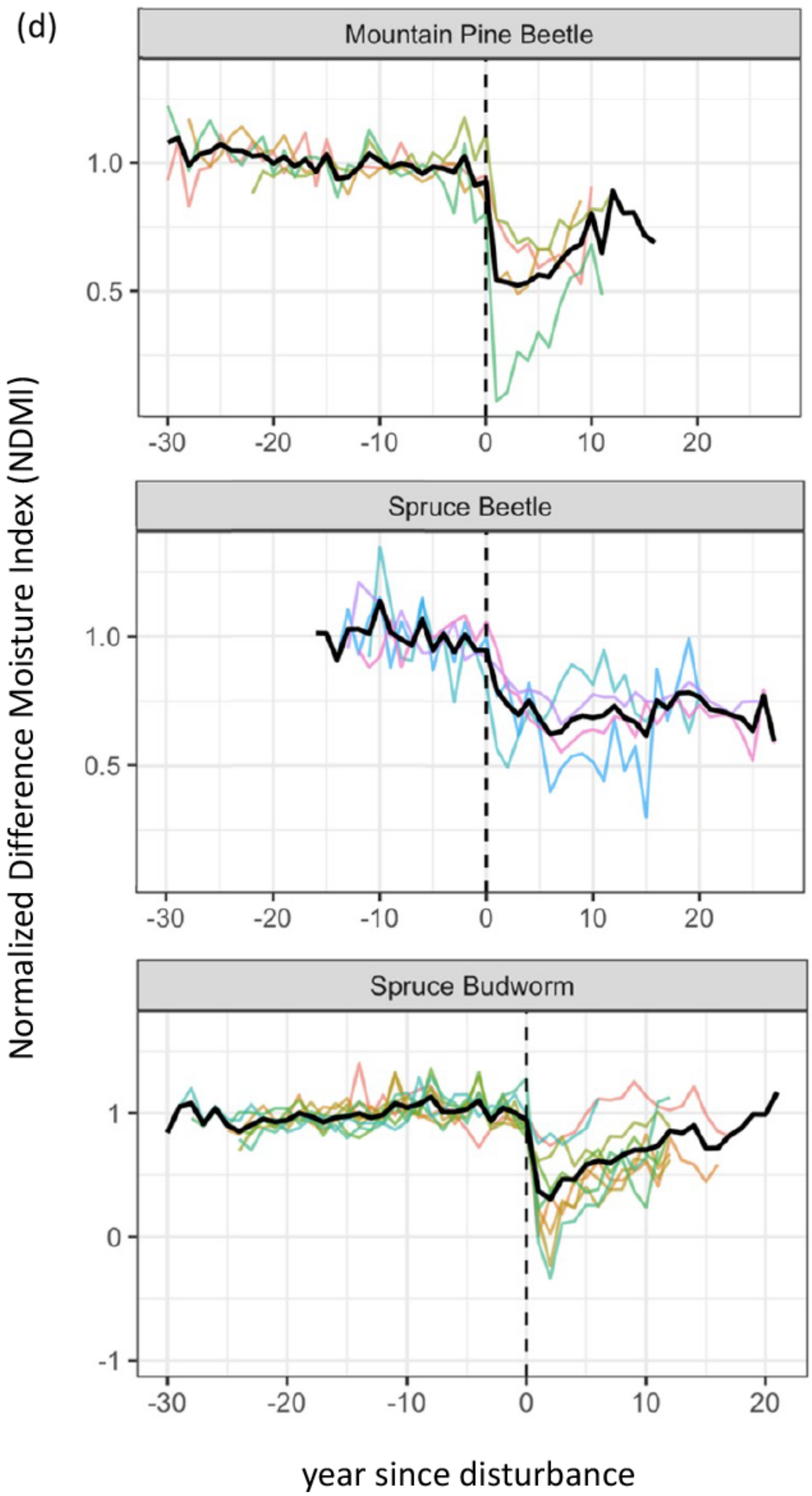

Figure 3D—Insect outbreaks are variable in severity, outbreak duration and rate, and recovery time. (d) Time series of Landsat-based Normalized Difference Moisture Index (NDMI) within severe outbreaks of mountain pine beetle. Top: mountain pine beetle; middle: spruce beetle; and bottom: western spruce budworm. Colored lines are individual case studies and black lines are means; reductions in NDMI indicate vegetation damage or loss. Licensed figure from Foster et al. 2022. Figures licensed under a Creative Commons Attribution 4.0 International License (http://creativecommons.org/licenses/by/4.0). Parts of two original figures were combined.

2.2 Defoliators, Sucking Insects, and Diseases

The second set of biotic agents attacks and damages trees but does not necessarily kill them. Agents important for conifers of the western U.S. (excluding Hawaii and Alaska) in this set include defoliating and sucking insects and tree pathogens (tables 2 and A.1). Defoliating insects feed on needles, which can be partially or fully consumed, leading to a reddish or gray tree coloration (fig. 2). Defoliation typically progresses from the top of the crown downward, although the opposite occurs for western hemlock looper (*Lambdina fiscellaria lugubrosa*) (Ciesla 2006).

Western spruce budworm has been the most destructive defoliator in western coniferous forests, (Furniss and Carolin 1977), followed by Douglas-fir tussock moth (Berryman and Wright 1978). Sucking insects (e.g., balsam woolly adelgid (BWA), *Adelges piceae*) feed on buds, twigs, branches, and stems and, as with defoliators, are also capable of causing tree mortality. The BWA life cycles range from one to multiple generations per year. Feeding may occur only earlier in the growing season, as for western spruce budworm. Important forest pathogens attack conifer roots, stems, branches, and needles.

These agents typically cause more subtle tree damage, at least initially, than tree-killing bark beetles. Needle loss causes parts of trees, or entire trees, to appear gray. Webbing produced by western spruce budworm binds needles, causing them to turn red at their tips, causing a reddish crown and eventual branch and tip dieback. Annual damage rates can be high (table A.1). Trees recover if damage is less severe or shorter in duration; faster growing tree species recover more quickly (Atkinson et al. 2014). Attacks by these agents on individual trees can last one year or decades. Repeated damage leads to stunted growth and crown deformities (fig. 2). In addition to these responses, sucking insects and pathogens can cause branch flagging, crown thinning (loss of needles), and, in the case of balsam woolly adelgid, gouting (bud and branch swelling). Following severe, prolonged attacks, conifers can be killed by these agents. Needles turn red as a result, following a progression and set of responses similar to the mortality caused by bark beetles.

Stands attacked by these agents can experience different combinations of low versus high severity damage and short- versus long-term outbreaks, depending on the agent and conditions. Defoliator outbreaks are most severe in multilayered, dense stands that allow caterpillars to disperse from overstory trees with high insect populations to understory trees. Sucking insects and pathogens can attack trees of any size. Root diseases spread from tree to tree via root contact, resulting in expanding circles of mortality (fig. 4). Some defoliator outbreaks can be severe and widespread, others less severe and chronic. Disease-damaged trees tend to be scattered across a landscape yet are widely distributed (Healey et al. 2016).

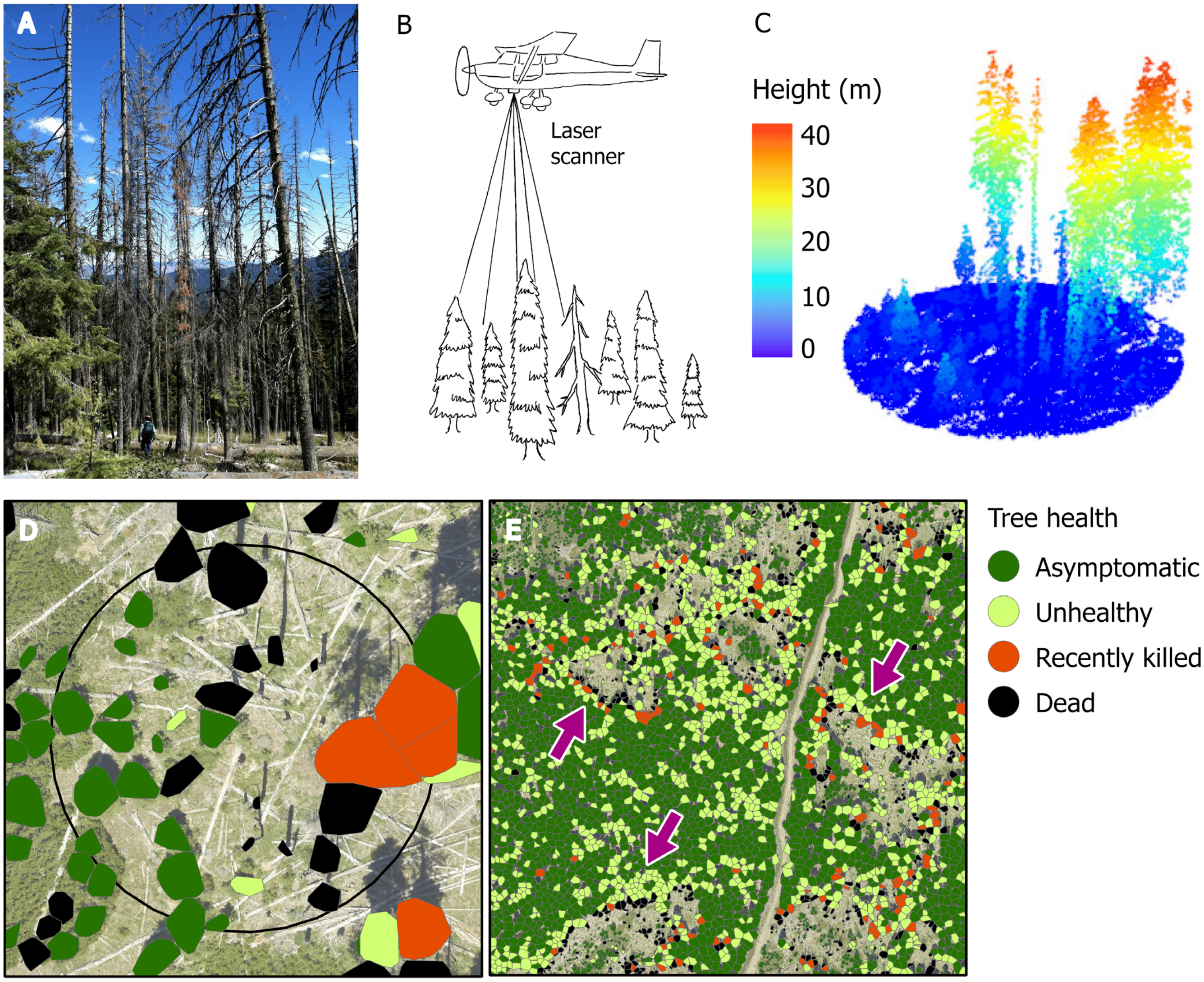

Figure 4—Methods and results from a study that mapped (a) trees killed by Armillaria root rot in Oregon. (b) Airborne or satellite-based lidar is an active sensor that can be used to derive forest structure information such as (c) tree crown heights (shown by colors) and crown diameters. By combining structure and reflectances from lidar data with multispectral reflectances, trees in asymptomatic (dark green), unhealthy (light green), recently killed (red), and dead (black) conditions were mapped. (d) This is the same area as in (c). (e) Part of the study area illustrating expanding centers of damage that occurs from root diseases (purple arrows). USDA Forest Service images from Oblinger et al. 2022.

2.3 Tree, Stand, and Landscape Responses

Based on a variety of biotic disturbance agents (tables 2 andA.1), we developed a list of general responses of trees, stands, and landscapes that are potentially relevant for characterization by remote sensing technologies and/or methods for detection and attribution (table 3). Note that some of the responses have been used repeatedly in forest entomology applications in remote sensing (e.g., foliage color change), whereas others have yet to be used or become well-established or may not be feasible (e.g., gouting by balsam woolly adelgid).

Table 3—Generalized responses of trees, stands, and landscapes to insect and disease outbreaks potentially relevant for using remote sensing for detection and attribution.

Type of response	Response	Change	Cause	Responsible agent	Remote sensing signature (potential technology or method)
Type of tree damage	Foliage color	Entire tree changes color: yellowish, brown, red; eventual change to gray following needle loss	Loss of chlorophyl in killed trees	Bark beetles, other agents that kill trees	Changes in visible (and other regions) reflectance (multispectral, hyperspectral)
		Color change within individual tree parts (top, or branches)	Needles damaged by partial feeding or by webbing; Feeding pattern (location of bark beetle attack on bole, location of overwintering insect stages relative to foliage)	All	
			Silken webs produced by some insects	Defoliators	
	Foliage amount	Defoliation, twig/branch dieback, topkill	Feeding	All	Changes in visible, near-infrared, shortwave infrared reflectance and microwave radiation (multispectral, hyperspectral, radar, lidar, structure-from-motion)
		Loss of foliage from entire tree	Needlefall from killed trees	Bark beetles, other agents that kill trees	
	Crown deformities, including gouting	Abnormal crown shape	Feeding location	All	Differences from a normal crown shape (lidar, structure-from-motion)
	Foliage water content	Decrease in water content	Needle structure change and desiccation following damage or mortality, or reduction in foliage amount	All	Changes in near-infrared, shortwave infrared reflectance (multispectral, hyperspectral, radar)
	Crown temperature	Increase in temperature	Reduction in foliage transpiration and associated cooling from defoliation or tree mortality	All	Changes in needle/crown temperature (thermal infrared radiation)

Table 3 continued.

Type of response	Response	Change	Cause	Responsible agent	Remote sensing signature (potential technology or method)
Temporal	Seasonal progression of damage, mortality, and/or recovery	Progression, timing, rate, and/or permanence of above tree responses to damage or mortality within one year (e.g., timing of tree fading or defoliation; recovery from defoliation)	See tree responses above	Various	Tree responses above considered from spring through fall (analysis of multiple intra-annual images or data)
	Interannual progression of damage, mortality, and/or recovery	Progression, timing, rate, and/or permanence of above tree responses to damage or mortality for multiple years (for example, multiple years of damage that can lead to either recovery or mortality; or rapid mortality that causes trees to move through predictable stages and is permanent)	See tree responses above	Various	Tree responses above considered over multiple years (analysis of multiple interannual images or data)
Spatial	Severity of damage or mortality	Number of damaged or killed trees within an area (stand or landscape)	See tree responses above	Various	Tree responses above considered for area of interest
	Canopy position of damage	Damage to overstory and/or understory trees	Dispersal of feeding caterpillars from overstory to understory; location of attacks on tree	All	Foliage amount and color (above)
	Spatial patterns of damage or mortality	Expanding centers of tree mortality	Pathogens transmitted between host trees through root contact	Root diseases	Tree responses above (spatial pattern of damage/mortality, including mapping old and newly killed trees)

Many insects and pathogens are host specific. Some bark beetle species prefer several related tree species (pines for mountain pine beetle, spruces for spruce beetle). Some defoliators (e.g., western spruce budworm) and pathogens (e.g., Armillaria) attack a wide range of conifer species. Some tree species experience significant damage or mortality from only one main biotic agent, such as Engelmann spruce and spruce beetle. Other tree species are damaged and killed by a suite of agents. For example, subalpine fir (*Abies lasiocarpa*) is attacked by fir engraver, western balsam bark beetle (*Dryocoetes confusus*), western spruce budworm, and balsam woolly adelgid, each of which has caused substantial damage or mortality to subalpine firs in the western U.S.

A variety of responses related to tree morphology can inform remote-sensing studies. Changes in needle color from green to red or yellow are caused by biotic agents. Such changes can indicate mortality (if entire tree changes color), but can also indicate defoliator, sucking insect, or pathogen attack. One color change is not necessarily indicative of one biotic agent: extensive feeding by defoliators can turn trees red or gray (similar to mortality caused by bark beetles), and spruce beetle-killed trees can turn yellow or red. Some insects such as Douglas-fir tussock moth and western hemlock looper produce silken webs that give the crown a silver appearance (Furniss and Carolin 1977; Pederson et al. 2020). Changes in foliage amount caused by biotic agents range from crown thinning, to top-kill and dieback, to whole-tree defoliation. Responses occur because of insects feeding on needles, insect attacks on other parts of the tree, or needlefall following tree mortality. Crown deformities can occur following attack by many biotic agents resulting in stunted growth, abnormal tops, or gouting. Needle and crown (whole tree) water content decreases as needles are killed or lost by consumption, partial crown dieback, and/or whole tree mortality. As a result of the loss of cooling from transpiration, the crown temperature of damaged or killed trees increases.

Temporal and spatial responses occur following attack by biotic agents. The timing and progression of damage within one year varies among agents, with some agents attacking earlier in spring or summer and others later in summer. Tree responses may be immediate, as with defoliation, or delayed, such as color change following bark beetle attack (with the amount of delay varying among beetle species). Trees may recover from attack, as for light defoliation, or may be killed. Over longer periods, less severe defoliation may result in recovery in one year (Eidson et al. 2021).

Severe damage from defoliating or sucking insects or diseases for multiple years, or attack from bark beetles, can kill trees, causing these trees to progress through stages of foliage color change and drop. Damage or mortality of individual trees as well as within stands and landscapes can be chronic and longer term, as with some outbreaks of western spruce budworm or balsam woolly adelgid, or rapid, severe, and extensive, as with damage or mortality within one year from defoliators and bark beetles when populations are high. Rates of damage progression and recovery over the course of years vary within and among outbreaks and among biotic agents (fig. 3). Human activities (e.g., salvage logging) that may occur following disturbance will alter recovery trajectories and affect the remote sensing signals.

Spatial patterns are highly variable within and among biotic agents. Damage or mortality can be diffuse and widely scattered within stands and landscape. Under suitable climate (often warm and/or dry) and stand (host species in susceptible age, size, and density categories) conditions, outbreaks of insects and diseases can lead to very high severity and extent of damage or mortality within both stands and landscapes. Defoliator outbreaks occur in multistory stands in which dispersing caterpillars in search of food can descend and feed on understory trees. Diseases tend to be scattered but widespread across landscapes but can cause severe damage or mortality locally. A further signal of root diseases that results from the spread of the pathogen through root contact is the spatial pattern of an expanding circle of damage and mortality, with the earliest attacked trees in the center.

We note that many of these responses occur as a result of other disturbance agents, particularly those that kill trees (Ciesla 2006). Trees killed by drought exhibit similar morphological changes as those killed by biotic agents, including changes in foliage color and water content change and subsequent needlefall. Trees scorched by wildfires, but whose foliage is not consumed (burned), can also exhibit similar changes (Ciesla 2006).

3. Relevant Characteristics of Remote Sensing Technologies and Methods

In this section we review characteristics of remote sensing technologies (sensors and platforms) and methods (processing, algorithms, etc.) relevant to forest insects and diseases (summarized in table 4).

Table 4A-B—Characteristics of remote sensing relevant for detecting and attributing tree damage and mortality.

Table 4A—Technology characteristics

Technologies	Aspects of sensors or platforms
Spectral	Bands: location, number, contiguity Shortwave: multispectral, hyperspectral, thermal infrared, microwave
Passive versus active (or passive and active) sensors	Active: lidar, microwave/radar Passive: all others
Reflectances and products	Surface reflectance, vegetation indices, forest structure/function
Spatial	Resolution, extent
Temporal	Resolution, extent, seasonal timing
Geometric	View zenith angle
Platform	Satellites, airplanes, helicopters, UASs, ground-based (terrestrial laser scanner, cell phone)

Table 4B—Methods characteristics

Methods	Choices of analyst, study
Timing of acquisition	Selected imagery for analysis; for instance, immediately after feeding or attack, at end of growing season, in winter, in next growing season Once per year versus multiple times per year
Damage or mortality metric	Classification into damage/mortality or undamaged; continuous metric of percent damage/mortality
Spatial resolution of metric	Pixel-based (different sizes) or object-based (minimum mapping unit size)
Reference data	Field measurements, on-screen analysis, use of finer spatial resolution products than study remote sensing data
Imagery used	Single image or multiple images (including time series), sensor type
Statistical method	Classification algorithm, regression model
Evaluation method	Confusion matrix, resampling/cross-validation, model fit metrics
Cloud computing	Use of high-performance computing, as from Google Earth Engine
Combining multiple remote sensing data types	Fine spatial resolution/coarse temporal resolution (e.g., RapidEye) with coarse spatial resolution/fine temporal resolution (e.g., Landsat)
Ancillary data	Inclusion of cover type, topography, etc. in addition to remote sensing data

3.1 Spectral Regions of Interest

Because remote sensing relies on electromagnetic radiation for observations, we first discuss the regions of the electromagnetic spectrum that are modified by tree responses to insects and diseases. In the shortwave part of the spectrum, healthy (green) vegetation creates characteristic patterns of reflectance and scattering (fig. 5). Relatively lower reflectance occurs in the visible region (0.4–0.7 µm), with a local peak in the green region caused by the absorption of blue and red wavelengths by chlorophyll. Reflectance peaks in the near-infrared (NIR) region (0.8–1.2 µm) associated with scattering and lack of absorption within the leaf. Reflectance then declines in the shortwave infrared (SWIR) region (1.4–2.4 µm), with particularly low reflectance in regions with absorption by water (around 1.4 and 1.9 µm).

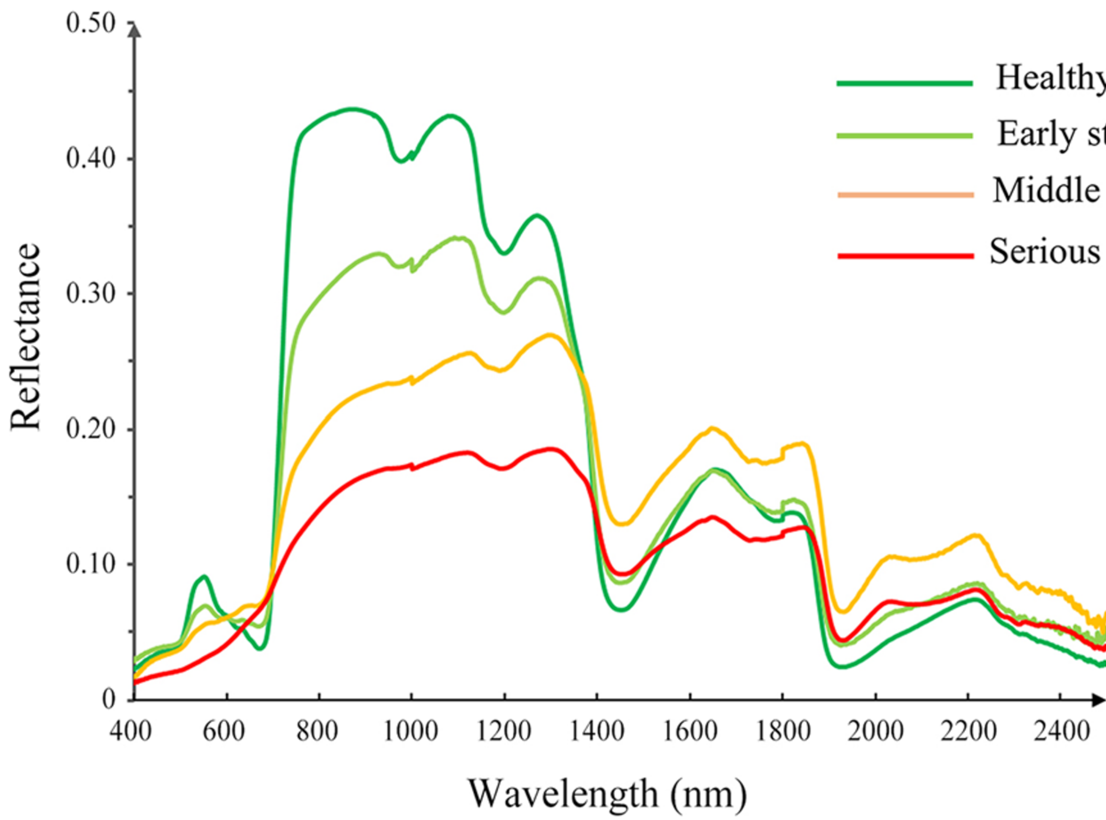

Figure 5—Shortwave reflectance spectra of healthy pines and pines at different stages following attack by pine wilt disease. Licensed figure from Yu et al. (2021b). Figure licensed under a Creative Commons Attribution 4.0 International License (http://creativecommons.org/licenses/by/4.0). Figure modified to remove original panel letter ("(a)").

Trees (or parts of trees) respond to attacks from biotic agents in several ways that alter the shortwave reflectance spectrum (Ahern 1988; Heller 1968; Niemann et al. 2015; Yu et al. 2015b), (fig. 5). Needles lose chlorophyll, causing increases in blue and red reflectance as absorption in those spectral regions decreases. The needles turn red or yellow as a result, altering the visible part of the spectrum. Trees that appear gray have uniform reflectance across the visible region, which may be higher (greater) than for healthy vegetation. Changes in the internal structure of affected needles reduce the internal scattering and therefore the NIR reflectance (Slaton et al. 2001). Needles also desiccate, then fall, exposing twigs, branches, and the stem. Such changes reduce the water content of the canopy, reducing the absorption in the SWIR region and increasing reflectance.

Reflectance in spectral regions, combinations of reflectances, and spectral indices are used in remote sensing studies to exploit these varied responses. Spectral indices are ratios or combinations of reflectances in different spectral regions or are first derivatives of the reflectance spectrum (when using hyperspectral data). These spectral indices minimize the background noise associated with variability (from, e.g., different illumination conditions) through normalization.

Vegetation indices are used to take advantage of the difference between healthy and damaged trees. Examples that use these differences include the (1) Red-Green Index (RGI) calculated from visible reflectances (Coops et al. 2006); (2) the Normalized Difference Vegetation Index (NDVI) (Rouse et al. 1973; Tucker 1979), which takes advantage of the large difference between visible and NIR reflectance that is reduced in damaged trees; (3) indices that compare reflectance in the NIR and SWIR regions such as the Normalized Difference Moisture Index (NDMI) (Wilson and Sader 2002) or Normalized Burn Ratio (NBR) (Key and Benson 2006); and (4) combinations of reflectances in multiple parts of the spectrum, such as the Tasseled Cap indices (Crist 1985), which are computed using visible, NIR, and SWIR reflectances (table 5).

Besides the shortwave region, other parts of the electromagnetic spectrum have been used in studies of forest insects and diseases. At longer wavelengths, thermal infrared radiation (around 3–20 µm) emitted by the Earth is a function of temperature. Killed trees have lost the cooling effect of transpiration, and as a results, canopy temperatures increase(e.g. Heller 1968). Microwave radiation (1 mm–1 meter wavelengths, equivalent to frequencies of 300–40,000 Hz) is sensitive to vegetation water content and structure and, at longer wavelengths, is not affected by cloud cover or aerosols (Hollaus and Vreugdenhil 2019).

Table 5—Examples of spectral indices and combinations commonly used in remote sensing applications of forest disturbances. ρ is reflectance; subscripts indicate different regions of the electromagnetic spectrum.

Name (abbreviation)	Equation	Reference
Excess Green (ExG) Index	$(2 * \rho_{\mathrm{green}}) - \rho_{\mathrm{red}} - \rho_{\mathrm{blue}}$	Woebbecke et al. 1995
Green Leaf Index (GLI)	$\frac{(\rho_{\mathrm{green}} - \rho_{\mathrm{red}}) + (\rho_{\mathrm{green}} - \rho_{\mathrm{blue}})}{(2 * \rho_{\mathrm{green}}) + \rho_{\mathrm{red}} + \rho_{\mathrm{blue}}}$	Hunt et al. 2011
Mean Red-Green-Blue (meanRGB) Index	$(\rho_{\mathrm{red}} + \rho_{\mathrm{green}} + \rho_{\mathrm{blue}})/3$	Clay et al. 1997
Normalized Burn Ratio (NBR)	$(\rho_{\mathrm{NIR}} - \rho_{\mathrm{SWIR2}})/(\rho_{\mathrm{NIR}} + \rho_{\mathrm{SWIR2}})$	Key and Benson 2006
Normalized Difference Moisture Index (NDMI)	$(\rho_{\mathrm{NIR}} - \rho_{\mathrm{SWIR1}})/(\rho_{\mathrm{NIR}} + \rho_{\mathrm{SWIR1}})$	Wilson and Sader 2002
Normalized Difference Red Edge (NDRE) Index	$(\rho_{\mathrm{NIR}} - \rho_{\mathrm{rededge}})/(\rho_{\mathrm{NIR}} + \rho_{\mathrm{rededge}})$	Hunt et al. 2011
Normalized Difference Vegetation Index (NDVI)	$(\rho_{\mathrm{NIR}} - \rho_{\mathrm{red}})/(\rho_{\mathrm{NIR}} + \rho_{\mathrm{red}})$	Rouse et al. 1973
Red-Blue Index (RBI)	$\rho_{\mathrm{red}}/\rho_{\mathrm{blue}}$	Perez et al. 2018
Red-Green Index (RGI)	$\rho_{\mathrm{red}}/\rho_{\mathrm{green}}$	Gamon and Surfus 1999
Simple ratio (SR)	$\rho_{\mathrm{NIR}}/\rho_{\mathrm{red}}$	Woebbecke et al. 1995
Tasseled Cap	Orthogonal transformation to produce greenness, wetness, brightness	Crist 1985

3.2 Sensors and Platforms

Spectral Information

Spectral information is one of the most important characteristics for most remote sensing instruments. Multispectral sensors record reflectance in a small number of bands, typically in the shortwave part of the spectrum (i.e., about 0.3–2.5 μm). A panchromatic band records radiation across a broad spectral region and is often included in a sensor because of its greater signal strength and therefore capacity for finer spatial resolution than narrower bands. Commonly included bands are in the blue, green, and red part of the visible region as well as in the NIR region. Bands have been added in other regions (for instance, in the SWIR) as technology has improved. Early sensors had relatively broad bands, whereas more recent sensors have much narrower bands that allow for more resolved observations of the reflectance spectrum and associated improved detection of land surface types.

Hyperspectral sensors record reflectance across a broad spectral range using hundreds of contiguous, narrow bands. The resulting fine spectral resolution allows for the sensing of narrow spectral features that may be missed with broader bands, such as

(1) chlorophyll absorption bands, (2) calculation of first derivatives of the reflectance spectrum, and (3) testing of large number of spectral regions unconstrained by the placement of bands in multispectral sensors, which may be important for detecting insect or disease damage (e.g., Donovan et al. 2021; Gao et al. 2023). The spectral region of hyperspectral sensors typically includes the visible and NIR regions (e.g., Gao et al. 2023), with some sensors used in forest insect or disease studies also including the SWIR region (Donovan et al. 2021).

Hyperspectral sensors have advantages and disadvantages as compared with multispectral sensors. The wide spectral range and fine spectral resolution allow researchers using hyperspectral data to test which regions of the shortwave spectrum are useful for detecting tree damage and mortality. In addition, the continuous nature of the data allows for the calculation of first derivatives of the spectrum, which may prove useful (e.g., Niemann et al. 2015). If the bands of multispectral sensors are placed in spectral regions sensitive to tree responses, the advantages of multispectral sensors (reduced cost and complexity, finer spatial resolution) may outweigh the lack of observations across the full spectrum. Hyperspectral sensors produce much greater amounts of data than multispectral sensors, and because the radiation received by very narrow bands (4–10 nm) is less than for the wider bands of multispectral sensors (50 nm or greater for advanced multispectral sensors), spatial resolution is often coarser.

Multispectral and hyperspectral imagery is useful for observing changes in foliage color, amount, water content, damage severity, progression, timing at stand and landscape scales; and spatial patterns associated with root diseases (table 3).

Multiple sensor technologies exist for observing radiation outside the shortwave region of the spectrum. Bands in the thermal infrared part of the spectrum (i.e., around 3–20 μm) allow for sensing land surface (tree or canopy) temperature. Microwave sensors detect radiation at 1-mm to 1-meter wavelengths and can be passive or active. Passive sensors record reflected or emitted radiation from the Earth's surface, whereas active sensors generate pulses of radiation that are reflected back to the sensor. Because passive microwave sensors record low amounts of radiation, spatial resolution is coarse (5–50 km), limiting their usefulness in studies of insect or disease outbreaks.

Radar remote sensing uses active microwave sensors (radars) that transmit pulses of radiation to the Earth's surface and record the backscatter. Radar data are sensitive to the vegetation amount and water content (table 3). Spatial resolutions range from 0.25–100 m for active microwave sensors, and studies have reported the potential of these sensors for detecting tree damage (Bae et al. 2022; Hollaus and Vreugdenhil 2019). Different radar sensors, including those using C-, X-, and L-bands, have been used to study forest disturbances, including insect outbreaks. Longer wavelength L-band radars penetrate the canopy better than shorter wavelength C- and X-band radars but, as a result, are more influenced by larger disturbances and less able to detect smaller scale disturbances such as insect outbreaks (Hollaus and Vreugdenhil 2019). However, recent studies found that despite fine spatial resolution, the C-band radar of Sentinel-1 was not useful for detecting insect outbreak areas (Huo et al. 2021; König et al. 2023).

Active sensors. Another characteristic of sensors is whether they are passive or active. Active sensors (defined above) include radar, as discussed above, and lidar (Light Detection and Ranging). Lidar sensors generate pulses of radiation and record the reflected radiation (fig. 4). By measuring the time required for pulses to return from target surfaces, three-dimensional representations of targets are generated. Lidar systems typically use the NIR region of the electromagnetic spectrum but can use the green (usually for bathometric applications) or SWIR region. Across the 400–2500 nm region of the electromagnetic spectrum, healthy green vegetation reflectance is highest in the NIR region (1062 nm), and across the visible domain, highest in the green region (531 nm). Lidar data can be discrete, in which one to multiple returns are recorded for each reflected pulse, or waveform, which records the full distribution of the reflected pulse. Multiple returns generally occur in forests because of reflections from the different parts of a tree's crown and the ground.

Early lidar acquisitions were from airplanes, which continues today. Later, space-based lidar data became available, although it is currently limited in forest disturbance applications. More recently, UAS- and ground-based collections have increased in number. Lidar data have typically been used to characterize the three-dimensional structure of an individual tree or canopy (table 3). The magnitude of energy reflected back to the lidar sensor, often referred to as return intensity or reflectance, is related to vegetation condition (photosynthetic versus nonphotosynthetic) (Wing et al. 2015) that can be used as an indicator of tree health (Meng et al. 2018; Oblinger et al. 2022; Shendryk et al. 2016). However, return intensity also varies by range (distance of the lidar sensor to the target) and lidar system settings (e.g., automatic gain control). Therefore, range normalization and calibration of lidar intensity values are usually advantageous when using lidar intensity for tree condition characterization (Korpela et al. 2010). Combining coincident multispectral imagery with lidar can also increase the utility of lidar for characterization of forest health conditions (Campbell et al. 2020; Kamińska et al. 2018; Oblinger et al. 2022).

Spatial and Temporal Resolution and Extent

Spatial and temporal resolution and extent are other key sensor/platform characteristics and are often linked (fig. 6). For forest disturbance applications, image spatial resolution varies from <10 cm from UASs (e.g., Cessna et al. 2021) to 250 m from the Moderate Resolution Imaging Spectroradiometer (MODIS) (Spruce et al. 2019). For applications seeking to map damage on parts of a tree crown (e.g., top-kill, flagging), resolutions finer than 10–30 cm are probably needed. Finer spatial resolution occurs with ad hoc aerial or UAS imagery; at this resolution, methods need to account for reflectance differences in sunlit versus shaded sides of individual trees. Currently, the finest resolution multispectral imagery from a commercial satellite is 1–4 m (fig. 6), similar to the area of individual crowns. Such imagery may be associated with a coincident panchromatic image (e.g., at 0.45–0.8 μm), which can allow finer-resolution pan-sharpened imagery to be generated by combining the multispectral and panchromatic imagery (e.g., Dennison et al. 2010). Mapping of whole-tree damage at this resolution can be accomplished with this resolution with high accuracy because sunlit and shaded sides of a crown are averaged together, improving separation from non-forest vegetation while still allowing for mapping individual tree crowns (Meddens et al. 2011).

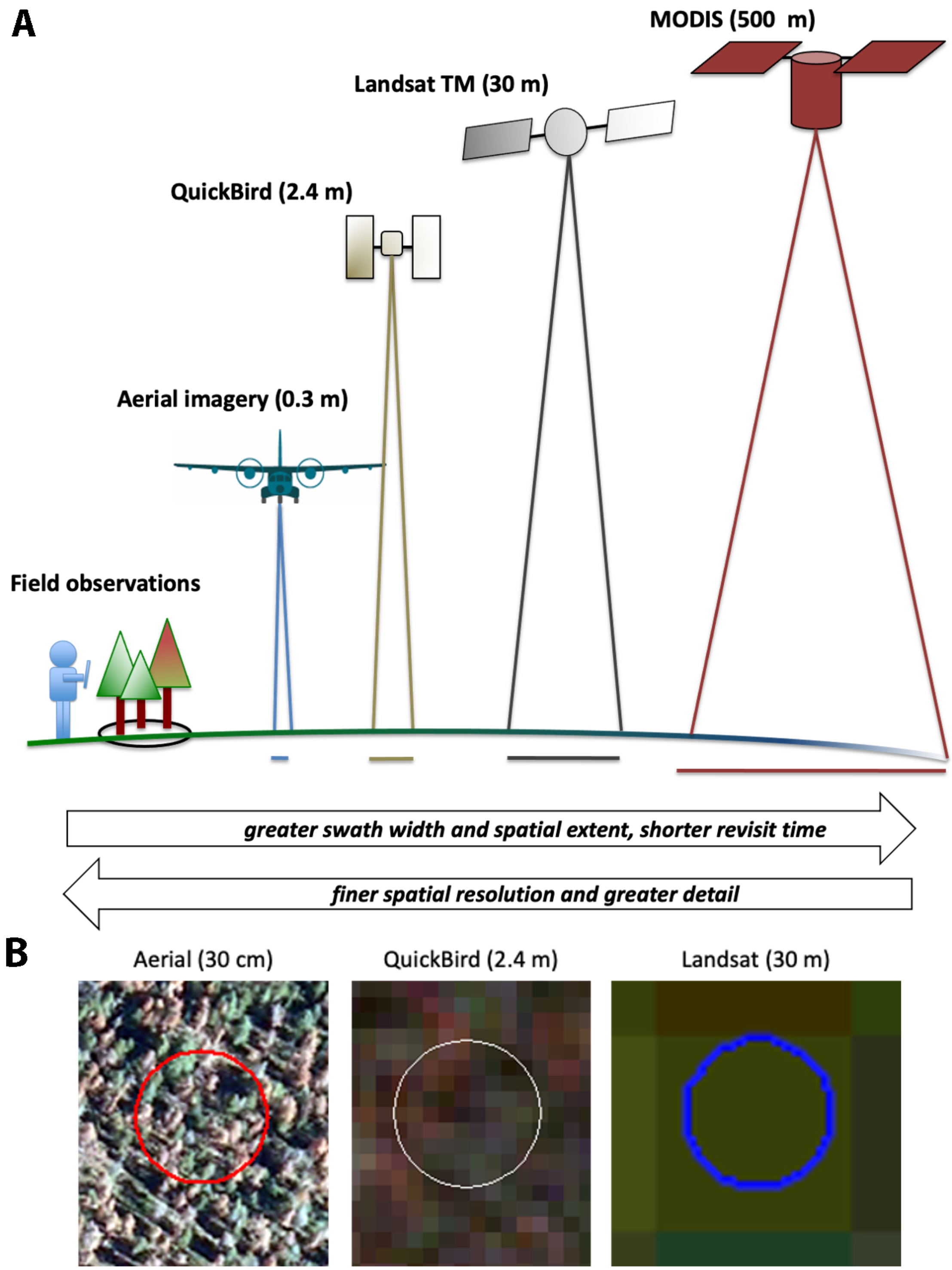

Figure 6—Spatial characteristics of imagery relative to insect and disease damage and mortality. (a) Spatial resolution, image swath width, and temporal frequency (revisit time) are linked (recent launches of constellations of fine-resolution satellites increase their frequency). (b) Aerial, QuickBird, and Landsat images of red-orange lodgepole pines killed by mountain pine beetle, illustrating the reduction in detail as resolution becomes coarser.

Still coarser resolution imagery (10-30 m and coarser; Landsat, a commonly used sensor, has 30-m resolution) detects responses of groups of trees within one pixel, representing plot- or stand-level data. The advantages of coarser resolutions of satellite imagery include the larger spatial extent of acquisitions, more frequent revisit times, and sometimes longer records of available data. Sensor swath width defines the spatial extent of an overpass or acquisition and affects the temporal resolution.

Temporal resolution (repeat time for observing one location) for satellites varies from 1–2 times per day (MODIS) to once every 16 days (Landsat) or more. Some fine-resolution satellite sensors such as Worldview-3, once tasked, acquire images off-nadir (resulting in images with higher view zenith angles, VZA) to increase the repeat time. Sensors on multiple satellites operating simultaneously (e.g., MODIS Terra and Aqua, RapidEye, Sentinel-2, or Planet Dove) can increase the repeat frequency. Temporal extent varies greatly among satellites; long time series have been achieved through linking images from one or more Landsat sensors (e.g., Huang et al. 2010; Kennedy et al. 2010; Meddens et al. 2013; Zhu and Woodcock 2014).

The combinations of spatial and temporal characteristics result in tradeoffs of image characteristics (fig. 6). Fine (tree-level) resolution is desired for studying damage and mortality, and multiple years are often needed. Operational monitoring is best achieved with acquisitions over large areas (regions). However, fine resolution usually occurs with limited spatial extent, and time series of images are available for only a few satellite sensors. Multiscale approaches that relate fine-resolution imagery to coarser-resolution imagery for landscape-level mapping of severe tree mortality have proven effective (Meddens et al. 2013). High-altitude aerial imagery from the National Agriculture Imagery Program (NAIP; https://datagateway.nrcs.usda.gov), with a spatial resolution of 1 m and a three-year refresh time, has been used to map tree crown health (Monahan et al. 2022). A promising approach is the use of images from constellations of satellites, which can result in daily images at fine spatial resolution (Dalponte et al. 2023; Trubin et al. 2023).

Viewing Geometry

View zenith angle (VZA; the angle between nadir, a pixel, and the sensor) is an important sensor and platform characteristic for forestry applications. Low VZA observations (angles close to nadir) minimize distortion of tree geometry. High VZA occurs with pixels that are more distant from nadir and can occur with low-altitude platforms (e.g., UASs) or pointable satellite-based sensors. Trees are distorted at high VZA because different pixels observe the tops and bottoms of the trees, creating a layover effect, thereby adversely influencing area calculations and potentially obscuring neighboring trees. However, these situations are exploited by algorithms that compute three-dimensional canopies from overlapping images using structure-from-motion, which uses photogrammetric processing to produce three-dimensional point clouds (Strunk et al. 2020; Westoby et al. 2012). Furthermore, such situations might enhance the capability for detecting defoliation in the upper crown and minimizing reflectance from the ground (not trees) (Leckie et al. 2005).

Illumination Geometry

In steep terrain, the slope, aspect, and position of the sun (solar azimuth and zenith angles) combine to illuminate hillsides differently. In the Northern Hemisphere, north-facing slopes appear darker (have lower reflectance) than south-facing slopes because of reduced solar energy per m^2 and more prominent shadows, and because north-facing slopes are wetter and can support denser and therefore darker forests. The use of reflectance ratios, as in spectral vegetation indices, reduces the adverse effects of illumination differences. Topographic corrections have also been developed (e.g. Meyer et al. 1993). Hicke and Logan 2009, with demonstrated variability in the green band associated with solar illumination and in the Red-Green Index in their study of mountain pine beetle outbreaks. As a result, they partitioned the study area into five illumination bins and ran separate classifications for each bin.

Sensor Platforms

Different platforms have been used to assess tree damage and mortality. Imagery and data have been acquired with satellites and airplanes for decades. The U.S. Forest Service has used thermal airborne sensors to map fires since 1962. The agency currently uses Phoenix infrared sensors that can be flown in small aircraft such as the Cessna Citation or the Beechcraft King Air 200.

The Forest Health Protection (FHP) program of the Forest Service has used near-infrared and color imagery to investigate insect activity since the 1970s (Ciesla 2000). The use of hyperspectral imagery to investigate forest health concerns started in 2014 (Cook et al. 2013) and continues to show promise in the FHP detection monitoring workflow (Baeza et al. 2021; Hanavan et al. 2015; Oblinger et al. 2022). Recently, FHP has acquired two Mobile Onboard Terrestrial Hyperspectral whiskbroom scanners (MOTH) with 256 spectral bands and a 0.4–2.5 µm spectral range. These MOTH sensors are capable of near real-time image processing with matched filter and anomaly detection, along with georectified chips and context imagery. Ground-based remote sensing, such as lidar data from terrestrial laser scanning instruments (Atkins et al. 2020) or multispectral data from cell phones (Kälin et al. 2019), are also becoming useful tools.

A newer platform that has become increasingly popular is the UAS. Advantages of UASs include the relatively low cost for the platform and sensors, the ability to be operated by (certified) individuals with minimal training, and the ability to be flown in many locations and situations. Timing of data collection is flexible and can be repeated to fit the research or monitoring question. The rapid development of sensor technology has allowed fine-resolution multispectral, hyperspectral, thermal, and/or lidar sensors to be flown on UASs. Flights can occur under some cloud conditions that would restrict the use of satellites or higher-altitude aircraft. Overlapping acquisitions can permit observations of the three-dimensional (i.e., vertical) structure of a forest from photogrammetric point clouds produced with structure-from-motion algorithms. Studies using UAS data are particularly good for developing and testing sensors and methods (Cardil et al. 2017; Zhang et al. 2018).

Disadvantages of UAS data include the cost of equipment and software and the investment in time and effort to fly the UAS and process the data. A significant disadvantage of UAS data is the limited spatial extent of acquisition resulting from limited battery capacity, flight speeds, and operator time and effort. To make use of UAS data in forested settings despite these limitations, studies have taken a multiscale approach that combines UAS with satellite and sometimes airborne datasets (e.g., Campbell et al. 2020).

Hardware Processing Speed and Turnaround Time

Fast processing by hardware associated with sensors permits more rapid product delivery, important for near-real-time applications. The near-real-time image processing capabilities inherited with the MOTH sensors shows great promise in generating a faster turnaround time on products and more realistic assistance to forest managers. The MOTH sensors have already demonstrated their ability to generate real-time image processing on previous campaigns; FHP's goal is to incorporate these sensors into their detection monitoring program in the coming years. Technology that further enables on-board processing of imagery (Qi et al. 2018). will further reduce time from data acquisition to image utilization.

3.3 Methods

Timing of Data Acquisition

Imagery acquisitions have been timed to occur after trees respond to an attack, which varies by insect or pathogen (Section 2 and table 3). Trees killed by bark beetles often turn red in the year following attack; mid- to late summer image dates maximize capturing this response (e.g., Meddens et al. 2013). Defoliators feed in late spring or early summer, and trees appear reddened or brown by mid-summer. Therefore, mid-summer images are useful for mapping current-year defoliation (e.g., Bhattarai et al. 2020). A winter acquisition with snow on the ground allows the understory to be masked, increasing the amount of snow visible when the crown is defoliated or in the gray stage following beetle attack. Baker et al. (2017) calculated wintertime subpixel viewable gap fraction from MODIS products using spectral mixture analysis, which yielded high R^2 values of 0.92 compared with a Landsat-based classification of tree mortality.

Single or Multiple Images Used

Single images or multiple images have been used for mapping damage or mortality. Classifications have used single images when attacked trees were easily separated from healthy trees, as when trees turned red following bark beetle attack and the severity (per-pixel fraction of killed trees) was high (e.g., Hicke and Logan 2009; Meddens et al. 2011). Studies of more subtle trees responses, such as defoliation (e.g., Donovan et al. 2021), or less severe outbreaks (for instance, when using coarser resolution imagery; Spruce et al. 2019) have used change detection (two images from before and after the damage).

Time series of imagery have been used in multiple studies of forest disturbances. Time series have been constructed using one image per year, often chosen to occur after the tree damage has become most apparent and for scenes with minimal cloud cover, haze, and smoke (e.g., Meddens et al. 2013) Time series analysis can take advantage of a number of years prior to an outbreak to establish the spectral variability of healthy trees (Meddens et al. 2013) (fig. 7). Other time series-based algorithms have been developed that calculate a set of metrics from spectral trajectories of moderate-resolution imagery time series for use in identifying disturbance onset, magnitude, and recovery, including, e.g., Landsat-based detection of Trends in Disturbance and Recovery (LandTrendr) (Kennedy et al. 2010), Continuous Change Detection and Classification (CCD) (Zhu and Woodcock 2014), and Vegetation Change Tracker (VCT) (Huang et al. 2010). Recent studies have demonstrated increased disturbance detection accuracies with ensemble approaches, in which results from various time series algorithms are combined (Cohen et al. 2018; Healey et al. 2018). These methods have been applied to detect (tables A.2, A.3) and attribute (table A.5, Section 4.5) biotic disturbances.

Recent studies have taken advantage of intra-annual imagery (i.e., multiple images per year) in remote sensing applications. Use of more frequent imagery allows for improved detection of short-duration disturbance events (aiding attribution, for instance), a higher probability of finding cloud- and haze-free scenes for analysis, and earlier detection of tree damage and mortality (Zhu et al. 2022). The additional images provided by intra-annual imagery can lead to high accuracy for mapping disturbances (Koltunov et al. 2020; Ye et al. 2021). The ForWarn system (Hargrove et al. 2009; https://forwarn.forestthreats.org) uses 250-m MODIS NDVI data to provide early detection of disturbances based on anomalies relative to long-term mean values. ForWarn products are produced every eight days, are available online (https://forwarn.forestthreats.org), and have been used for multiple biotic and abiotic disturbance events (https://forwarn.forestthreats.org/disturbance-events). Mulverhill et al. (2023) used a harmonized Landsat Sentinel-2 time series together with a change detection algorithm to demonstrate continuous monitoring and early warning of non-stand-replacing disturbances.

Although using a time series of moderate-resolution imagery can increase detection accuracy (Meddens et al. 2013), reliable detection of lower severity damage with such data (<50% of a pixel) remains a challenge (Meddens et al. 2013; Rodman et al. 2021) (fig. 7).

A

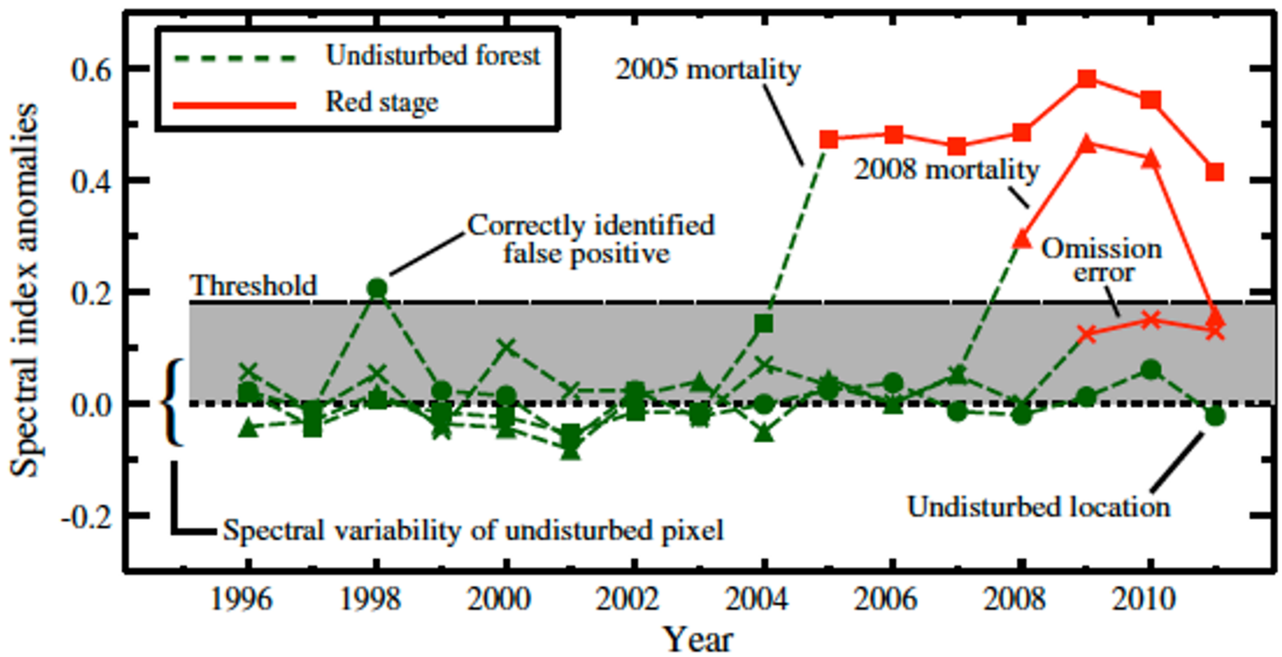

B

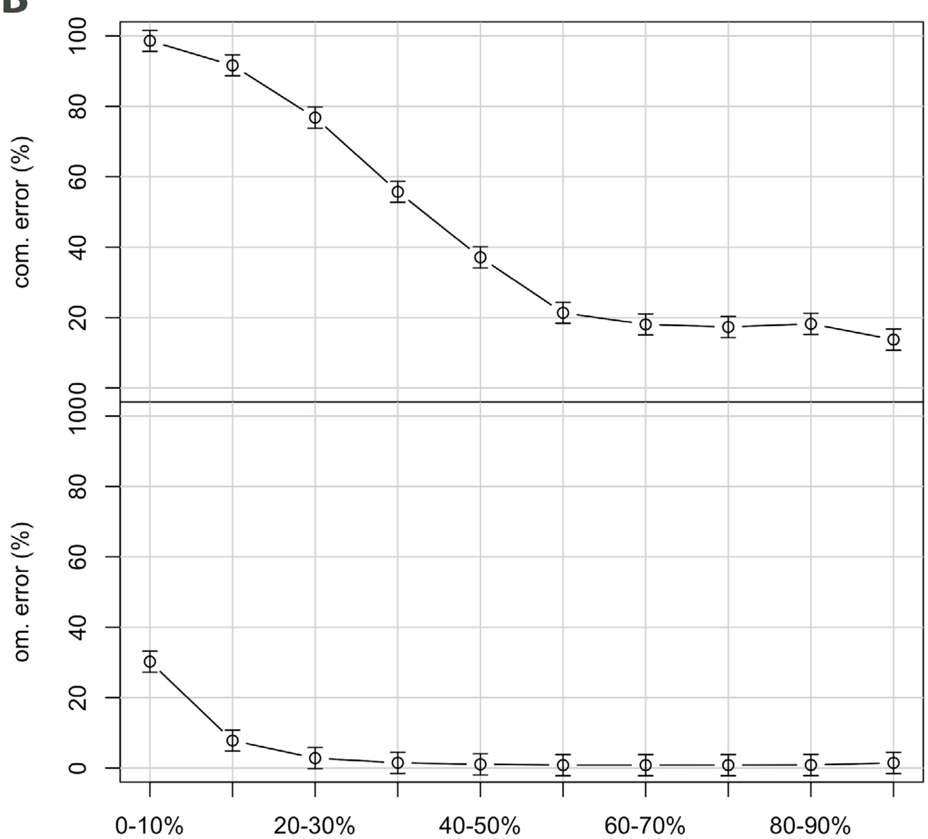

Figure 7A-B—Methods and results from studies using Landsat to map a mountain pine beetle outbreak in lodgepole pine in Colorado. (a) Use of time series of a spectral index for classifying tree mortality. Licensed figure by Elsevier, from Meddens et al. 2013. (b) Omission ("om.") and commission ("com.") errors of the disturbed tree class as a function of the percentage of pixel that is occupied by killed (red) trees (determined using a finer-resolution aerial image). Licensed figure by Elsevier, from Meddens et al. 2013.

C

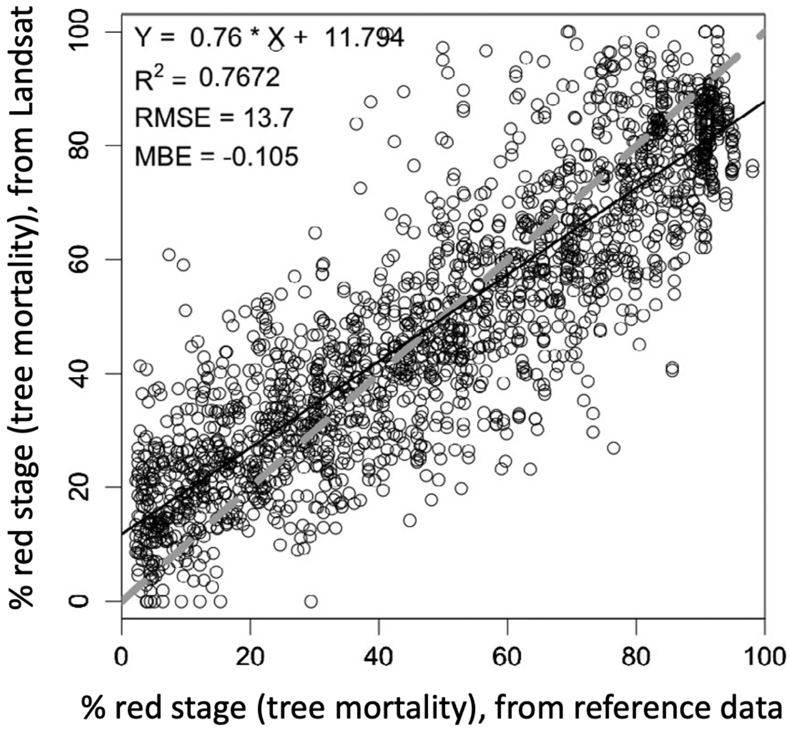

D

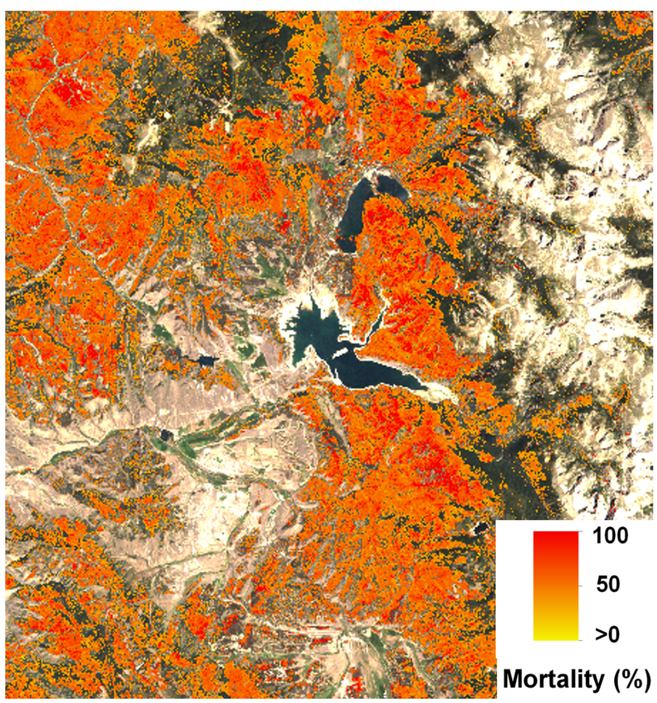

Figure 7C-D—Methods and results from studies using Landsat to map a mountain pine beetle outbreak in lodgepole pine in Colorado. (c) Comparison of regression model estimate of percent of a pixel in red stage (y-axis) and independent reference data (x-axis). Licensed figure by Elsevier, from Meddens and Hicke 2014. (d) Resulting cumulative percent mortality after applying regression model for part of the study area. Licensed figure by Elsevier, from Meddens and Hicke 2014.

Damage or Mortality Metric

Classification methods assign one of a set of non-forest (e.g., herbaceous vegetation) and forest type (e.g., green/heathy, red stage/killed) classes to individual pixels (e.g., Hicke and Logan 2009) or objects (groups of pixels representing, e.g., tree crowns) (e.g., Oblinger et al. 2022). Some studies have used continuous metrics, including the fraction of killed trees within a pixel (Meddens and Hicke 2014; Steel et al. 2023) (fig. 7) or amount of defoliation (Thapa et al. 2022). Continuous damage metrics such as amount of defoliation may also be assigned to one of a few levels of defoliation (e.g., Bhattarai et al. 2020).

Spatial Resolution of Object of Interest

To date, most studies have used pixel-based mapping of damage or mortality. In contrast, some studies that used imagery at much finer resolution than a tree crown area (1–2 m) have analyzed objects (trees). Segmentation of imagery into trees is accomplished with either spectral data (Chen et al. 2019; Erikson 2004; Guo et al. 2007; Huang et al. 2018; Lassalle et al. 2022; Näsi et al. 2015) or three-dimensional crown shapes derived from lidar data (Jakubowskiä et al. 2013; Li et al. 2012), or structure-from-motion data (Cardil et al. 2017; Minarik et al. 2020), or a combination of lidar and spectral data (Dalponte and Coomes 2016; Oblinger et al. 2022).

When using fine-resolution imagery, differences in reflectance can occur for sunlit versus shaded parts of one tree, making identification of a killed tree challenging (Meddens et al. 2011) (although the active nature of lidar data avoids this problem). Studies have addressed this issue by using the brightest pixels within a tree for classification (Cessna et al. 2021; Leckie et al. 2004). Other challenges of defining objects (trees) include using a canopy height model to separate trees in dense canopies (Sparks et al. 2022), occlusion of the lower parts of crowns by the upper crown (as in lidar data) or by neighboring trees (Lindberg and Holmgren 2017), and separating understory trees from overstory trees (Cao et al. 2023; Dalponte and Coomes 2016; Reitberger et al. 2009).

Reference Data for Model Development and Evaluation

Studies have assembled reference data for model training and testing from a variety of sources. Many studies have used field measurements of damage or mortality, which provide high-confidence reference data (e.g., Das et al. 2022; Meddens et al. 2011), but are costly in terms of time and effort of collecting data. Furthermore, plot sizes should approximate image pixel sizes and account for image geolocation accuracy and pixel footprint after reprojection. Some studies have used products from imagery at finer spatial resolution as reference data (Campbell et al. 2020; Hart and Veblen 2015, Schwantes et al. 2016). For instance, in their study of Landsat imagery, Meddens et al. (2013) used a 2.4-m classified image (itself trained and tested with field measurements; Meddens et al. 2011) for reference data. Aerial surveys have been used as reference data (e.g., Franklin et al. 2003; Rahimzadeh-Bajgiran et al. 2018), although these have important considerations (table 1).

In situations when the spatial resolution of the imagery allows for the detection of individual trees, or when damage occurs for a large fraction of a pixel, changes in reflectance have allowed scientists to develop reference data sets through on-screen identification or photointerpretation of affected pixels (e.g., Bright et al. 2020; Hicke and Logan 2009). Such an approach is especially useful when an analyst can use true-color imagery to separate damaged or killed trees from healthy vegetation. Confidence in this method has been demonstrated by including example zoom images (Bright et al. 2020; Hicke and Logan 2009). Trees in the gray stage following bark beetle attack or that have been defoliated have been identified in this manner, although the signature can be less clear than with red trees (e.g., Bright et al. 2020).

Statistical or Analytical Method

Studies have used different approaches to identify damage or mortality from biotic agents. Many studies have classified pixels or objects in one of several classes, one or more of which is associated with biotic agents. Traditional and well-established classification algorithms have been employed, such as maximum likelihood (e.g., Hicke and Logan 2009). More recent studies have used other classification algorithms, including random forest, support vector machines, and neural networks and convolutional neural networks. Studies comparing these algorithms for mapping biotic disturbances have reported only marginal differences in accuracy. For example, Donovan et al. (2021) and Bhattarai et al. (2020) reported that random forests produced slightly higher accuracies than support vector machines, and Gao et al. (2023) reported that a convolutional neural network yielded slightly higher accuracy than a random forest classification.

Regression methods have also been used to map continuous metrics of damage or mortality. Meddens et al. (2014) used multiple linear and generalized additive models to estimate the fraction of bark beetle-caused tree mortality within a Landsat pixel. Thapa et al. (2022) used linear, nonlinear, and mixed-effect models to estimate defoliation severity caused by spruce budworm (*Choristoneura fumiferana*) and jack pine budworm (*Choristoneura pinus*).

Spectral mixture analysis (SMA) retrieves the fractional contribution of individual classes from a pixel's reflectance spectrum (or bands). Classes can represent green vegetation, nonphotosynthetic vegetation (bark, twigs, dry needles), soil, and shadow, among others. The typical reflectance spectra for these classes can be taken from the imagery itself or from spectral libraries. SMA has been used only rarely in studies of damage by biotic agents. Radeloff et al. (1999) unmixed Landsat Thematic Mapper reflectances to shade, green vegetation, and nonphotosynthetic vegetation end members, and found a strong negative relationship between green vegetation and populations of jack pine budworm.

Evaluation Method

Evaluations of results have taken different forms. Commonly used approaches for classifications (categorical data) have included confusion matrices that provide omission and commission errors for each class and overall accuracy (e.g., Meddens et al. 2011), possibly using area-weighted errors (Olofsson et al. 2013). For continuous variables, comparisons of predicted values against reference data have been reported; metrics have included the linear regression equation, R^2, root-mean-squared error (RMSE), and mean bias error (MBE) (e.g., Meddens and Hicke 2014). Resampling or cross-validation to produce multiple models for evaluation against withheld test data has been commonly used in studies (e.g., Meddens et al. 2011). For spatial resolutions coarser than 1-4 m, several issues may hinder comparing pixel-level results against field measurements, including errors in field-measured coordinates, or image georegistration, or possible tree distortion from high VZA. Adding a buffer to field points is one solution (Hicke and Logan 2009; White et al. 2005).

Software Processing and Turnaround Time

Faster production of results is assisted by rapid preprocessing and availability of input remote sensing products (e.g., surface reflectance), fast analysis and evaluation of results, and established workflows that aid subsequent application. Generation of products for mapping and monitoring tree damage and mortality can be greatly facilitated by using preprocessed imagery.

Radiometric calibration, geo- or co-registration of images, and conversion from digital numbers to reflectance are important processing steps. Analysis time may be shortened by using established products, such as surface reflectance or vegetation indices from MODIS or Landsat or other derived attributes of forest ecosystem structure or function such as leaf area index or surface temperature (Bright et al. 2013). Relatively rapid preprocessing of imagery is facilitated by Google Earth Engine (GEE) and for MODIS/VIIRS specifically by the NASA Land, Atmosphere Near-real-time Capability for EOS (LANCE) project.

Analyzing imagery has become easier and more rapid (2–3-week latency for Landsat imagery) with the development of GEE, a cloud-based platform. The GEE platform provides easy and efficient access to a large repository of relevant remote sensing data and allows scientists to access, process, and analyze this imagery with high-performance computing (Gorelick et al. 2017). By negating the need for large local storage and CPU capacity, GEE facilitates the processing of remotely sensed datasets across regional to global spatial extents in significantly shorter time frames than previously possible (Amani et al. 2020; Pérez-Cutillas et al. 2023). Commonly used algorithms in forest disturbance studies, such as LandTrendr have been implemented on GEE and applied to mapping insect outbreaks (Bright et al. 2020; Rodman et al. 2021).

The NASA LANCE project provides near-real-time Level 0–3 MODIS and VIIRS data, generally within three hours of satellite data acquisition (Zhang et al. 2022). Vegetation indices produced from NASA LANCE data in the continental U.S., including NDVI and the vegetation condition index (VCI), can be applied to detect forest disturbances at rapid turnaround times.

Finer resolution imagery is typically commercial, is tasked to acquire specific targets, and is not as available as coarser resolution imagery. This imagery still requires substantial preprocessing and analysis. Recent advances include an application program interface (API) for orthorectifying and calibrating imagery to top-of-atmosphere reflectance and image stitching of very high-resolution satellite imagery (Neigh et al. 2019), and a new NASA portal (Global Imagery Browse Services (GIBS)—www.earthdata.nasa.gov/eosdis/science-system-description/eosdis-components/gibs—for browsing and downloading imagery within a few hours of satellite image acquisition.

Combining Multiple Remote Sensing Data Types

Merging different remote sensing data sets with different spectral, spatial, and/or temporal characteristics can improve detection and attribution of forest disturbances (Gao et al. 2015), although few studies have directly addressed insects or diseases. Combining the fine resolution but limited frequency and extent from 6.5-m RapidEye images with coarser resolution, but repeated Landsat imagery led to higher accuracies of detection of defoliation of sparse broadleaved trees in Asia (Gärtner et al. 2016). Harmonized Landsat-Sentinel-2 imagery (Claverie et al. 2018) was used to detect different disturbance types (including insect outbreaks) in Canada with high accuracy (Mulverhill et al. 2023). Canopy defoliation was quantified in eastern oak forests using a combination of hyperspectral imagery and lidar (Meng et al. 2018) and estimates of leaf area index and basal area related to outbreaks of eastern spruce budworm were made using a combination of optical and synthetic aperture radar (SAR) imagery (Bhattarai et al. 2022).

Other approaches combined hyperspectral or multispectral data (used to identify damaged or killed trees) with lidar or structure-from-motion data, which were used to delineate tree crowns for object-oriented classification (Campbell et al. 2020; Cessna et al. 2021; Navarro-Cerrillo et al. 2019; Oblinger et al. 2022) (fig. 4) or as a forest mask (Kantola et al. 2016). Lidar returns may also help with classification via structural metrics (Navarro-Cerrillo et al. 2019) or apparent reflectance in the SWIR range (Cessna et al. 2021).

Including Ancillary Data

Data sets not directly related to damage or mortality caused by biotic agents have been used in detection or attribution studies. Land cover (forest and non-forest classes), forest type, or tree species data sets focus remote sensing efforts on forests or particular tree species and have aided attributing a disturbance to a particular damage agent (e.g., He et al. 2019; Schleeweis et al. 2020; Senf et al. 2015). Aerial survey products provide information about both tree species and insect or disease damage, thus adding information to disturbance locations mapped with remote sensing (Meigs et al. 2015). Wildfire information (burned area perimeters, severity) has been used for identifying fires (Schroeder et al. 2017). Other factors that influence insect or disease outbreaks, such as topography or climate, have been included to improve mapping accuracy (e.g., Campbell et al. 2023; Kennedy et al. 2015).

4. Applications of Remote Sensing

In this section we apply our framework to examples of insect and diseases in the western United States and discuss the application of remote sensing technologies and methods to the detection and attribution of tree damage or mortality caused by insects and diseases. Within groups of biotic agents, we list the tree, stand, and landscape responses that have been exploited and describe examples of published case studies.

4.1 Bark Beetles

Outbreaks of bark beetles have been reported extensively by remote sensing studies. Multiple characteristics of bark beetle outbreaks allow for higher accuracy in remote sensing studies. Many tree species killed by bark beetles turn red, providing a strong contrast to healthy, green trees. Attacks by some bark beetle species in some locations (e.g., spruces killed by spruce beetle in the Rocky Mountains of the conterminous U.S.) can cause host trees to turn yellow or yellow-green instead of red, a more challenging detection scenario based on visible wavelengths alone. Foster et al. (2017) found that the Red-Green Index was able to differentiate attacked from unattacked spruces in this area, but with lower accuracy than from NIR and SWIR reflectances.

Because many important bark beetle species typically kill trees, the whole crown changes, making detection easier compared with the responses to other biotic agents that may result in changes in only part of the crown. The killed trees are permanent (i.e., do not recover) and progress from red to gray. This facilitates detection of past beetle attacks, in contrast with other biotic agents, which may cause only temporary damage. Trees in the gray stage present a more subtle visual change from healthy trees than red trees but are still detectable (Hart and Veblen 2015; Meddens et al. 2011).

Changes in the internal structure of needles and decreases in canopy water content also occur following a bark beetle attack. These changes have been exploited in studies using visible reflectances (e.g., RGI) and indices calculated from multiple spectral regions (e.g., NDVI, NBR, Tasseled Cap). Studies have reported moderate to high overall and class accuracies of bark beetle outbreaks (Hall et al. 2016). Images from a single date as well as from time series have been used, with a comparison revealing similar accuracies (Meddens et al. 2013).

Studies have mapped red and gray stages using a variety of sensor resolutions. Higher accuracies were achieved with very fine aerial (e.g., Meddens et al. 2011) and satellite (e.g., Hicke and Logan 2009; White et al. 2004) imagery. Accuracies with 30-m resolution imagery can also be high if the outbreak is sufficiently severe (Meddens et al. 2013) (fig. 7b). Bark beetle outbreaks can kill a large fraction of trees in a stand, and tree mortality can be extensive across the landscape; both characteristics facilitate detection by coarser resolution imagery such as 250-m MODIS data (Spruce et al. 2019).

Meddens et al. (2013) used Landsat imagery following bark beetle outbreaks to assess class errors as a function of the percentage of a pixel covered by red-stage trees. They found that omission and commission errors were below 20 percent when 60 percent or more of a pixel was occupied by killed trees (fig. 7b). We speculate that this result is likely to be resolution-independent as well as disturbance type-independent, thereby providing guidance about the resolution required to detect a disturbance of a specified severity with a desired accuracy.

Bark beetle outbreaks have killed trees in woodlands across large areas (e.g., piñon pines killed by piñon ips; Hicke et al. 2020). These situations can be challenging for detection because of the low tree density and bright, often reddish, soil reflectance that are apparent between trees (Ciesla et al. 2015). However, studies using both fine (2.4 m; Clifford et al. 2011) and coarser (30 m; Schwantes et al. 2016) satellite imagery achieved higher accuracies of detection of dead trees in these environments.

Using remote sensing to map green-attack trees (also known as previsual conditions) is very attractive to scientists and managers because it allows for early detection of outbreaks. An early review of this topic (Wulder et al. 2009) identified several factors that limit using remote sensing to detect green-attack, including uncertainty in timing of bark beetle attacks and infestation periods, necessity of timing the remote sensing acquisition with tree responses and favorable weather conditions, and the need for finer spatial and spectral resolution to separate green-attack from healthy trees.

Since Wulder et al. 2009, advances in methods have allowed studies to take advantage of the early tree responses (reduction in canopy water content or increase in canopy temperature) (Heller 1968). The NIR and SWIR reflectance and related vegetation indices (e.g., the Normalized Difference Water Index) are the most important shortwave bands for detecting green attack because of their sensitivity to needle water content and pigmentation (Abdullah et al. 2019b; Bárta et al. 2021; Foster et al. 2017; Mandl and Lang 2023). However, Zabihi et al. (2021) noted that compared to visible reflectance, these longer wavelengths have higher variability related to leaf physiology, tree species diversity and age, and season, contributing to increased uncertainties in models used to detect green-attack trees.

Studies have assessed multiple spatial resolutions in green-attack studies. Abdullah et al. (2019b) have shown higher accuracies of green attack detection using Sentinel data (67 percent of classified pixels matched the reference pixel data set) compared with Landsat data (36 percent accuracy). Immitzer and Atzberger (2014) used all eight bands of 2-m WorldView-2 multispectral imagery to classify healthy, green-attack, and dead trees, achieving an overall accuracy of approximately 75 percent averaged among three images. Ortiz et al. (2013) used SAR and RapidEye multispectral imagery for early detection of green-attack, reporting higher classification accuracy with data from both sensors than for data from either sensor alone (Ortiz et al. 2013). Niemann et al. (2015) used fine-resolution hyperspectral (2-m spatial resolution, 2.5 nm and 5.6 nm spectral resolutions) and lidar data with to show differences in spectral absorption by needle pigments of green-attack trees compared to healthy and red trees.

Recently, UASs have been used for multispectral and hyperspectral remote sensing of green-attack. For European spruce bark beetle attacks in Norway spruce, Huo et al. (2023) reported a green-attack detection accuracy of 15 percent at 5 weeks after initial infestation, when the red-edge and green bands showed significant differences, and 90 percent at 10 weeks, when the red band showed significant differences. Cessna et al. (2021) integrated multispectral imagery and structure-from-motion point cloud data from a drone as well as point cloud data from the NASA G-LiHT sensor to detect green-attack. Spectral-structural fusion models resulted in higher overall accuracy (~78 percent) than a spectral-only (~59 percent) model and slightly higher accuracy than a structural-only model (~76 percent).

Studies of green-attack have also used thermal information from handheld and satellite-based sensors. Majdák et al. (2021) reported that trunk temperatures of bark beetle-infested trees in the interior and edges of forest stands were significantly higher than uninfested trees measured using a handheld thermal sensor. Abdullah et al. (2019a) showed that canopy surface temperatures derived from Landsat-8's TIR sensor were more important than vegetation indices for detecting previsual conditions.

4.2 Defoliators

Trees damaged by defoliating insects can be more challenging than bark beetle outbreaks for detection and attribution by remote sensing because a range of defoliation conditions (defoliation severity, and mortality versus recovery) can occur. Defoliation can cause parts of or the entire tree crown to appear gray or reddish-brown. Severe defoliation can cause tree mortality and may turn any remaining foliage red. Light or moderate defoliation makes detection difficult, and trees can recover after defoliation. As with bark beetles, changes in tree color, needle structure, and canopy water content have been utilized in remote sensing studies of defoliation. Published studies about defoliators have used multispectral imagery, and most have relied on change detection compared with a pre-outbreak scene.

In contrast to studies of bark beetle outbreaks, studies of defoliator outbreaks in the western U.S. or North America are few; we found only three (table A.2). Meigs et al. (2011) compared Landsat time series metrics to aerial surveys and field observations, finding that western spruce budworm exhibited long, slow outbreaks. Meigs et al. (2015) used Landsat imagery to refine western spruce budworm outbreak locations within polygons mapped by aerial surveys. Senf et al. (2015) investigated western spruce budworm outbreaks in British Columbia, Canada, finding class omission and commission errors of 10–11 percent.

We also reviewed remote sensing studies from eastern North American conifer forests for defoliator species related to those in the western U.S., including spruce budworm, jack pine budworm, and hemlock looper (table A.2). The defoliator outbreaks in eastern North America provide useful information because insect and trees species and tree responses are similar to those in western North America. Studies addressed either annual or cumulative (multiyear) defoliation and typically used multidate change detection. Detection (presence/absence) accuracies were higher (table A.2), and as expected, accuracy decreased when multiple levels of defoliation severity were evaluated. Goodbody et al. (2018) found that spectral metrics were more effective at identifying defoliation severity than structural metrics. Thapa et al. (2022) used winter imagery to enhance the sensitivity to budworm defoliation. Most studies used Landsat imagery and had moderate classification accuracies. Studies that used finer resolution imagery reported a higher R^2 value (Goodbody et al. 2018) or classification accuracy (Leckie et al. 2005).

4.3 Sucking Insects

Tree responses to the major sucking insect species in the western U.S., balsam woolly adelgid (BWA), range from subtle to substantial. The subtle responses include gouting or crown deformities, which may affect only parts of a host tree, posing significant challenges for remote sensing. The more substantial signal of tree mortality, which results in changes in needle color and subsequent needlefall, is easier to detect, yet may only occur in severe outbreaks or potentially after years of attack.

Two remote sensing studies of BWA in the western U.S. have been published. Cook et al. (2010) used a handheld spectroradiometer to separate branches from infested and uninfested trees with a classification accuracy of 93 percent. Campbell et al. (2023) developed models of field-observed BWA damage severity in Utah using only Landsat satellite imagery, using only climate and terrain data, and using both. With cross-validation, they found that the satellite-only model produced moderately accurate models (R^2=0.54 and RMSE=0.11 (range of 0–1)), and the climate-only and combined data produced more accurate models. The lower accuracy of the satellite-based model may have occurred because of the coarse spatial resolution relative to the within-pixel extent of damaged trees or because of the subtle signals of field-measured damage (e.g., gouting, deformities).

Multiple studies of BWA in eastern North America, as well as of hemlock woolly adelgid (*Adelges tsugae*, HWA), a related species also found in eastern North America, have addressed damage in conifer stands (table A.3); these studies are likely applicable to BWA in the western U.S. Most studies used change detection, either over time or among damage or infestation amounts. Studies used multispectral (Landsat or airborne) or airborne hyperspectral imagery to relate to adelgid-caused damage, with high R^2 values. Studies that used imagery to classify into presence/absence or multiple damage levels reported higher accuracies for presence/absence or fewer classes or for finer resolution imagery, and lower accuracies for multiple damage levels or for coarser resolution imagery (e.g., Landsat). Terrestrial or airborne lidar data were used to assess the canopy structural changes from HWA damage.

4.4 Diseases

As with defoliators and sucking insects, tree diseases cause a range of symptoms with a range of severities. Reduced growth, crown deformities, and crown thinning are subtle signals difficult for remote sensing studies to identify, especially when coupled with low severity and/or chronic damage. Trees killed by diseases can have identifiable responses. One signal of root diseases in conifer-dominated forests is the expanding circles of damage and the distinct pattern of treefall, with the oldest damage and downed trees in the center and the newest damage on the perimeter. However, although this signature is readily observable on imagery (Heller and Bega 1973), its progression is slow and of low severity, making detection of new damage by moderate resolution imagery challenging. Thus, existing studies have typically used high-resolution imagery for disease detection (table A.4).

Only three studies used remote sensing to detect disease in conifer-dominated forests in western North America, one for Armillaria (Oblinger et al. 2022), one for laminated root rot (Leckie et al. 2004), and one for white pine blister rust (Hatala et al. 2010) (table A.4). Moderate to high accuracies were achieved for multiple classes of damage severity, with more difficulty detecting low-severity damage (as expected). Studies of forest diseases on other continents reported similar accuracies for classifications. One study reported an R^2=0.74 when comparing the change in NDVI of gray dragon spruces (*Picea asperata*) that were damaged by *Lophodermium piceae* (Luo et al. 2022). As expected, studies reported higher accuracies with fewer classes (e.g., live versus dead) and greater confusion between neighboring classes when more classes were included, especially those classes with light damage. As with other damage agents, combining spectral data from passive imagery with point cloud data from laser scanning increased classification accuracies and made classification of individual trees possible across small spatial extents (Dalponte et al. 2022; Oblinger et al. 2022; Yu et al. 2021a).

Forest pathologists have an increased interest in using remote sensing methods to detect signatures not capable of being detected with visual survey methods. Large-scale, landscape-level events such as oak decline (*Phytophthora ramorum*), oak wilt (*Bretziella fagacearum*), and Rapid Ohia Death (*Ceratocyctis* fungi) have resulted in an increased demand for detection monitoring efforts that can map the extent and severity of these fungal events. Combinations of field-based leaf spectroscopy, laboratory-based chemical analysis, and airborne remote sensing have shown promise for mapping these and other forest diseases (Crocker et al. 2023; Perroy et al. 2020; Sapes et al. 2022).

4.5 Attribution

In the context of this document, we use “attribution” to mean identifying the cause of detected disturbances (e.g., separating wildfire disturbances from bark beetle disturbances). To date, almost all effort and studies have addressed the detection, not attribution, of insect or disease damage. This is understandable given that detection itself is challenging, and attribution studies that separate biotic and abiotic disturbances pose additional difficulties. Tree damage or mortality from insects or diseases can be less severe (number of damaged trees per area), slower, or longer in duration within a stand or pixel than other disturbance types such as wildfire or logging, suggesting differences that might be exploited by attribution studies (Stahl et al. 2023). Because of possibly lower severity and, for some biotic agents such as bark beetles, the preference for larger trees and thus avoidance of smaller trees, recovery at the stand level can be faster than assumed for biotic disturbances in some attribution studies. Thus, outbreaks are highly variable in terms of severity, duration, and rates of damage and recovery within a stand or pixel (fig. 3), leading to difficulties in making assumptions about spatial or temporal characteristics for use in attribution.

We reviewed and analyzed published studies that used automated methods and remotely sensed imagery to make predictions about attributing forest disturbances to insects or diseases. We were interested in studies that distinguished these biotic disturbance agents from other abiotic disturbance agents such as wildfire or harvest or that separated different types of biotic agents. We selected studies that included insects from a recent review of studies of biotic and abiotic forest disturbances (Stahl et al. 2023), and we added articles following an updated literature search. We identified a total of 18 studies that addressed attribution to biotic agents (table A.5). All studies addressed insect outbreaks; no attribution study looked at diseases explicitly, although some Study Type 1 studies (next paragraph) mentioned diseases as part of their lumped category.

We categorized studies by specificity of biotic agent, identifying three “Study Types” that ranged from very general (Study Type 1) to very specific (Study Type 3). The nine studies in Study Type 1 lumped insect outbreaks into a more general class (e.g., “stress”, “non-stand-replacing”, “other”) that also included other disturbance types such as drought, harvest, and wildfire, depending on the study. Often these studies spanned a large geographic extent and thus needed to account for many types of forest disturbance.

We found seven studies that either addressed only one insect species or lumped all insect species into one class, and attributed forest disturbances to that insect class versus other classes such as fire or harvest (Study Type 2). An additional two studies distinguished different insect species (Study Type 3). Ahmed et al. (2017) separated disturbances caused by spruce budworm (*Choristoneura griseicoma*) from forest tent caterpillar (*Malacosoma disstria*) as well as including other five other (non-insect) classes. Senf et al. (2015) separated insect disturbances from harvest and wildfire, then distinguished western spruce budworm disturbances from mountain pine beetle disturbances in a second step.

All studies used Landsat time series as the remote sensing imagery; some studies added ancillary data sets in their classification such as topography. Typically, disturbance algorithms such as LandTrendr (e.g., Senf et al. 2015), Vegetation Change Tracker (e.g., Zhao et al. 2015), or Continuous Change Detection and Classification (e.g., Zhang et al. 2022) were used to identify breaks and segments in the pixel-based time series, which were then used in a classification of disturbance types. These algorithms have been used in attribution of insect and disease outbreaks by noting that different disturbance types (biotic and abiotic) have different typical signatures of the trajectory metrics (Coops et al. 2020; Meigs et al. 2011). These attribution studies assume that some disturbance types such as wildfire or harvest induce rapid changes in reflectance or spectral indices. Biotic disturbance types (which are often lumped in with types in a “stress” or “non-stand-replacing” type) are assumed to be slow, multiyear disturbances (e.g., Moisen et al. 2016).

Other studies, however, have illustrated variability in disturbance characteristics within and among biotic agents (Foster et al. 2022; Goodwin et al. 2008; Meigs et al. 2011) (fig. 3). Tree mortality from bark beetles is typically widespread but slow-moving, and of low severity, but occasionally, outbreaks cause rapid, high-severity tree mortality (Cole and Amman 1980; Hicke et al. 2020; Meddens and Hicke 2014). Defoliation is assumed to be a long, slow process, but outbreaks of defoliator species in the western U.S. can be short (1–4 years) and severe (table A.1) (Foster et al. 2022). These assumptions about the dynamics of different biotic (and abiotic) disturbance types are also influenced by severity within a remote sensing pixel and are therefore scale-dependent: pixels at coarser resolutions experience lower severity and longer outbreaks (Meddens and Hicke 2014).

The above studies reported a range of omission and commission errors (<10% to >80%) for insect-caused tree damage (fig. 8). Studies in Study Types 1 and 2 spanned this range, and error rates were likely dependent on which classes were included, the type of reference data, and the number of reference data points. The two Study Type 3 studies had class error rates of 5-40%. Variability in the temporal characteristics of insect outbreaks, as noted above, likely contributed to the range of error values. Furthermore, the spatial variability in severity of tree damage or mortality from insects may have posed challenges to classification algorithms. Finally, the grouping of disturbance types was also probably important in determining errors. For example, grouping outbreaks with wildfire in one class for comparison with urbanization, or lumping all insect species into one class, may have increased within-class variability and therefore increased omission and commission errors as compared with a situation in which each disturbance type was put into a separate class. It is possible that more refined groups of disturbance types would result in lower errors; whether grouping types increases or decreases errors depends on the variability of explanatory variables (remote sensing inputs) within groups (classes).

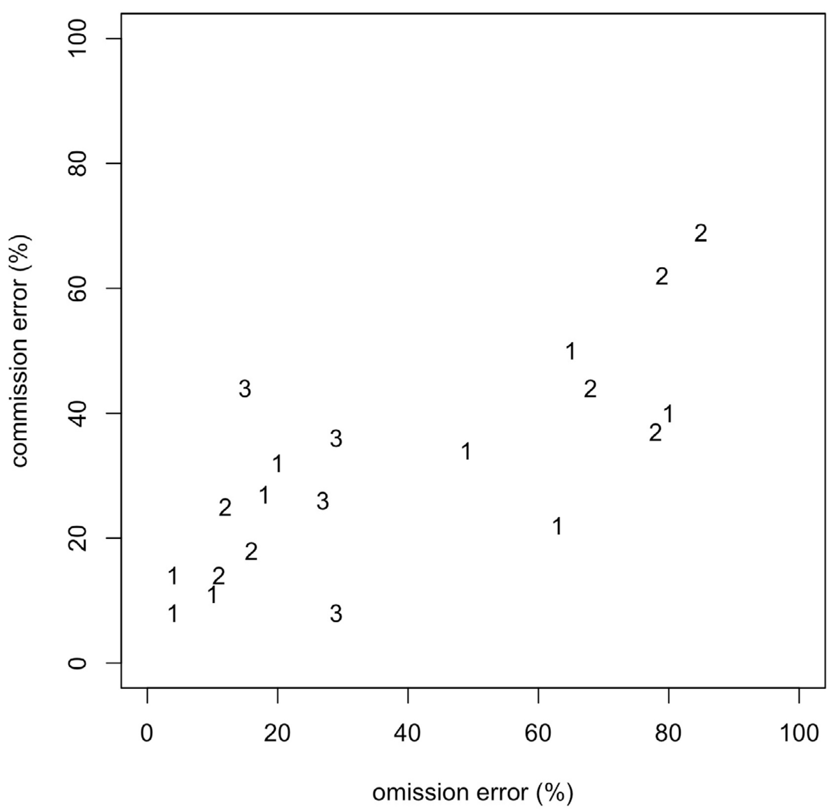

Figure 8—Omission and commission errors of classes associated with biotic agents reported by attribution studies (table A5); number indicates study type (Type 1: studies that lump insects with other disturbance types; Type 2: studies that separate one insect guild/species class from other disturbance types; Type 3: studies that separate >1 insect guild/species). Errors are for insect classes only. The two Study Type 3 studies (Ahmed et al. 2017 and Senf et al. 2015) reported errors for two insect species each. Havašová et al. 2017 and Schroeder et al. 2017: representative values from different years or scenes. Oeser et al. 2017: values from all-site model.

Another form of attribution has been achieved by combining aerial surveys, which provide information about host tree species and biotic agent, with remote sensing products, which could refine the spatial resolution of the damage and fill in temporal gaps. Meigs et al. 2015 combined Landsat imagery with aerial surveys to study mountain pine beetle and western spruce budworm outbreaks in Oregon and Washington. The aerial surveys were used to identify locations of these outbreaks and separate species, and the Landsat imagery provided finer-resolution mapping within survey polygons.

5. Knowledge Gaps and Opportunities

Despite decades of research, a number of knowledge gaps and opportunities exist for advancing remote sensing of insect and disease outbreaks (table 6). We highlight opportunities for significantly advancing our understanding (potential priority investments) in bold in table 6.

Table 6—Knowledge gaps and opportunities. Bold text indicates potential priority investments.

Knowledge gaps and opportunities	Description
Insects and diseases	Progression of tree responses; **additional remote sensing studies in western U.S. of defoliators, sucking insects, and diseases, including across severities and of incipient populations**
Subtle tree damage	**Ability of remote sensing to capture crown thinning and deformities, top-kill, flagging, etc., from defoliators, sucking insects, and diseases**
Early detection and near-real-time mapping	**Detecting green-attack stage of bark beetles; rapid turnaround time from acquisition to map product**
Regional to national maps	**Repeated maps of forest disturbances attributed to insects and diseases (e.g., annually)**
Host tree characteristics	**Maps of tree species and structure that inform susceptibility to insects or diseases for aiding detection and attribution**
Coarse-resolution imagery	Use of 250- to 1000-m imagery, which has the advantages of high revisit rates and multiple products
Viewing geometry and conditions	Detection using high viewing zenith angle or winter imagery
Sensitivity to radiometric normalization	Influence of lack of radiometric calibration on accuracies
Attribution	**Attribution to insect guilds (bark beetles versus defoliators) or species**
Direct sensing of insects	Capability of detecting insects themselves instead of tree responses

Insects and diseases

Although bark beetle outbreaks are well-studied, gaps in knowledge remain that affect remote sensing efforts. Few remote sensing studies exist for defoliators, sucking insects, and diseases in western North America. Case studies of similar biotic agents exist for other regions, and new studies are needed to assess whether the methods used in other regions can be successfully applied in western North America. Studies that address incipient defoliation or bark beetle attack, or the source and spread rate of disease events, will aid monitoring efforts. Assessing accuracies across a range of damage severity (both within individual trees and at stand levels) from biotic agents and for different damage types (e.g., crown thinning or top-kill) will increase understanding (see fig. 7b for an example using bark beetles).

Subtle Tree Damage

Newer remote sensing characteristics (technologies and methods) could be employed to improve detection of more subtle damage such crown thinning and deformities, top-kill, and flagging by defoliators, sucking insects, and diseases. Possible avenues for advancing understanding include using lidar, radar, or structure-from-motion data, perhaps in combination with spectral data, to evaluate the three-dimensional structure changes of the crown (see Section 3).

Mapping damage with structural (or spectral) data could be based on images acquired pre- and post-damage to allow for change detection (Boucher et al. 2020), although repeated lidar or structure-from-motion acquisitions within outbreak areas are uncommon to date. Damaged trees could be mapped with single-date data by, for instance, comparing damaged trees with other undamaged or less damaged trees in the area (Atkins et al. 2020) or by using on-screen interpretation of easily identifiable tree condition classes, as from multispectral structure-from-motion data.

As with whole-tree mortality, flagging may be detectable by needle color change with sufficiently fine spatial resolution (Shrestha et al. 2024). Studies might investigate mapping deformities or thinning using single-date structural data, as is done visually by field crews, although a challenge will be to identify a “normal” crown shape for comparison. Goodbody et al. (2018) used an aerial image and structure-from-motion to show that at a spatial resolution of 20 m, spectral metrics were more sensitive to defoliation severity by spruce budworm than structural metrics. Given the subtleties of these tree responses, future studies could evaluate methods at very fine resolutions, e.g., tree level or finer, or with multidate imagery, which may lead to higher accuracy.

Early Detection and Near-real-time Mapping

Continued advances in early detection and near-real-time monitoring mapping of outbreaks and damage progression with remote sensing would be valuable for forest managers. Progress on detecting beetle-killed trees in the green-attack stage and tree responses to other biotic agents early in the growing season is needed, including additional ecophysiological and remote sensing studies of the progression of tree responses such as transpiration following an attack. Studies that demonstrate capabilities for frequent application over large areas would be useful, and efforts are needed to operationalize these methods when ready. Operational, near-real-time attribution of damage to insect guilds (e.g., bark beetle versus defoliators) or individual species is highly desirable for monitoring. Additional studies and evaluation of methods that use intra-annual imagery may be useful.

Relevant to this topic, significant tradeoffs occur among spatial resolution, spatial extent, and temporal resolution. Satellite instruments with high repeat frequency and greater spatial extent typically have coarser spatial resolution (e.g., the global daily coverage of 250–500-m MODIS imagery, or the 17-day repeat times of 30-m Landsat imagery). However, constellations of satellites, such as Planet DOVE (Dalponte et al. 2023, Trubin et al. 2023) or the planned Landsat Next (landsat.gsfc.nasa.gov/satellites/landsat-next) satellite systems, may address these tradeoffs. There may be potential issues of radiometric calibration and coregistration with these newly available sensors and platforms. However, programs like the Landsat Next mission have been proactive in addressing these concerns because the new Landsat platforms and sensors are designed to ensure continuity with current Landsat and Sentinel sensors and backward compatibility with archival Landsat data (Wulder et al. 2022).

Decreasing the production time of maps of insect and disease disturbances is advantageous for more rapid advancement of scientific understanding as well as for near-real-time monitoring. Long turnaround time on products together with a general sense of overpromising on capabilities have been issues of new technologies. As discussed above, significant advances have occurred in computational capabilities and the availability of moderate- and high-resolution multispectral satellite imagery along with the increased push to integrate sensors into airborne forest health detection monitoring efforts. Continued development of both hardware and software will speed processing and reduce time from data acquisition to image utilization.

Regional to National Maps

A significant objective (and a major challenge) is to provide repeated maps of biotic disturbances at regional to national scales and reasonably fine resolution (10–30 m or finer). Such products could be used retrospectively (for use in subsequent studies of forest disturbance ecology) as well as for seasonal or annual monitoring (e.g., product delivery within several months of the end of the growing season). Additional utility would be achieved if disturbances were attributed (see *Attribution* below). To achieve improved detection and attribution accuracy, spatial resolution finer than 10–30 m would provide more information (e.g., potentially at the tree level). Object-oriented methods are useful when the image spatial resolution is finer than the nominal size of the objects (trees) of interest. Aerial lidar in forests is currently collected at 8–16 points/m2, thus oversampling tree crowns to facilitate object-oriented tree delineation. Such tree-level mapping could improve detectability of attacked trees or the accuracy of agent attribution, especially in conjunction with spectral data.

Other potentially useful remote sensing data sources include Landsat or Sentinel imagery time series, imagery from satellite constellations of fine spatial resolution sensors such as Planet DOVE (Dalponte et al. 2023, Trubin et al. 2023), or airborne imagery from the National Agriculture Imagery Program (NAIP) (USDA:NRCS:Geospatial Data Gateway:Home) (Monahan et al. 2022).

Fixed-wing or hybrid drones are able to cover larger areas than rotor-style drones and may become viable data sources (particularly if collected at key time intervals) to complement other sources in near future (Baena et al. 2018; Fraser and Congalton

2019). Such a national effort would require substantial research and development effort, computer power and storage, and dedication of personnel for operational production.

Host Tree Characteristics

Detection and attribution of biotic disturbances could be improved by incorporating tree and stand information. For example, Senf et al. (2015) found higher attribution accuracies in monospecific stands with only host tree species as compared with mixed species stands. Tree species, size, age, and density influence susceptibility to attack by biotic agents (e.g., Shore and Safranyik 1992). Information about these characteristics could aid detection and attribution by identifying locations that could experience disturbance by a particular insect or pathogen species. Finer spatial resolution is more useful than moderate (e.g., 30-m) resolution, given that many forests contain mixtures of characteristics, and many biotic disturbances are less severe and less apparent at coarser resolutions. Data sets based on imputing field plots are available at 30-m spatial resolution (GNN/LEMMA, lemma.forestry.oregonstate.edu/data; TreeMap; Riley et al. 2021). Repeated maps in time are useful for identifying disturbances, although even one time period can be helpful.

Tree species mapping will aid with detection and attribution of insect and pathogen outbreaks that attack only one or a few host tree species (table A.1). Multiple types of tree species maps are currently or potentially available. Hand-drawn maps of tree species ranges produced using observations (e.g., Little 1971) are available for individual species but have coarse spatial resolution that limit their utility in many disturbance applications. Results of species distribution models developed from observations with climate, topography, or other predictor values representing drivers of ranges can provide finer spatial resolution at more local (e.g., Williams et al. 2017) or more regional scales (e.g., Rehfeldt et al. 2006) scales, but have the disadvantage of predicting potential, not actual, locations of tree species.

Forest type maps, which include one or more species, have been produced (e.g., Ruefenacht et al. 2008) although maps of individual trees species would improve the utility. Studies have modeled individual tree species using climate, soils, and satellite imagery. Examples of larger spatial extents include Bhattarai et al. (2021), who mapped host species of spruce budworm in an area of northern New Brunswick, Canada, the imputation data sets mentioned above, and the National Individual Tree Species Atlas, available at 1–km spatial resolution (Ellenwood et al. 2015). Tree-scale species mapping at moderate to high accuracy has been reported in studies using drones (Abdollahnejad and Panagiotidis 2020), helicopters (Kuzmin et al. 2016), and airborne lidar data (Michałowska and Rapiński 2021) data.

Other tree or stand characteristics contribute to susceptibility to attack. Bark beetles attack older, larger trees in denser stands, and defoliators prefer multistory, dense stands (table A.1). Regional and national maps of forest structure are available from the imputation data sets discussed above and from data sets produced for use as inputs to the Forest Service National Insect and Disease Risk Map (Krist et al. 2014). Structural information at finer spatial resolution is available from lidar or structure-from-motion data; such information, however, is not available for large areas.

Coarse-resolution Imagery

Coarse spatial resolution imagery (250–8000 m) has some advantages over finer spatial resolution data but has not been used much in studies of forest disturbances by biotic agents. Examples include the Advanced Very-High Resolution Radiometer (AVHRR) data set, started in 1982, and MODIS, started in 2000. Substantial effort has been applied toward developing temporally consistent products that correct for sensor drift and differences and that provide both surface reflectance and biophysical products (e.g., Los et al. 2000; Vermote et al. 2002), which are advantages for biotic disturbance applications. Furthermore, these products have fine (daily) temporal resolution, allowing for developing cloud-free time series and for use in early warning systems (Hargrove et al. 2009). Several studies of biotic disturbances have been published (e.g., de Beurs and Townsend 2008; Gnilke and Sanders 2022), but only one in the western U.S. (Spruce et al. 2019). The coarse spatial resolution is a significant disadvantage of such imagery relevant to biotic disturbances, but additional studies may be able to assess or exploit the advantages.

Viewing Geometry and Conditions

Leckie et al. 2005 tested the capability of imagery acquired at higher VZA (more oblique) using a forward-looking sensor on an airplane as compared with a similar nadir-pointing sensor. The authors found no increase in differentiation or accuracy of locations of defoliation by jack pine budworm in eastern Canada, but because of some imagery differences and limitations, called for additional testing of this technology.

As crowns thin and the canopy opens following damage and mortality by biotic agents, the understory may become more visible, thereby potentially muting or hiding the overstory tree response. One study found a high correlation between gray-stage trees killed by mountain pine beetle and winter imagery when the ground (and understory) was covered in snow but the overstory trees were snow-free (Baker et al. 2017). Greater sensitivity of reflectances to defoliation under conditions of lower sun elevation angles (as in late summer) occurs because of shading of the understory, which is therefore less able to influence satellite measurements (Ekstrand 1990). The extent to which the effect of understory adversely influences detection accuracy of insect or disease disturbances is unknown.

Sensitivity to Radiometric Normalization

Historically, authors of studies about biotic disturbances applied significant time and effort to radiometric normalization for the multiple images used in change detection and time series analysis (Hall et al. 2016). More recent studies have not tested or modified imagery to address this issue, perhaps because of the ready availability of easily downloaded imagery that has already been preprocessed to top-of-atmosphere reflectance and atmospherically corrected. Detecting the effects of insects and diseases often requires the ability to separate subtle signals of damage that may not differ much from the signals of heathy trees, suggesting that radiometric normalization is an important step. Additional studies to assess this effect are needed.

Attribution

Additional studies are needed to advance understanding and demonstrate capability for attributing forest disturbances to different biotic agents, including separating bark beetle damage from defoliation and attributing disturbance to individual insect species or diseases. Advancement of national-scale attribution studies to separate biotic disturbances from other disturbance types will aid monitoring. The utility of combining remotely sensed imagery with aerial surveys, continuing the work of Meigs et al. (2015), should be explored.

Type of tree response and permanence of damage (tree mortality versus temporary damage followed by recovery) may aid attribution efforts. Including maps of tree species and other characteristics (above) may be helpful, although challenges exist because one insect or disease may attack multiple host tree species (table A.1). Furthermore, multiple agents may attack one tree species. For instance, Douglas-fir beetles (*Dendroctonus pseudotsugae*) often kill Douglas-firs (*Pseudotsuga menziesii*) stressed by western spruce budworm or Douglas-fir tussock moth, (Furniss and Kegley 2014); ponderosa pines are attacked by mountain pine beetle, western pine beetle (*Dendroctonus brevicomis*), and pine engraver (*Ips pini*) (Ciesla et al. 2015); and subalpine fir are host to western balsam bark beetle, fir engraver, western spruce budworm, balsam woolly adelgid, and annosus root disease, among other agents (Uchytil 1991). Analysis of the specific tree responses and permanence over time may assist attribution studies in these cases.

Foliage color change (green to red or yellow) is a significant signature of bark beetle-killed trees, thereby allowing separation of bark beetle outbreaks from some other biotic and abiotic disturbance types. Furthermore, differences in foliage color may assist with attribution within bark beetle species or attacked host tree species. These differences may be greater (as between yellow-green spruce trees and red lodgepole pines) or more subtle (such as the deeper red of killed lodgepole pine versus the more orange of ponderosa pine) (fig. 2, table A.1). Studies using different spectral indices based on visible reflectances, such as the Red-Green Index, can take advantage of these signatures. Some attribution methods that use color may require observations of very narrow spectral regions (as with hyperspectral imagery) to assess differences.

Possibilities also exist for attributing tree damage and/or mortality to defoliators. The transition directly to gray, as can occur in some situations, could be exploited, as could recovery instead of mortality. The reddish hue of crowns of trees attacked by defoliators may provide clues about current year versus previous year defoliation and the defoliator species. The rapid population increase and short outbreak cycles with defoliators such as western hemlock looper might allow differentiation from extended, less severe outbreaks of other defoliator species (e.g., western spruce budworm; Meigs et al. 2011), although more studies are needed to characterize these dynamics for a range of outbreaks. Silken webs produced by some defoliators may allow separation from other biotic agents, although detection might be challenging.

The wide range of host tree species and variety of tree responses make attribution of damage or mortality to diseases difficult. One unique characteristic of root diseases is the expanding centers of mortality that have been documented with remote sensing studies (Oblinger et al. 2022) (fig. 4). Whether this characteristic or other tree responses can be used for attribution remains to be determined.

Direct Sensing of Insects

The vast majority of remote sensing studies of insects and diseases have used tree responses. In a few situations, the direct study of insects has been reported. During epidemics of insects, weather radars have captured dispersal flights of mountain pine beetle (Jackson et al. 2008) and spruce budworm (Boulanger et al. 2017), providing insight about dispersal methods and dynamics. Other situations are very challenging for current remote sensing technologies and methods, but future research may be able to identify useful approaches.

6. Recommendations for Future Studies: Study Design and Reporting

When developing the methods for a study that will detect or attribute tree damage or mortality from insects or diseases, authors should be cognizant of the variability in severity, damage progression, and recovery. Higher accuracy may result if studies separate low- and high-severity disturbances into different classes (even for the same biotic agent), although class accuracy of severity levels may be lower in this situation compared with presence/absence of damage. Authors should describe the damage characteristics of the study (severity, extent, timing) as determined from other sources (i.e., the reference data) so that study methods and findings can be more easily understood and applied to other situations in future studies. For instance, for a defoliation study, it is important to use reference data to describe the extent of defoliation for trees within the study area (and avoid relying on any model product that is the outcome of the study).

Careful selection of reference data (Section 3.3) is critical for model training and evaluation. As noted above, field measurements, finer spatial resolution products, on-screen identification, and aerial surveys have advantages and disadvantages. Furthermore, we recommend that authors provide detailed evaluations of their results. Classifications should report confusion matrices that include overall accuracy as well as omission and commission errors of individual classes. For models of continuous data, studies should report multiple metrics (e.g., RMSE, R^2). The use of test data (independent data not used in model development) in evaluations is ideal; reporting goodness-of-fit of the model to the data used in model development is helpful but not as powerful. Resampling, cross-validation, out-of-bag, or jackknife methods are ways to characterize statistical confidence with withheld observations. Demonstration of accuracy with image zooms of true-color imagery together with classifications or products increases confidence of results.

To increase the utility of their results for subsequent studies, authors might consider an analytical method that identifies the most important variables (bands, spectral indices, etc.) for explaining variability in the damage or mortality response variable as well as the relationships between each explanatory variable and the response variable. Such an analysis is not always necessary if, for instance, the study objective is only to map tree damage within the study area for the study time period. However, reporting this information allows the study findings to be applied to other situations. If such an analysis is performed, the authors need to consider multicollinearity among the explanatory variables, which is known to adversely affect variable importance and relationships (e.g., Graham 2003). Note that using some popular methods, including random forest classification and regression (Cutler et al. 2007) and VSURF for variable selection (Genuer et al. 2015), does not eliminate multicollinearity. Model overfitting needs to be guarded against; jackknifing or cross-validation are robust methods that assist with model evaluation where or when reference data may be lacking.

The inclusion of ancillary variables that represent drivers of damage or mortality by biotic agents (e.g., climate, topography) can increase model accuracy over models that rely on remote sensing observations alone. As with correlated explanatory variables, including these ancillary variables may be warranted if the study objective is to provide the best map possible. However, if identifying important variables is a study objective, including ancillary variables may increase multicollinearity among explanatory variables. Furthermore, combining variables representing observations of damage or mortality with variables representing drivers may alter variable importance and relationships. Subsequent studies seeking to use this remote sensing-based damage product of interest to identify drivers will be hampered because driver variables were used to create the map, causing potential circularity in the driver analysis.

Studies should discuss how their findings about accuracy, variable importance, and relationships with the response variables match ecological theory and understanding. Instances where findings do not match understanding should be called out, perhaps as scientific advances or errors, and authors are encouraged to speculate about their confidence in any new understanding that they report.

To aid the adoption of newly published methodologies, authors could share instructions, descriptive code, and/or test data, and possibly a subset of the data set, in public repositories as part of publication. A review of publicly available code in ecological research found that 73 percent of the literature failed to provide code used in the methodology (Culina et al. 2020). Furthermore, Roche et al. (2015) reported that 56 percent of ecological research literature that provided data were incomplete–where completeness was assessed on the clarity and detail of metadata and reproducibility of methodology with provided data. Such sharing would make methodologies more accessible to new users and facilitate methodologies being applied to novel situations and study areas. The online guide of the LandTrendr implementation in GEE is an excellent example (https://emapr.github.io/LT-GEE/; Kennedy et al. 2018).

7. Synthesis and Conclusions

Relevant to remote sensing, there is a range of tree responses to different insects or diseases, providing a significant challenge for remote sensing studies of detection and attribution. Major bark beetle species cause whole-tree mortality, resulting in foliage color change to red or yellow, needle degradation and fall and reductions in canopy water content. The other groups of biotic disturbance agents (defoliators, sucking insects, and diseases) can cause similar and significant tree responses, for example, following substantial feeding by defoliators or tree mortality following severe and repeated damage. However, these other agents can also generate more subtle tree responses (e.g., defoliation, crown thinning, or deformities), which may be more common. Other responses, including damage progression, severity, spatial extent, and post-disturbance progression of living or killed trees, depend on specific situations, even for the same insect or disease. Substantial variability of tree- and stand-level damage severity occurs within and among agents.

Many remote sensing studies detecting bark beetle outbreaks in western North America have been published, likely due to interest in the large spatial extent and high severity of these disturbances. Fewer detection studies of defoliators, sucking insects, or diseases exist for this region, perhaps related to challenges of detecting the more subtle responses or the smaller outbreak areas. More studies exist for other regions (such as eastern North America), illustrating a knowledge gap. Studies of bark beetle outbreaks can produce higher accuracies or sensitivities than those of defoliators, sucking insects, or diseases. This result likely occurs because of the strong signals from bark beetle outbreaks (whole-tree mortality, foliage color change, high severity, large extent) that are detectable with remote sensing. Many studies, however, did not report the condition of the attacked trees or severity (proportion of damaged trees). For agents other than bark beetles, lower accuracy could have occurred because of more subtle tree responses or fewer damaged trees within pixels. Conversely, higher accuracy could have been reported because of tree mortality (instead of damage that did not cause mortality). One or more studies of each biotic agent type reported high accuracies or sensitivities (R^2), suggesting that mapping disturbances by these agents can be achieved with high confidence, at least for some situations. Far fewer attribution studies have been published, and those have often reported large class errors likely associated with variability in tree, stand, and landscape responses.

In summary, remote sensing is a powerful tool for mapping damage and mortality from forest insects and diseases, both retrospectively and for near-real-time monitoring. Although aerial surveys are a valuable resource, safety concerns about flights and collection gaps increase the value of a remote sensing approach. Our review highlights the underlying responses of trees, stands, and landscapes that provide signals detectable by remote sensing technologies and methods (fig. 1). Recent studies in both technologies and methods have produced exciting advances for detection and attribution, and continued development is likely to produce greater understanding and capability in the near future. Although we developed our framework describing tree responses and remote sensing technologies and methods (fig. 1) from conditions in the western conterminous United States, the framework is general and can be applied to disturbances caused by other forest insects and diseases outside of western North America as well as other disturbance types such as drought.

References

Abdollahnejad, A.; Panagiotidis, D. 2020. Tree species classification and health status assessment for a mixed broadleaf-conifer forest with UAS multispectral imaging. Remote Sensing. 12(22): 3722. https://doi.org/10.3390/rs12223722

Abdullah, H.; Darvishzadeh, R.; Skidmore, A.K.; [et al.]. 2019a. Sensitivity of Landsat-8 OLI and TIRS data to foliar properties of early stage bark beetle (*Ips typographus*, L.) infestation. Remote Sensing. 11(4): 398. https://doi.org/10.3390/rs11040398

Abdullah, H.; Skidmore, A.K.; Darvishzadeh, R.; [et al.]. 2019b. Sentinel-2 accurately maps green-attack stage of European spruce bark beetle (*Ips typographus*, L.) compared with Landsat-8. Remote Sensing in Ecology and Conservation. 5: 87-106. https://doi.org/10.1002/rse2.93

Ahern, F.J. 1988. The effects of bark beetle stress on the foliar spectral reflectance of lodgepole pine. International Journal of Remote Sensing. 9: 1451-1468. https://doi.org/10.1080/01431168808954952

Ahmed, O. S.; Wulder, M.A.; White, J.C.; [et al.]. 2017. Classification of annual non-stand replacing boreal forest change in Canada using Landsat time series: A case study in northern Ontario. Remote Sensing Letters. 8: 29-37. https://doi.org/10.1080/2150704X.2016.1233371

Allen, B.; Dalponte, M.; Hietala, A.M.; [et al.]. 2022a. Detection of root, butt, and stem rot presence in Norway spruce with hyperspectral imagery. Silva Fennica. 56(2): 10606. https://doi.org/10.14214/sf.10606

Allen, B.; Dalponte, M.; Ørka, H.O.; [et al.]. 2022b. UAV-based hyperspectral imagery for detection of root, butt, and stem rot in Norway spruce. Remote Sensing. 14(15): 3830. https://doi.org/10.3390/rs14153830

Allen, T.R.; Kupfer, J.A. 2001. Spectral response and spatial pattern of Fraser fir mortality and regeneration, Great Smoky Mountains, USA. Plant Ecology. 156: 59-74. https://doi.org/10.1023/A:1011948906647

Amani, M.; Ghorbanian, A.; Ahmadi, S.A.; [et al.]. 2020. Google Earth Engine cloud computing platform for remote sensing big data applications: A comprehensive review. IEEE Journal of Selected Topics in Applied Earth Observations and Remote Sensing. 13: 5326-5350. https://doi.org/10.1109/JSTARS.2020.3021052

Atkins, J. W.; Bond-Lamberty, B.; Fahey, R.T.; [et al.]. 2020. Application of multidimensional structural characterization to detect and describe moderate forest disturbance. Ecosphere. 11(6): e03156. https://doi.org/10.1002/ecs2.3156

Atkinson, R.; Burrell, M.; Rose, K.; [et al.]. The dynamics of recovery and growth: How defoliation affects stored resources. Proceedings of the Royal Society B: Biological Sciences. 281: 20133355. https://doi.org/10.1098/rspb.2013.3355

Audley, J.P.; Fettig, C.J.; Munson, A.S.; [et al]. 2021. Dynamics of beetle-killed snags following mountain pine beetle outbreaks in lodgepole pine forests. Forest Ecology and Management. 482: 118870. https://doi.org/10.1016/j.foreco.2020.118870

Bae, S.; Müller, J.; Förster, B.; [et al.]. 2022. Tracking the temporal dynamics of insect defoliation by high-resolution radar satellite data. Methods in Ecology and Evolution. 13: 121-132. https://doi.org/10.1111/2041-210X.13726

Baena, S., Boyd, D.S.; Moat, J. 2018. UAVs in pursuit of plant conservation - Real world experiences. Ecological Informatics. 47: 2-9. https://doi.org/10.1016/j.ecoinf.2017.11.001

Baeza, A.; Martin, R.E.; Stephenson, N.L.; [et al.]. 2021. Mapping the vulnerability of giant sequoias after extreme drought in California using remote sensing. Ecological Applications. 31: e02395. https://doi.org/10.1002/eap.2395

Baker, E.H.; Painter, T.H.; Schneider, D. [et al.]. 2017. Quantifying insect-related forest mortality with the remote sensing of snow. Remote Sensing of Environment. 188: 26-36. https://doi.org/10.1016/j.rse.2016.11.001

Bárta, V.; Lukeš, P.; Lukeš, L. 2021. Early detection of bark beetle infestation in Norway spruce forests of Central Europe using Sentinel-2. International Journal of Applied Earth Observation and Geoinformation. 100: 102335. https://doi.org/10.1016/j.jag.2021.102335

Bentz, B.J.; Régnière, J.; Fettig, C.J. [et al.]. 2010. Climate change and bark beetles of the western United States and Canada: Direct and indirect effects. BioScience. 60(8): 602-613. https://doi.org/10.1525/bio.2010.60.8.6

Berryman, A.A.; Wright, L.C. 1978. Defoliation, tree condition, and bark beetles. In: Brookes, M.H.; Stark, R.W.; Campbell, R.W., eds. The Douglas-fir tussock moth: A synthesis. Tech. Bull. 1585. Washington, D.C.: U.S. Department of Agriculture, Forest Service. pp. 81-88.

Betlejewski, F.; Goheen, D.J.; Angwin, P.A.; [et al.]. 2011. Port-Orford-Cedar root disease. Forest Insect & Disease Leaflet 131. Washington, D.C.: U.S. Department of Agriculture, Forest Service. 12 p. Online: https://www.fs.usda.gov/Internet/FSE_DOCUMENTS/stelprdb5345454.pdf [Accessed 10 September 2024]

Bhattarai, R.; Rahimzadeh-Bajgiran, P.; Weiskittel, A.; [et al.]. 2022. Estimating species-specific leaf area index and basal area using optical and SAR remote sensing data in Acadian mixed spruce-fir forests, USA. International Journal of Applied Earth Observation and Geoinformation. 108: 102727. https://doi.org/10.1016/j.jag.2022.102727

Bhattarai, R.; Rahimzadeh-Bajgiran, P.; A. Weiskittel, A.; [et al.]. 2020. Sentinel-2 based prediction of spruce budworm defoliation using red-edge spectral vegetation indices. Remote Sensing Letters. 11: 777-786. https://doi.org/10.1080/2150704X.2020.1767824

Bhattarai, R.; Rahimzadeh-Bajgiran, P.; Weiskittel, A.; [et al.]. 2021. Spruce budworm tree host species distribution and abundance mapping using multi-temporal Sentinel-1 and Sentinel-2 satellite imagery. ISPRS Journal of Photogrammetry and Remote Sensing. 172: 28-40. https://doi.org/10.1016/j.isprsjprs.2020.11.023

Boucher, P.B.; Hancock, S.; Orwig, D.A. [et al.]. 2020. Detecting change in forest structure with simulated GEDI lidar waveforms: A case study of the hemlock woolly adelgid (HWA; *Adelges tsugae*) infestation. Remote Sensing. 12(8): 1304. https://doi.org/10.3390/rs12081304

Boulanger, Y.; Fabry, F.; Kilambi, A.; [et al.]. 2017. The use of weather surveillance radar and high-resolution three dimensional weather data to monitor a spruce budworm mass exodus flight. Agricultural and Forest Meteorology. 234: 127-135. https://doi.org/10.1016/j.agrformet.2016.12.018

Bright, B.C.; Hicke, J.A.; Meddens, A.J.H. 2013. Effects of bark beetle-caused tree mortality on biogeochemical and biogeophysical MODIS products. Journal of Geophysical Research: Biogeosciences. 118(3): 974-982. https://doi.org/10.1002/jgrg.20078

Bright, B.C.; Hudak, A.T.; Meddens, A.J.; [et al.]. 2020. Mapping multiple insect outbreaks across large regions annually using Landsat time series data. Remote Sensing. 12(10): 1655. https://doi.org/10.3390/rs12101655

Campbell, M.J; Dennison, P.E.; Tune, J.W.; [et al.]. 2020. A multi-sensor, multi-scale approach to mapping tree mortality in woodland ecosystems. Remote Sensing of Environment. 245: 111853. https://doi.org/10.1016/j.rse.2020.111853

Campbell, M.J.; Williams, J.P.; Berryman, E.M. 2023. Using remote sensing and climate data to map the extent and severity of balsam woolly adelgid infestation in northern Utah, USA. Forests. 14(7): 1357. https://doi.org/10.3390/f14071357

Cao, Y.; Ball, J.G.C.; Coomes, D.A.; [et al.]. 2023. Benchmarking airborne laser scanning tree segmentation algorithms in broadleaf forests shows high accuracy only for canopy trees. International Journal of Applied Earth Observation and Geoinformation. 123: 103490. https://doi.org/10.1016/j.jag.2023.103490

Cardil, A.; Vepakomma, U.; Brotons, L. 2017. Assessing pine processionary moth defoliation using unmanned aerial systems. Forests 8(10): 402. https://doi.org/10.3390/f8100402

Cessna, J.; Alonzo, M.G.; Foster, A.C.; [et al.]. 2021. Mapping boreal forest spruce beetle health status at the individual crown scale using fused spectral and structural data. Forests. 12(9): 1145. https://doi.org/10.3390/f12091145

Chen, Y.; Hou, C.; Tang,Y.; [et. al.]. 2019. Citrus tree segmentation from UAV images based on monocular machine vision in a natural orchard environment. Sensors. 19: 5558. https://doi.org/10.3390/s19245558

Ciesla, W.; Stephens, S.; Howell, B.; [et al.]. 2015. Aerial signatures of forest damage in Colorado and adjoining states. Fort Collins, CO: Colorado State University, Colorado State Forest Service. https://www.fs.usda.gov/Internet/FSE_DOCUMENTS/fseprd861963.pdf [Accessed 10 September 2024]

Ciesla, W.M. 2000. Remote sensing in forest health protection. FHTET Rep. No. 00-03. Salt Lake City, UT: U.S. Department of Agriculture, Forest Service, Remote Sensing Applications Center. 266 p.

Ciesla, W.M. 2006. Aerial signatures of forest insect and disease damage in the western United States. FHTET-01-06. Fort Collins, CO: U.S. Department of Agriculture, Forest Service, Forest Health Technology Enterprise Team. 94 pp. https://www.fs.usda.gov/foresthealth/technology/pdfs/AerialSignatures.pdf [Accessed 10 September 2024]

Claverie, M.; Ju, J.; Masek, J.G.; [et al.]. 2018. The Harmonized Landsat and Sentinel-2 surface reflectance data set. Remote Sensing of Environment. 219: 145-161. https://doi.org/10.1016/j.rse.2018.09.002

Clay, G.R.; Marsh, S.E. 1997. Spectral analysis for articulating scenic color changes in a coniferous landscape. Photogrammetric Engineering & Remote Sensing. 63: 1353-1362. Online: https://www.asprs.org/wp-content/uploads/pers/1997journal/dec/1997_dec_1353-1362.pdf [Accessed 10 September 2024]

Clifford, M.J.; Cobb, N.S.; M. Buenemann, M. 2011. Long-term tree cover dynamics in a pinyon-juniper woodland: Climate-change-type drought resets successional clock. Ecosystems. 14: 949-962. https://doi.org/10.1007/s10021-011-9458-2

Clifford, M.J.; Rocca, M.E.; Delph, R. 2008. Drought induced tree mortality and ensuing bark beetle outbreaks in southwestern pinyon-juniper woodlands. In: Gottfried, G.J.; Shaw, J.D.; Ford, P.L., compilers. 2008. Ecology, management, and restoration of pinon-juniper and ponderosa pine ecosystems: Combined proceedings of the 2005 St. George, Utah and 2006 Albuquerque, New Mexico workshops. Proceedings RMRS-P-51. Fort Collins, CO: U.S. Department of Agriculture, Forest Service, Rocky Mountain Research Station. pp. 39-51. Online: https://research.fs.usda.gov/treesearch/31240 [Accessed 10 September 2024]

Cohen, W. B.; Yang, Z.; Healey, S.P.; [et al.]. 2018. A LandTrendr multispectral ensemble for forest disturbance detection. Remote Sensing of Environment. 205: 131-140 https://doi.org/10.1016/j.rse.2017.11.015

Cole, W. E.; Amman, G.D. 1980. Mountain pine beetle dynamics in lodgepole pine forests Part I: Course of an infestation. Gen. Tech. Rep. INT-GTR-89. Ogden, UT: U.S. Department of Agriculture, Forest Service, Intermountain Forest and Range Experiment Station. 59 p.

Cook, B.D.; Corp, L.A.; Nelson, R.F.; [et al.]. 2013. NASA Goddard's LiDAR, Hyperspectral and Thermal (G-LiHT) Airborne Imager. Remote Sensing. 5(8): 4045-4066. https://doi.org/10.3390/rs5084045

Cook, S.P.; Humes, K.S.; Hruska, R.; [et al.]. 2010. Identifying subalpine fir (*Abies lasiocarpa*) attacked by the balsam woolly adelgid (*Adelges piceae*) using spectral measurements of the foliage. International Journal of Forestry Research. 2010:498189. https://doi.org/10.1155/2010/498189

Coops, N.C.; Johnson, M.; Wulder, M.A. [et al.]. 2006. Assessment of QuickBird high spatial resolution imagery to detect red attack damage due to mountain pine beetle infestation. Remote Sensing of Environment. 103: 67-80. https://doi.org/10.1016/j.rse.2006.03.012

Coops, N.C.; Shang, C.; Wulder, M.A.; [et al.]. 2020. Change in forest condition: Characterizing non-stand replacing disturbances using time series satellite imagery. Forest Ecology and Management. 474: 118370. https://doi.org/10.1016/j.foreco.2020.118370

Coops, N.C.; Tompalski, P.; Goodbody, T.R.H.; [et al.]. 2023. Framework for near real-time forest inventory using multi source remote sensing data. Forestry. 96: 1-19. https://doi.org/10.1093/forestry/cpac015

Cotrozzi, L. 2022. Spectroscopic detection of forest diseases: A review (1970–2020). Journal of Forestry Research. 33: 21-38. https://doi.org/10.1007/s11676-021-01378-w

Crist, E.P. 1985. A TM Tasseled Cap equivalent transformation for reflectance factor data. Remote Sensing of Environment. 17(3): 301-306. https://doi.org/10.1016/0034-4257(85)90102-6

Crocker, E.; Gurung, K.; Calvert, J.; [et al.].. 2023. Integrating GIS, remote sensing, and citizen science to map oak decline risk across the Daniel Boone National Forest. Remote Sensing. 15(9): 2250. https://doi.org/10.3390/rs15092250

Culina, A.; Van Den Berg, I.; Evans, S.; [et al.]. 2020. Low availability of code in ecology: A call for urgent action. PLOS Biology. 18(7): e3000763. https://doi.org/10.1371/journal.pbio.3000763

Cutler, D.R.; Edwards Jr, T.C.; Beard, K.H.; [et al.]. 2007. Random forests for classification in ecology. Ecology. 88: 2783-2792. https://doi.org/10.1890/07-0539.1

Dalponte, M.; Cetto, R.; Marinelli, D.; [et al.]. 2023. Spectral separability of bark beetle infestation stages: A single-tree time-series analysis using Planet imagery. Ecological Indicators. 153: 110349. https://doi.org/10.1016/j.ecolind.2023.110349

Dalponte, M.; Coomes, D.A. 2016. Tree-centric mapping of forest carbon density from airborne laser scanning and hyperspectral data. Methods in Ecology and Evolution. 7: 1236-1245. https://doi.org/10.1111/2041-210X.12575

Dalponte, M.; Solano-Correa, Y.T.; Ørka, H.O.; [et al.]. 2022. Detection of heartwood rot in Norway spruce trees with lidar and multi-temporal satellite data. International Journal of Applied Earth Observation and Geoinformation. 109: 102790. https://doi.org/10.1016/j.jag.2022.102790

Das, A.J.; Slaton, M.R.; Mallory, J.; [et al.]. 2022. Empirically validated drought vulnerability mapping in the mixed conifer forests of the Sierra Nevada. Ecological Applications. 32: e2514. https://doi.org/10.1002/eap.2514

de Beurs, K.M.; Townsend, P.A. 2008. Estimating the effect of gypsy moth defoliation using MODIS. Remote Sensing of Environment. 112(10):983-3990. https://doi.org/10.1016/j.rse.2008.07.008

Dennison, P.E.; Brunelle,A.R.; Carter, V.A. 2010. Assessing canopy mortality during a mountain pine beetle outbreak using GeoEye-1 high spatial resolution satellite data. Remote Sensing of Environment 114(11): 2431-2435. https://doi.org/10.1016/j.rse.2010.05.018

Dickinson, D.; Kohler, G.R. 2020. Western hemlock looper. Forest Insect & Disease Leaflet 186. Washington, D.C.: U.S. Department of Agriculture, Forest Service. 11 p. https://www.fs.usda.gov/sites/default/files/users/user3914/FHP-files/FIDL-186-WesternHemlockLooper.pdf [Accessed 10 September 2024]

Donovan, S.D.; MacLean, D.A.; Zhang, Y.; [et al.]. 2021. Evaluating annual spruce budworm defoliation using change detection of vegetation indices calculated from satellite hyperspectral imagery. Remote Sensing of Environment. 253: 112204. https://doi.org/10.1016/j.rse.2020.112204

Eidson, E.; Eckberg, T.; Davis, G.; [et al.]. 2021. 2021 Idaho Douglas-fir tussock moth monitoring report. Report. Report No. IDL 21-2. Boise, ID: Idaho Department of Lands. 30 p. https://www.idl.idaho.gov/wp-content/uploads/sites/2/2022/02/2021_Idaho_DFTM_Report_Final.pdf [Accessed 10 September 2024]

Ekstrand, S. 1990. Detection of moderate damage on Norway spruce using Landsat TM and digital stand data. IEEE Transactions on Geoscience and Remote Sensing. 28(4): 685-692. https://doi.org/10.1109/TGRS.1990.572982

Ellenwood, J.R.; Krist, Jr., F.J.; Romero, S.A. 2015. National individual tree species atlas. FHTET-15-01. Fort Collins, CO: U.S. Department of Agriculture, Forest Service, Forest Health Technology Enterprise Team. 320 p. https://www.fs.usda.gov/foresthealth/technology/pdfs/FHTET_15_01_National_Individual_Tree_Species_Atlas.pdf [Accessed 10 September 2024]

Erikson, M. 2004. Species classification of individually segmented tree crowns in high-resolution aerial images using radiometric and morphologic image measures. Remote Sensing of Environment. 91: 469-477. https://doi.org/10.1016/j.rse.2004.04.006

Fellin, D.G.; Dewey, J.E. 1986. Western spruce budworm. Forest Insect & Disease Leaflet 53. Washington, D.C.: U.S. Department of Agriculture, Forest Service. 10 p. https://www.fs.usda.gov/Internet/FSE_DOCUMENTS/fsbdev2_043655.pdf [Accessed 10 September 2024]

Ferrell, G.T. 1986. Fir engraver. Forest Insect & Disease Leaflet 13. Washington, D.C.: U.S. Department of Agriculture, Forest Service. 7 p. https://www.fs.usda.gov/Internet/FSE_DOCUMENTS/fsbdev2_043751.pdf [Accessed 10 September 2024]

Foster, A.C.; Walter, J.A.; Shugart, H.H.; [et al.]. 2017. Spectral evidence of early-stage spruce beetle infestation in Engelmann spruce. Forest Ecology and Management. 384:347-357. https://doi.org/10.1016/j.foreco.2016.11.004

Foster, A.C.; Wang, J.A.; Frost, G.V.; [et al.]. 2022. Disturbances in North American boreal forest and Arctic tundra: Impacts, interactions, and responses. Environmental Research Letters. 17:113001 https://doi.org/10.1088/1748-9326/ac98d7

Franklin, S.; S. Robitaille. 2020. Forest insect defoliation and mortality classification using annual Landsat time series composites: a case study in northwestern Ontario, Canada. Remote Sensing Letters. 11: 1175-1180. https://doi.org/10.1080/2150704X.2020.1828659

Franklin, S.; Wulder, M.; Skakun, R.; [et al.]. 2003. Mountain pine beetle red-attack forest damage classification using stratified Landsat TM data in British Columbia, Canada. Photogrammetric Engineering & Remote Sensing. 69: 283-288. https://doi.org/10.14358/PERS.69.3.283

Franklin, S.E.; Bowers, W.W.; Ghitter, G. 1995. Discrimination of adelgid-damage on single balsam fir trees with aerial remote sensing data. International Journal of Remote Sensing. 16: 2779-2794. https://doi.org/10.1080/01431169508954591

Franklin, S.E.; Fan, H.; Guo, X. 2008. Relationship between Landsat TM and SPOT vegetation indices and cumulative spruce budworm defoliation. International Journal of Remote Sensing. 29: 1215-1220. https://doi.org/10.1080/01431160701730136

Fraser, B.T.; Congalton, R.G. 2019. Evaluating the effectiveness of unmanned aerial systems (UAS) for collecting thematic map accuracy assessment reference data in New England forests. Forests 10: 24. https://doi.org/10.3390/f10010024

Fraser, R.H.; Latifovic, R. 2005. Mapping insect-induced tree defoliation and mortality using coarse spatial resolution satellite imagery. International Journal of Remote Sensing. 26: 193-200. https://doi.org/10.1080/01431160410001716923

Furniss, R.; Carolin,V.M. 1977. Western forest insects. Misc. Pub. No. 1339. Washington, D.C.: U.S. Department of Agriculture, Forest Service. 654 p.

Furniss, M.; Kegley, S. 2014. Douglas-fir beetle. Forest Insect & Disease Leaflet 5. Washington, D.C.: U.S. Department of Agriculture, Forest Service. 12 p. https://www.fs.usda.gov/Internet/FSE_DOCUMENTS/fsbdev2_043201.pdf [Accessed 10 September 2024]

Gamon, J.; Surfus J. 1999. Assessing leaf pigment content and activity with a reflectometer. The New Phytologist. 143: 105-117. https://doi.org/10.1046/j.1469-8137.1999.00424.x

Gao, B.T.; Yu, L.F.; Ren, L.L.; [et al.]. 2023. Early detection of *Dendroctonus valens* infestation with machine learning algorithms based on hyperspectral reflectance. Remote Sensing. 14: 1373. https://doi.org/10.3390/rs14061373

Gao, F.; Hilker, T.; Zhu, X.; [et al.]. 2015. Fusing Landsat and MODIS data for vegetation monitoring. IEEE Geoscience and Remote Sensing Magazine. 3: 47-60. https://doi.org/10.1109/MGRS.2015.2434351

Gärtner, P.; Förster, M.; Kleinschmit, B. 2016. The benefit of synthetically generated RapidEye and Landsat 8 data fusion time series for riparian forest disturbance monitoring. Remote Sensing of Environment. 177:237-247. https://doi.org/10.1016/j.rse.2016.01.028

Genuer, R.; Poggi, J.-M.; Tuleau-Malot, C. 2015. VSURF: An R package for variable selection using random forests. The R Journal. 7: 19-33. https://journal.r-project.org/articles/RJ-2015-018/ [Accessed 24 September 2024]

Gibson, K.; Kegley, S.; Bentz, B. 2009. Mountain pine beetle. Forest Insect and Disease Leaflet 2. Portland, OR: U.S. Department of Agriculture, Forest Service, Pacific Northwest Region. https://www.fs.usda.gov/foresthealth/docs/fidls/FIDL-02-MtnPineBeetle.pdf [Accessed 24 September 2024]

Gnilke, A.; Sanders, T.G.M. 2022. Distinguishing abrupt and gradual forest disturbances with MODIS-based phenological anomaly series. Frontiers in Plant Science. 13: 863116. https://doi.org/10.3389/fpls.2022.863116

Goodbody, T.R.H.; Coops, N.C.; Hermosilla, T.; [et al.]. 2018. Digital aerial photogrammetry for assessing cumulative spruce budworm defoliation and enhancing forest inventories at a landscape-level. ISPRS Journal of Photogrammetry and Remote Sensing. 142: 1-11. https://doi.org/10.1016/j.isprsjprs.2018.05.012

Goodwin, N.R.; Coops,N.C.; Wulder, M.A.; [et al.]. 2008. Estimation of insect infestation dynamics using a temporal sequence of Landsat data. Remote Sensing of Environment. 112: 3680-3689. https://doi.org/10.1016/j.rse.2008.05.005

Gorelick, N.; Hancher, M.; Dixon, M.; [et al.]. 2017. Google Earth Engine: Planetary-scale geospatial analysis for everyone. Remote Sensing of Environment. 202: 18-27. https://doi.org/10.1016/j.rse.2017.06.031

Graham, M.H. 2003. Confronting multicollinearity in ecological multiple regression. Ecology. 84: 2809-2815. https://doi.org/10.1890/02-3114

Guo, Q.; Kelly, M.; Gong, P.; [et al.]. 2007. An object-based classification approach in mapping tree mortality using high spatial resolution imagery. GIScience & Remote Sensing. 44: 24-47. https://doi.org/10.2747/1548-1603.44.1.24

Hagle, S.; Gibson, K.; Tunnock, S. 2003. Field guide to diseases and insect pests of northern and central Rocky Mountain conifers. Forest Health Protection Report. Missoula, MT: U.S. Department of Agriculture, Forest Service, Northern Region, State and Private Forestry. 197 p.

Hagle, S.K.; Filip, G.M. 2010. Schweinitzii root and butt rot of western conifers. Forest Insect and Disease Leaflet 177. Portland, OR: U.S. Department of Agriculture, Forest Service, Pacific Northwest Region. 8 p. https://www.fs.usda.gov/Internet/FSE_DOCUMENTS/fsbdev2_043575.pdf [Accessed 24 September 2024]

Hall, R.; Castilla, G.; White, J.; [et al.]. 2016. Remote sensing of forest pest damage: A review and lessons learned from a Canadian perspective. The Canadian Entomologist. 148: S296-S356. https://doi.org/10.4039/tce.2016.11

Hanavan, R.P.; Kamoske, A.G.; Schaaf, A.N. [et al.]. 2022. Supplementing the forest health national aerial survey program with remote sensing during the COVID-19 pandemic: Lessons learned from a collaborative approach. Journal of Forestry. 120: 125-132. https://doi.org/10.1093/jofore/fvab056

Hanavan, R.P.; Pontius, J.; Hallett, R. 2015. A 10-year assessment of hemlock decline in the Catskill Mountain Region of New York State using hyperspectral remote sensing techniques. Journal of Economic Entomology. 108: 339-349. https://doi.org/10.1093/jee/tou015

Hargrove, W.W.; Spruce, P.J.; Gasser, G.E.; [et al.]. 2009. Toward a national early warning system for forest disturbances using remotely sensed canopy phenology. Photogrammetric Engineering and Remote Sensing. 75: 1150-1156.

Hart, S.J.; Veblen, T.T. 2015. Detection of spruce beetle-induced tree mortality using high- and medium-resolution remotely sensed imagery. Remote Sensing of Environment. 168: 134-145. https://doi.org/10.1016/j.rse.2015.06.015

Hatala, J.A.; Crabtree, R.L.; Halligan, K.Q.; [et al.]. 2010. Landscape-scale patterns of forest pest and pathogen damage in the Greater Yellowstone Ecosystem. Remote Sensing of Environment. 114: 375-384. https://doi.org/10.1016/j.rse.2009.09.008

Havašová, M.; Ferenčík, J.; Jakuš, R. 2017. Interactions between windthrow, bark beetles and forest management in the Tatra national parks. Forest Ecology and Management. 391: 349-361. https://doi.org/10.1016/j.foreco.2017.01.009

He, Y.A.; Chen, G.; Potter, C.; [et al.]. 2019. Integrating multi-sensor remote sensing and species distribution modeling to map the spread of emerging forest disease and tree mortality. Remote Sensing of Environment. 231: 111238. https://doi.org/10.1016/j.rse.2019.111238

Healey, S.P.; Cohen, W.B.; Yang, Z.; [et. al.]. 2018. Mapping forest change using stacked generalization: An ensemble approach. Remote Sensing of Environment. 204: 717-728. https://doi.org/10.1016/j.rse.2017.09.029

Healey, S.P.; Raymond, C.L.; Lockman, I.B. [et al.]. 2016. Root disease can rival fire and harvest in reducing forest carbon storage. Ecosphere. 7: e01569. https://doi.org/10.1002/ecs2.1569

Heller, R.C. 1968. Previsual detection of ponderosa pine trees dying from bark beetle attack. Proceeds of the Fifth Symposium on Remote Sensing of Environment; University of Michigan; Ann Arbor, MI. pp. 387-434.

Heller, R.C.; V. Bega, R.V. 1973. Detection of forest diseases by remote sensing. Journal of Forestry. 71: 18-21. https://doi.org/10.1093/jof/71.1.18

Hermosilla, T.; Wulder, M.A.; White, J.C.; [et al.]. 2015. Regional detection, characterization, and attribution of annual forest change from 1984 to 2012 using Landsat-derived time-series metrics. Remote Sensing of Environment. 170: 121-132. https://doi.org/10.1016/j.rse.2015.09.004

Hermosilla, T.; Wulder, M.A.; White, J.C.; [et al.]. 2016. Mass data processing of time series Landsat imagery: Pixels to data products for forest monitoring. International Journal of Digital Earth. 9: 1035-1054. https://doi.org/10.1080/17538947.2016.1187673

Hessburg, P.F.; Goheen, D.J.; Bega; R.V. 1995. Black stain root disease of conifers. Forest Insect and Disease Leaflet 145. Portland, OR: U.S. Department of Agriculture, Forest Service, Pacific Northwest Region. https://www.fs.usda.gov/foresthealth/docs/fidls/FIDL-145-BlackStainRootDisease.pdf [Accessed 24 September 2024]

Hicke, J.A.; Allen, C.D.; Desai, A.R.; [et al.]. 2012. Effects of biotic disturbances on forest carbon cycling in the United States and Canada. Global Change Biology. 18: 7-34. https://doi.org/10.1111/j.1365-2486.2011.02543.x

Hicke, J.A.; Logan, J. 2009. Mapping whitebark pine mortality caused by a mountain pine beetle outbreak with high spatial resolution satellite imagery. International Journal of Remote Sensing. 30: 4427-4441. https://doi.org/10.1080/01431160802566439

Hicke, J.A.; Meddens, A.J.; Kolden, C.A. 2016. Recent tree mortality in the western United States from bark beetles and forest fires. Forest Science. 62: 141-153. https://doi.org/10.5849/forsci.15-086

Hicke, J.A., Xu, B.; Meddens, A.J.; Egan, J.M. 2020. Characterizing recent bark beetle-caused tree mortality in the western United States from aerial surveys. Forest Ecology and Management. 475: 118402 https://doi.org/10.1016/j.foreco.2020.118402

Hollaus, M.; Vreugdenhil, M. 2019. Radar satellite imagery for detecting bark beetle outbreaks in forests. Current Forestry Reports. 5: 240-250. https://doi.org/10.1007/s40725-019-00098-z

Holsten, E.H.; Thier, R.W.; Munson, A.S.; [et al.]. 1999. The spruce beetle. Forest Insect and Disease Leaflet 127. Washington, D.C.: U.S. Department of Agriculture, Forest Service. https://www.fs.usda.gov/foresthealth/docs/fidls/FIDL-127-SpruceBeetle.pdf [Accessed 24 September 2024]

Homicz, C.S.; Fettig, C.J.; Munson, A.S.; [et al.]. 2022. Western pine beetle. Forest Insect and Disease Leaflet 1. Washington, D.C.: U.S. Department of Agriculture, Forest Service. https://www.fs.usda.gov/foresthealth/docs/fidls/FIDL-01-WesternPineBeetle.pdf [Accessed 24 September 2024]

Huang, C.; S. N. Goward, S.N.; Masek, J.G.; [et al.]. 2010. An automated approach for reconstructing recent forest disturbance history using dense Landsat time series stacks. Remote Sensing of Environment. 114: 183-198. https://doi.org/10.1016/j.rse.2009.08.017

Huang, C.Y.; Anderegg, W.R.L.; Asner, G.P. 2019. Remote sensing of forest die-off in the Anthropocene: From plant ecophysiology to canopy structure. Remote Sensing of Environment. 231: 111233. https://doi.org/10.1016/j.rse.2019.111233

Huang, H.; Li, X.; Chen, C. 2018. Individual tree crown detection and delineation from very-high-resolution UAV images based on bias field and marker-controlled watershed segmentation algorithms. IEEE Journal of Selected Topics in Applied Earth Observations and Remote Sensing. 11:2253-2262. https://doi.org/10.1109/JSTARS.2018.2830410

Hubbard, R.M.; Rhoades, C.C.; Elder, K.;[et al.]. 2013. Changes in transpiration and foliage growth in lodgepole pine trees following mountain pine beetle attack and mechanical girdling. Forest Ecology and Management. 289:312-317. https://doi.org/10.1016/j.foreco.2012.09.028

Hunt, E.R.; Daughtry, C.; Eitel, J.U.; [et al.]. 2011. Remote sensing leaf chlorophyll content using a visible band index. Agronomy Journal. 103:1090-1099. https://doi.org/10.2134/agronj2010.0395

Huo, L.; Lindberg, E.; Bohlin, J.; [et al.]. 2023. Assessing the detectability of European spruce bark beetle green attack in multispectral drone images with high spatial- and temporal resolutions. Remote Sensing of Environment. 287:113484. https://doi.org/10.1016/j.rse.2023.113484

Huo, L.; Persson, H.J.; Lindberg, E. 2021. Early detection of forest stress from European spruce bark beetle attack, and a new vegetation index: Normalized distance red & SWIR (NDRS). Remote Sensing of Environment. 255:112240. https://doi.org/10.1016/j.rse.2020.112240

Huo, L.-Z.; Boschetti, L.; Sparks, A.M. 2019. Object-based classification of forest disturbance types in the conterminous United States. Remote Sensing. 11:477. https://doi.org/10.3390/rs11050477

Immitzer, M.; Atzberger, C. 2014. Early detection of bark beetle infestation in Norway spruce (*Picea abies*, L.) using WorldView-2 data. Photogramm. Fernerkund. Geoinf 5:351-367. https://doi.org/10.1127/1432-8364/2014/0229

Jackson, P.L.; Straussfogel, D.; Lindgren, B.S.; [et al.]. 2008. Radar observation and aerial capture of mountain pine beetle, *Dendroctonus ponderosae* Hopk. (Coleoptera: Scolytidae) in flight above the forest canopy. Canadian Journal of Forest Research. 38:2313-2327. https://doi.org/10.1139/X08-06

Jakubowski, M.K.; Li, W.; Guo, Q.; [et al.]. 2013. Delineating individual trees from LiDAR data: A comparison of vector-and raster-based segmentation approaches. Remote Sensing. 5:4163-4186. https://doi.org/10.3390/rs5094163

Jones, C.; Song, C.H.; Moody, A. 2015. Where's woolly? An integrative use of remote sensing to improve predictions of the spatial distribution of an invasive forest pest the hemlock woolly adelgid. Forest Ecology and Management. 358: 222-229. https://doi.org/10.1016/j.foreco.2015.09.013

Kälin, U.; Lang, N.; Hug, C. [et al.]. 2019. Defoliation estimation of forest trees from ground-level images. Remote Sensing of Environment. 223: 143-153. https://doi.org/10.1016/j.rse.2018.12.021

Kamińska, A.; Lisiewicz, M.; Stereńczak, K.; [et al.]. 2018. Species-related single dead tree detection using multi-temporal ALS data and CIR imagery. Remote Sensing of Environment. 219: 31-43. https://doi.org/10.1016/j.rse.2018.10.005

Kantola, T.; Lyytikainen-Saarenmaa, P.; Coulson, R.N.; [et al.]. 2016. Development of monitoring methods for hemlock woolly adelgid induced tree mortality within a Southern Appalachian landscape with inhibited access. Iforest-Biogeosciences and Forestry. 9: 178-186. https://doi.org/10.3832/ifor1712-008

Kautz, M.; Meddens, A.J.H.; Hall,R.J.; [et al.]. 2017. Biotic disturbances in Northern Hemisphere forests—A synthesis of recent data, uncertainties and implications for forest monitoring and modelling. Global Ecology and Biogeography. 26: 533-552. https://doi.org/10.1111/geb.12558

Kearns, H.; Jacobi, W.; Johnson, D. 2005. Persistence of pinyon pine snags and logs in southwestern Colorado. Western Journal of Applied Forestry. 20: 247-252. https://doi.org/10.1093/wjaf/20.4.247

Kennedy, R.E.; Yang, Z.; Braaten, J.; [et al.]. 2015. Attribution of disturbance change agent from Landsat time-series in support of habitat monitoring in the Puget Sound region, USA. Remote Sensing of Environment. 166: 271-285. https://doi.org/10.1016/j.rse.2015.05.005

Kennedy, R.E.; Yang, Z.; Cohen, W.B. 2010. Detecting trends in forest disturbance and recovery using yearly Landsat time series: 1. LandTrendr—Temporal segmentation algorithms. Remote Sensing of Environment. 114: 2897-2910. https://doi.org/10.1016/j.rse.2010.07.008

Kennedy, R.E.; Yang, Z.; Gorelick, N.; [et al.]. 2018. Implementation of the LandTrendr Algorithm on Google Earth Engine. Remote Sensing. 10: 691. https://doi.org/10.3390/rs10050691

Key, C.H.; Benson, N.C. 2006. Landscape Assessment (LA). In: Lutes, D.C.; Keane, R.E.; Caratti, J.F.; [et al.]. 2006. FIREMON: Fire effects monitoring and inventory system. Gen. Tech. Rep. RMRS-GTR-164-CD. Fort Collins, CO: U.S. Department of Agriculture, Forest Service, Rocky Mountain Research Station. p. LA-1-55. https://research.fs.usda.gov/treesearch/24066 [Accessed 24 September 2024]

Koltunov, A.; Ramirez, C.M.; Ustin, S.L.; [et al.]. eDaRT: The Ecosystem Disturbance and Recovery Tracker system for monitoring landscape disturbances and their cumulative effects. Remote Sensing of Environment. 238: 111482. https://doi.org/10.1016/j.rse.2019.111482

König, S.; Thonfeld, F.; Förster, M.; [et al.]. 2023. Assessing combinations of Landsat, Sentinel-2 and Sentinel-1 time series for detecting bark beetle infestations. GIScience & Remote Sensing. 60(1): 2226515. https://doi.org/10.1080/15481603.2023.2226515

Korpela, I.; Ørka, H.O.; Hyyppä, J.; [et al.]. 2010. Range and AGC normalization in airborne discrete-return LiDAR intensity data for forest canopies. ISPRS Journal of Photogrammetry and Remote Sensing. 65: 369-379. https://doi.org/10.1016/j.isprsjprs.2010.04.003

Krist, F.J.; Ellenwood, J.R.; Woods, M.E.; [et al.]. 2015. 2013-2027 National Insect and Disease Forest Risk Assessment: Summary and data access. Chapter 6 in K.M. Potter and B.L. Conkling, eds., Forest Health Monitoring: National status, trends and analysis, 2014. Gen. Tech. Rep. SRS-209. Asheville, NC: U.S. Department of Agriculture, Forest Service, Southern Research Station. pp. 87-92. https://research.fs.usda.gov/treesearch/57824 [Accessed 24 September 2024]

Kuzmin, A.; Korhonen, L.; Manninen, T.; [et al.]. 2016. Automatic segment-level tree species recognition using high resolution aerial winter imagery. European Journal of Remote Sensing. 49: 239-259. https://doi.org/10.5721/EuJRS20164914

Lassalle, G.; Ferreira, M.P.; La Rosa, L.E.C.; [et al.]. 2022. Deep learning-based individual tree crown delineation in mangrove forests using very-high-resolution satellite imagery. ISPRS Journal of Photogrammetry and Remote Sensing. 189: 220-235. https://doi.org/10.1016/j.isprsjprs.2022.05.002

Latif, Q.S.; Dudley, J.G.; Dresser, M.A.; [et al.]. 2023. Snag persistence rates and patterns following mountain pine beetle epidemic in the Elkhorn Mountains, Montana, USA. Forest Ecology and Management. 544: 121230. https://doi.org/10.1016/j.foreco.2023.121230

Lausch, A.; Borg, E.; Bumberger, J.; [et al.]. 2018. Understanding forest health with remote sensing, Part III: Requirements for a scalable multi-source forest health monitoring network based on data science approaches. Remote Sensing. 10: 1120. https://doi.org/10.3390/rs10071120

Lausch, A.; Erasmi, S.; King, D.J.; [et al.]. 2016. Understanding forest health with remote sensing-Part I—A review of spectral traits, processes and remote-sensing characteristics. Remote Sensing. 8: 1029. https://doi.org/10.3390/rs8121029

Lausch, A.; Erasmi, S.; King, D.J.; [et al.]. 2017. Understanding forest health with remote sensing-Part II—A review of approaches and data models. Remote Sensing. 9: 129. https://doi.org/10.3390/rs9020129

Leckie, D.G.; Cloney, E.; Joyce, S.P. 2005. Automated detection and mapping of crown discolouration caused by jack pine budworm with 2.5 m resolution multispectral imagery. International Journal of Applied Earth Observation and Geoinformation. 7: 61-77. https://doi.org/10.1016/j.jag.2004.12.002

Leckie, D.G.; Jay, C.; Gougeon, F.A.; [et al.]. R 2004. Detection and assessment of trees with *Phellinus weirii* (laminated root rot) using high resolution multi-spectral imagery. International Journal of Remote Sensing. 25: 793-818. https://doi.org/10.1080/0143116031000139926

Lee, H.-S.; Lee, K.-S. 2019. Multi-temporal analysis of high-resolution satellite images for detecting and monitoring canopy decline by pine pitch canker. Korean Journal of Remote Sensing. 35: 545-560. https://doi.org/10.7780/kjrs.2019.35.4.5

Li, W.; Guo, Q.; Jakubowski, M.K.; Kelly, M. 2012. A new method for segmenting individual trees from the lidar point cloud. Photogrammetric Engineering & Remote Sensing. 78: 75-84. https://doi.org/10.14358/PERS.78.1.75

Lindberg, E., Holmgren, J. 2017. Individual tree crown methods for 3D data from remote sensing. Current Forestry Reports 3: 19-31. https://doi.org/10.1007/s40725-017-0051-6

Little, E.L. 1971. Atlas of United States Trees: Vol. 1.: Conifers and important hardwoods. Miscellaneous Pubication 1146. Washington, D.C.: U.S. Department of Agriculture, Forest Service.

Los, S.O.; Collatz, G. J.; Sellers, P.J.; [et al.]. 2000. A global 9-yr biophysical land surface dataset from NOAA AVHRR data. Journal of Hydrometeorology. 1: 183-199. https://doi.org/10.1175/1525-7541(2000)001<0183:AGYBLS>2.0.CO;2

Luo, X.; Feng, Q.; Jia, Y. [et al.]. 2022. The large-scale investigation and analysis of *Lophodermium piceae* in subalpine areas based on satellite multi-spectral remote sensing. Diversity. 14: 727. https://doi.org/10.3390/d14090727

Majdák, A.; Jakuš, R.; Blaženec, M. 2021. Determination of differences in temperature regimes on healthy and bark-beetle colonised spruce trees using a handheld thermal camera. iForest - Biogeosciences and Forestry. 14: 203. https://doi.org/10.3832/ifor3531-014

Mandl, L.; Lang, S. 2023. Uncovering early traces of bark beetle induced forest stress via semantically enriched Sentinel-2 data and spectral indices. PFG – Journal of Photogrammetry, Remote Sensing and Geoinformation Science. 91: 211-231. https://doi.org/10.1007/s41064-023-00240-4

McMillin, J.; Malesky, D.; Kegley, S. [et al.]. 2017. Western balsam bark beetle. Forest Insect & Disease Leaflet 184. Washington, D.C.: U.S. Department of Agriculture, Forest Service. 12 p. https://www.fs.usda.gov/Internet/FSE_DOCUMENTS/fseprd562421.pdf [Accessed 10 September 2024]

Meddens, A.J.H.; Hicke, J.A. 2014. Spatial and temporal patterns of Landsat-based detection of tree mortality caused by a mountain pine beetle outbreak in Colorado, USA. Forest Ecology and Management. 322: 78-88. https://doi.org/10.1016/j.foreco.2014.02.037

Meddens, A.J.H.; Hicke, J.A.; Ferguson, C.A. 2012. Spatiotemporal patterns of observed bark beetle-caused tree mortality in British Columbia and the western United States. Ecological Applications. 22: 1876-1891. https://doi.org/10.1890/11-1785.1

Meddens, A.J.H.; Hicke, J.A.; Vierling, L.A. 2011. Evaluating the potential of multispectral imagery to map multiple stages of tree mortality. Remote Sensing of Environment. 115: 1632-1642. https://doi.org/10.1016/j.rse.2011.02.018

Meddens, A.J.H.; Hicke, J.A.; Vierling, L.A.; [et al.]. 2013. Evaluating methods to detect bark beetle-caused tree mortality using single-date and multi-date Landsat imagery. Remote Sensing of Environment. 132:49-58. https://doi.org/10.1016/j.rse.2013.01.002

Meigs, G.W.; Kennedy, R.E.; Cohen, W.B. 2011. A Landsat time series approach to characterize bark beetle and defoliator impacts on tree mortality and surface fuels in conifer forests. Remote Sensing of Environment. 115:3707-3718. https://doi.org/10.1016/j.rse.2011.09.009

Meigs, G.W.; Kennedy, R.E.; Gray, A.N.; Gregory, M.J. 2015. Spatiotemporal dynamics of recent mountain pine beetle and western spruce budworm outbreaks across the Pacific Northwest Region, USA. Forest Ecology and Management. 339:71-86. https://doi.org/10.1016/j.foreco.2014.11.030

Meng, R.; Dennison, P.E.; Zhao, F.; [et al.]. 2018. Mapping canopy defoliation by herbivorous insects at the individual tree level using bi-temporal airborne imaging spectroscopy and LiDAR measurements. Remote Sensing of Environment. 215:170-183. https://doi.org/10.1016/j.rse.2018.06.008

Meyer, P.; Itten, K.I.; Kellenberger, T.; [et al.]. 1993. Radiometric corrections of topographically induced effects on Landsat TM data in an alpine environment. ISPRS Journal of Photogrammetry and Remote Sensing. 48:17-28. https://doi.org/10.1016/0924-2716(93)90028-L

Michałowska, M.; Rapiński, J. 2021. A review of tree species classification based on airborne LiDAR data and applied classifiers. Remote Sensing. 13:353. https://doi.org/10.3390/rs13030353

Miller, D.R.; Kimmey, J.W.; Fowler, M.E. 1959. White pine blister rust. Forest Pest Leaflet 36. Washington, D.C.: U.S. Department of Agriculture, Forest Service.

Minarik, R.; Langhammer, J.; Lendzioch, T. 2020. Automatic tree crown extraction from UAS multispectral imagery for the detection of bark beetle disturbance in mixed forests. Remote Sensing. 12:4081. https://doi.org/10.3390/rs12244081

Moisen, G.G.; Meyer, M.C.; Schroeder, T.A.; [et al.]. 2016. Shape selection in Landsat time series: A tool for monitoring forest dynamics. Global Change Biology. 22:3518-3528. https://doi.org/10.1111/gcb.13358

Monahan, W.B.; Arnspiger, C.E.; Bhatt, P.; [et al.]. 2022. A spectral three-dimensional color space model of tree crown health. PLoS ONE 17:e0272360. https://doi.org/10.1371/journal.pone.0272360

Mulverhill, C.; Coops, N.C.; Achim, A. 2023. Continuous monitoring and sub-annual change detection in high-latitude forests using Harmonized Landsat Sentinel-2 data. ISPRS Journal of Photogrammetry and Remote Sensing. 197:309-319. https://doi.org/10.1016/j.isprsjprs.2023.02.002

Mulvey, R.L.; Shaw, D.C.; Filip,G.M.; [et al.]. 2013. Swiss needle cast of Douglas-fir. Forest Insect and Disease Leaflet 181. Portland, OR: U.S. Department of Agriculture, Forest Service, Pacific Northwest Region. 16 p. https://www.fs.usda.gov/foresthealth/docs/fidls/FIDL-181-SwissNeedleCast.pdf [Accessed 24 September 2024]

Näsi, R.; Honkavaara, E.; Lyytikäinen-Saarenmaa, P.; [et al.]. 2015. Using UAV-Based photogrammetry and hyperspectral imaging for mapping bark beetle damage at tree-level. Remote Sensing. 7: 15467-15493. https://doi.org/10.3390/rs71115467

Navarro-Cerrillo, R.M.; Varo-Martínez, M.Á.C.; Acosta, G. P.; [et al.]. 2019. Integration of WorldView-2 and airborne laser scanning data to classify defoliation levels in *Quercus ilex* L. Dehesas affected by root rot mortality: Management implications. Forest Ecology and Management. 451: 117564. https://doi.org/10.1016/j.foreco.2019.117564

Negrón, J.F.; Wilson, J.L. 2003. Attributes associated with probability of infestation by the piñon ips, *Ips confusus* (Coleoptera: Scolytidae), in piñon pine, *Pinus edulis*. Western North American Naturalist. 63: 440-451. https://www.jstor.org/stable/41717318 [Accessed 24 September 2024]

Neigh, C.S.R.; Bolton, D.K.; Diabate, M.; [et al.]. 2014a. An automated approach to map the history of forest disturbance from insect mortality and harvest with Landsat time-series data. Remote Sensing. 6: 2782-2808. https://doi.org/10.3390/rs6042782

Neigh, C.S.R.; Bolton, D.K.; Williams, J.J.; [et al.]. 2014b. Evaluating an automated approach for monitoring forest disturbances in the Pacific Northwest from logging, fire and insect outbreaks with Landsat time series data. Forests. 5: 3169-3198. https://doi.org/10.3390/f5123169

Neigh, C.S.; Carroll, M.L.; Montesano, P.M.; [et al]. 2019. An API for spaceborne sub-meter resolution products for earth science. IGARSS 2019-2019 IEEE International Geoscience and Remote Sensing Symposium; July 28-August 2; Yokohama, Japan. 2016: 5397-5400. https://doi.org/10.1109/IGARSS.2019.8898358

Nelson, E.E.; Martin, N.E.; Williams, R.E. 1981. Laminated root rot of western conifers. Forest Insect and Disease Leaflet 159. Washington, D.C.: U.S. Department of Agriculture, Forest Service. 6 p. https://www.fs.usda.gov/foresthealth/docs/fidls/FIDL-159-LaminatedRootRot.pdf [Accessed 24 September 2024]

Niemann, K.O.; Quinn, G.; Stephen, R.; [et al.]. 2015. Hyperspectral remote sensing of mountain pine beetle with an emphasis on previsual assessment. Canadian Journal of Remote Sensing. 41: 191-202. https://doi.org/10.1080/07038992.2015.1065707

Oblinger, B.W.; Bright, B.C.; Hanavan, R.P.; [et al.]. 2022. Identifying conifer mortality induced by Armillaria root disease using airborne lidar and orthoimagery in south central Oregon. Forest Ecology and Management. 511: 120126. https://doi.org/10.1016/j.foreco.2022.120126

Oeser, J.; Pflugmacher, D.; Senf, C.; [et al.]. 2017. Using intra-annual Landsat time series for attributing forest disturbance agents in central Europe. Forests. 8: 251. https://doi.org/10.3390/f8070251

Olofsson, P.; Foody, G.M.; Stehman, S.V.; [et al.]. 2013. Making better use of accuracy data in land change studies: Estimating accuracy and area and quantifying uncertainty using stratified estimation. Remote Sensing of Environment. 129: 122-131. https://doi.org/10.1016/j.rse.2012.10.031

Oregon Department of Forestry. 2017. Spruce aphid. Forest Health Fact Sheet. 2 p. https://www.oregon.gov/ODF/Documents/ForestBenefits/Spruce_aphid_2017.pdf [Accessed 24 September 2024]

Ortiz, S.M.; Breidenbach, J.; Kändler, G. 2013. Early detection of bark beetle green attack using TerraSAR-X and RapidEye data. Remote Sensing. 5: 1912-1931. https://doi.org/10.3390/rs5041912

Pederson, L.; Eckberg, T.; Lowrey, L.; [et al.]. 2020. Douglas-fir tussock moth. Forest Insect & Disease Leaflet 86. Washington, D.C.: U.S. Department of Agriculture, Forest Service. 11 p. https://www.fs.usda.gov/Internet/FSE_DOCUMENTS/fsbdev2_043658.pdf [Accessed 10 September 2024]

Perez, D.; Lu, Y.; Kwan, C.; [et al.]. 2018. Combining satellite images with feature indices for improved change detection. In: 2018 9th IEEE Annual Ubiquitous Computing, Electronics & Mobile Communication Conference (UEMCON). IEEE. p. 438-444. https://doi.org/10.1109/UEMCON.2018.8796538

Pérez-Cutillas, P.; Pérez-Navarro, A.; Conesa-García, C.; [et al.]. 2023. What is going on within Google Earth Engine? A systematic review and meta-analysis. Remote Sensing Applications: Society and Environment. 29: 100907. https://doi.org/10.1016/j.rsase.2022.100907

Perroy, R.L.; Hughes, M.; Keith, L.M.; [et al.]. 2020. Examining the utility of visible near-infrared and optical remote sensing for the early detection of Rapid ʻŌhiʻa Death. Remote Sensing. 12: 1846. https://doi.org/10.3390/rs12111846

Pontius, J.; Hallett, R.; Martin, M. 2005. Using AVIRIS to assess hemlock abundance and early decline in the Catskills, New York. Remote Sensing of Environment. 97: 163-173. https://doi.org/10.1016/j.rse.2005.04.011

Pontius, J.; Hanavan, R.P.; Hallett, R.A.; [et al.]. 2017. High spatial resolution spectral unmixing for mapping ash species across a complex urban environment. Remote Sensing of Environment. 199: 360-369. https://doi.org/10.1016/j.rse.2017.07.027

Pouliot, D.; R. Latifovic, R. 2016. Land change attribution based on Landsat time series and integration of ancillary disturbance data in the Athabasca oil sands region of Canada. GIScience & Remote Sensing. 53: 382-401. https://doi.org/10.1080/15481603.2015.1137112

Radeloff, V.C.; Mladenoff, D.J.; Boyce, M.S. 1999. Detecting jack pine budworm defoliation using spectral mixture analysis: Separating effects from determinants. Remote Sensing of Environment. 69: 156-169. https://doi.org/10.1016/S0034-4257(99)00008-5

Raffa, K.F.; Berryman, A.A. 1987. Interacting selective pressures in conifer-bark beetle systems: A basis for reciprocal adaptations? American Naturalist. 129: 234-262. https://doi.org/10.1086/284633

Ragenovich, I.R.; Mitchell, R.G. 2006. Balsam woolly adelgid. Forest Insect & Disease Leaflet 118. Washington, D.C.: U.S. Department of Agriculture, Forest Service. 12 p. https://www.fs.usda.gov/Internet/FSE_DOCUMENTS/fsbdev2_043667.pdf [Accessed 10 September 2024]

Rahimzadeh-Bajgiran, P.; Weiskittel, A.R.; Kneeshaw, D. 2018. Detection of annual spruce budworm defoliation and severity classification using Landsat imagery. Forests. 9: 357. https://doi.org/10.3390/f9060357

Randall, C.B. 2012. Management guide for fir engraver. Washington, D.C.: U.S. Department of Agriculture, Forest Service, Forest Health Projection.

Rehfeldt, G.E.; Crookston, N.L.; Warwell, M.V. 2006. Empirical analyses of plant-climate relationships for the western United States. International Journal of Plant Sciences. 167(6): 1123-1150. https://doi.org/10.1086/507711

Reitberger, J.; Schnörr, C.; Krzystek, P.; [et al.]. 2009. 3D segmentation of single trees exploiting full waveform LIDAR data. ISPRS Journal of Photogrammetry and Remote Sensing. 64: 561-574. https://doi.org/10.1016/j.isprsjprs.2009.04.002

Rencz, A.; Nemeth, J. 1985. Detection of mountain pine beetle infestation using Landsat MSS and simulated thematic mapper data. Canadian Journal of Remote Sensing. 11: 50-58. https://doi.org/10.1080/07038992.1985.10855077

Rhoades, C.C.; Hubbard, R.M.; Hood, P.R.; [et al.]. 2020. Snagfall the first decade after severe bark beetle infestation of high-elevation forests in Colorado, USA. Ecological Applications. 30(3): e02059. https://doi.org/10.1002/eap.2059

Riley, K.L.; Grenfell, I.C.; Finney, M.A.; [et al.]. 2021. TreeMap, a tree-level model of conterminous U.S. forests circa 2014 produced by imputation of FIA plot data. Scientific Data. 8: 11. https://doi.org/10.1038/s41597-020-00782-x

Roche, D.G.; Kruuk, L.E.B.; Lanfear, R. [et al.]. 2015. Public data archiving in ecology and evolution: How well are we doing? PLOS Biology. 13: e1002295. https://doi.org/10.1371/journal.pbio.1002295

Rocky Mountain Region, Forest Health Protection. 2010. Field guide to diseases & insects of the Rocky Mountain Region. Gen. Tech. Rep. RMRS-GTR-241. Fort Collins, CO: U.S. Department of Agriculture, Forest Service, Rocky Mountain Research Station. 336 p. https://research.fs.usda.gov/treesearch/37290 [Accessed 24 September 2024]

Rodman, K.C.; Andrus, R.A.; Veblen, T.T.; [et al]. 2021. Disturbance detection in Landsat time series is influenced by tree mortality agent and severity, not by prior disturbance. Remote Sensing of Environment. 254:112244. https://doi.org/10.1016/j.rse.2020.112244

Rouse, J.W.; Haas, R.H.; Shell, J.A.; [et al.]. 1973. Monitoring vegetation systems in the Great Plains with ERTS-1. In: Third Earth Resources Technology Satellite-1 Symposium, Volume 1: Technical Presentations, Section A. p. 309-317. https://ntrs.nasa.gov/api/citations/19740022614/downloads/19740022614.pdf [Accessed 24 September 2024]

Royle, D.D.; Lathrop, R.G. 1997. Monitoring hemlock forest health in New Jersey using Landsat TM data and change detection techniques. Forest Science. 42(3): 327-335. https://doi.org/10.1093/forestscience/43.3.327

Royle, D.D.; Lathrop, R.G. 2002. Discriminating *Tsuga canadensis* hemlock forest defoliation using remotely sensed change detection. Journal of Nematology. 34: 213-221. https://journals.flvc.org/jon/article/view/69408/67068 [Accessed 24 September 2024]

Rudinsky, J.A. 1962. Ecology of Scolytidae. Annual Review of Entomology. 7: 327-348. https://doi.org/10.1146/annurev.en.07.010162.001551

Ruefenacht, B.; Finco, M.V.; Nelson, M.D.; [et al.]. 2008. Conterminous U.S. and Alaska forest type mapping using Forest Inventory and Analysis data. Photogrammetric Engineering and Remote Sensing. 74: 1379-1389. https://doi.org/10.14358/PERS.74.11.1379

Sapes, G.; Lapadat, C.; Schweiger, A.K. [et al.]. 2022. Canopy spectral reflectance detects oak wilt at the landscape scale using phylogenetic discrimination. Remote Sensing of Environment. 273: 112961. https://doi.org/10.1016/j.rse.2022.112961

Schleeweis, K.G.; Moisen, G.G.; Schroeder, T.A.; [et al.]. 2020. U.S. national maps attributing forest change: 1986–2010. Forests. 11: 653. https://doi.org/10.3390/f11060653

Schmid, J.M.; Mata, S.A.; Schaupp, W.C. 2009. Mountain pine beetle-killed trees as snags in Black Hills ponderosa pine stands. Res. Note. RMRS-RN-40. Fort Collins, CO: U.S. Department of Agriculture, Forest Service, Rocky Mountain Research Station. 6 p. https://research.fs.usda.gov/treesearch/33670 [Accessed 24 September 2024]

Schmitt, C.L.; Parmeter,J.R.; Kliejunas, J.T. 2000. Annosus root disease of western conifers. Forest Insect & Disease Leaflet 172. Washington, D.C.: U.S. Department of Agriculture, Forest Service. 10 p. https://www.fs.usda.gov/Internet/FSE_DOCUMENTS/fsbdev2_043641.pdf [Accessed 10 September 2024]

Schroeder, T A.; Schleeweis, K.G.; Moisen, G.G. [et al.]. 2017. Testing a Landsat-based approach for mapping disturbance causality in U.S. forests. Remote Sensing of Environment. 195: 230-243. https://doi.org/10.1016/j.rse.2017.03.033

Schultz, D.; Bedard, W.D. 1987. California fivespined ips. Forest Insect & Disease Leaflet 102. Washington, D.C.: U.S. Department of Agriculture, Forest Service. 8 p. https://www.fs.usda.gov/Internet/FSE_DOCUMENTS/fsbdev2_043643.pdf [Accessed 10 September 2024]

Schwantes, A.M.; Swenson, J.J.; Jackson, R.B. 2016. Quantifying drought-induced tree mortality in the open canopy woodlands of central Texas. Remote Sensing of Environment. 181: 54-64. https://doi.org/10.1016/j.rse.2016.03.027

Sebald, J.; Senf, C.; Seidl, R. 2021. Human or natural? Landscape context improves the attribution of forest disturbances mapped from Landsat in Central Europe. Remote Sensing of Environment. 262: 112502. https://doi.org/10.1016/j.rse.2021.112502

Senf, C.; Pflugmacher, D.; Wulder, M.A.; [et al.]. 2015. Characterizing spectral–temporal patterns of defoliator and bark beetle disturbances using Landsat time series. Remote Sensing of Environment. 170: 166-177. https://doi.org/10.1016/j.rse.2015.09.019

Senf, C.; Seidl, R. 2021. Storm and fire disturbances in Europe: Distribution and trends. Global Change Biology. 27(15): 3605-3619. https://doi.org/10.1111/gcb.15679

Senf, C.; Seidl, R.; Hostert, P. 2017. Remote sensing of forest insect disturbances: Current state and future directions. International Journal of Applied Earth Observation and Geoinformation. 60: 49-60. https://doi.org/10.1016/j.jag.2017.04.004

Senf, C.; Wulder, M.A.; Campbell, E.M.; [et al.]. 2016. Using Landsat to assess the relationship between spatiotemporal patterns of western spruce budworm outbreaks and regional-scale weather variability. Canadian Journal of Remote Sensing. 42: 706-718. https://doi.org/10.1080/07038992.2016.1220828

Shendryk, I.; Broich, M.; Tulbure, M.G.; [et al.]. 2016. Mapping individual tree health using full-waveform airborne laser scans and imaging spectroscopy: A case study for a floodplain eucalypt forest. Remote Sensing of Environment. 187: 202-217. https://doi.org/10.1016/j.rse.2016.10.014

Shore, T.L.; Safranyik, L. 1992. Susceptibility and risk rating systems for the mountain pine beetle in lodgepole pine stands. Information report BC-X-336. Forestry Canada. https://cfs.nrcan.gc.ca/pubwarehouse/pdfs/3155.pdf [Accessed 10 September 2024]

Shrestha, A.; Hicke, J.A.; Meddens, A.J.H.; [et al.]. 2024. Evaluating a novel approach to detect the vertical structure of insect damage in trees using multispectral and three-dimensional data from drone imagery in the northern Rocky Mountains, USA. Remote Sensing. 16: 1365. https://doi.org/10.3390/rs16081365

Slaton, M.R.; Raymond Hunt Jr., E.; Smith, W.K. 2001. Estimating near-infrared leaf reflectance from leaf structural characteristics. American Journal of Botany. 88: 278-284. https://doi.org/10.2307/2657019

Sparks, A.M.; Corrao, M.V.; Smith, A.M.S. 2022. Cross-comparison of individual tree detection methods using low and high pulse density airborne laser scanning data. Remote Sensing. 14(14): 3480. https://doi.org/10.3390/rs14143480

Spruce, J.P.; Hicke, J.A.; Hargrove, W.W.; [et al]. 2019. Use of MODIS NDVI products to map tree mortality levels in forests affected by mountain pine beetle outbreaks. Forests. 10: 811. https://doi.org/10.3390/f10090811

Stahl, A.T.; R. Andrus, R.; Hicke, J.A.; [et al.]. 2023. Automated attribution of forest disturbance types from remote sensing data: A synthesis. Remote Sensing of Environment. 285: 113416. https://doi.org/10.1016/j.rse.2022.113416

Steel, Z.L.; Jones, G.M.; Collins, B.M.; [et al.]. 2023. Mega-disturbances cause rapid decline of mature conifer forest habitat in California. Ecological Applications. 33: e2763. https://doi.org/10.1002/eap.2763

Strunk, J.L.; Gould, P.J.; Packalen, P.; [et al.]. 2020. Evaluation of pushbroom DAP relative to frame camera DAP and lidar for forest modeling. Remote Sensing of Environment. 237: 111535. https://doi.org/10.1016/j.rse.2019.111535

Sturrock, R.N.; Frankel, A.V.; Brown, P.E.; [et al.]. 2011. Climate change and forest diseases. Plant Pathology. 60: 133-149. https://doi.org/10.1111/j.1365-3059.2010.02406.x

Thapa, B.; Wolter, P.T.; Sturtevant, B.R.; [et al.]. 2022. Linking remote sensing and insect defoliation biology-A cross-system comparison. Remote Sensing of Environment. 281: 113236. https://doi.org/10.1016/j.rse.2022.113236

Torres, P.; Rodes-Blanco, M.; Viana-Soto, A.; [et al.]. 2021. The role of remote sensing for the assessment and monitoring of forest health: A systematic evidence synthesis. Forests. 12: 1134. https://doi.org/10.3390/f12081134

Trubin, A.; Kozhoridze, G.; Zabihi, K.; [et al.]. Detection of susceptible Norway spruce to bark beetle attack using PlanetScope multispectral imagery. Frontiers in Forests and Global Change. 6: 1130721. https://doi.org/10.3389/ffgc.2023.1130721

Tucker, C.J. 1979. Red and photographic infrared linear combinations for monitoring vegetation. Remote Sensing of Environment. 8: 127-150. https://doi.org/10.1016/0034-4257(79)90013-0

Uchytil, R.J. 1991. *Abies lasiocarpa*. Fire Effects Information System. U.S. Department of Agriculture, Forest Service, Rocky Mountain Research Station, Fire Sciences Laboratory. https://www.fs.usda.gov/database/feis/plants/tree/abilas/all.html [Accessed 30 June 2023]

Vermote, E.F.; El Saleous, N.Z.; Justice, C.O. 2002. Atmospheric correction of MODIS data in the visible to middle infrared: first results. Remote Sensing of Environment. 83: 97-111. https://doi.org/10.1016/S0034-4257(02)00089-5

Vogelmann, J.E.; Rock, B.N. 1988. Assessing forest damage in high-elevation coniferous forests in Vermont and New-Hampshire using thematic mapper data. Remote Sensing of Environment. 24: 227-246. https://doi.org/10.1016/0034-4257(88)90027-2

Weed, A.S.; Ayres, M.P.; Bentz, B.J. 2015. Population dynamics of bark beetles [Chapter 4]. In: Vega, F.E.; Hofstetter, R.W., eds. Bark beetles. San Diego, CA: Elsevier: p. 157-176. https://doi.org/10.1016/B978-0-12-417156-5.00004-6

Weed, A.S.; Ayres, M.P.; Hicke, J.A. 2013. Consequences of climate change for biotic disturbances in North American forests. Ecological Monographs. 84: 441-470. https://doi.org/10.1890/13-0160.1

Westoby, M.J.; Brasington, J.; Glasser, N.F.; [et al.]. 2012. 'Structure-from-Motion' photogrammetry: A low-cost, effective tool for geoscience applications. Geomorphology. 179: 300-314. https://doi.org/10.1016/j.geomorph.2012.08.021

White, J.C.; Wulder, M.A.; Brooks, D.; [et al.]. 2004. Mapping mountain pine beetle infestation with high spatial resolution satellite imagery. Forestry Chronicle. 80: 743-745. https://doi.org/10.5558/tfc80743-6

White, J.C.; Wulder, M.A.; Brooks, D.; [et al.]. 2005. Detection of red attack stage mountain pine beetle infestation with high spatial resolution satellite imagery. Remote Sensing of Environment. 96: 340-351. https://doi.org/10.1016/j.rse.2005.03.007

Williams, D.W.; Birdsey, R. 2003. Historical patterns of spruce budworm defoliation and bark beetle outbreaks in North American conifer forests: An atlas and description of digital maps. Gen. Tech. Rep. GTR NE-308. Newtown Square, PA: U.S. Department of Agriculture, Forest Service, Northeastern Research Station. 33 p. https://research.fs.usda.gov/treesearch/5521 [Accessed 24 September 2024]

Williams, J.P.; Hanavan, R.P.; Rock, B.N.; [et al.]. 2016. Influence of hemlock woolly adelgid infestation on the physiological and reflectance characteristics of eastern hemlock. Canadian Journal of Forest Research. 46: 410-426. https://doi.org/10.1139/cjfr-2015-0328

Williams, J.P.; Hanavan, R.P.; Rock, B.N.; [et al.]. 2017. Low-level *Adelges tsugae* infestation detection in New England through partition modeling of Landsat data. Remote Sensing of Environment. 190: 13-25 https://doi.org/10.1016/j.rse.2016.12.005

Williams, R.E.; Shaw, C.G.; Wargo, P.M.; [et al.]. 1986. Armillaria root disease. Forest Insect & Disease Leaflet 78. Washington, D.C.: U.S. Department of Agriculture, Forest Service. 7 p. Online: https://www.fs.usda.gov/Internet/FSE_DOCUMENTS/fsbdev2_043634.pdf [Accessed 4 September 2024]

Wilson, E.H.; Sader, S.A. 2002. Detection of forest harvest type using multiple dates of Landsat TM imagery. Remote Sensing of Environment. 80: 385-396. https://doi.org/10.1016/S0034-4257(01)00318-2

Wing, B.M.; Ritchie, M.W.; Boston, K.; [et al.]. 2015. Individual snag detection using neighborhood attribute filtered airborne lidar data. Remote Sensing of Environment. 163: 165-179. https://doi.org/10.1016/j.rse.2015.03.013

Woebbecke, D.M.; Meyer, G.E.; Von Bargen, K.; [et al.]. 1995. Color indices for weed identification under various soil, residue, and lighting conditions. Transactions of the ASAE. 38: 259-269.

Wulder, M.A.; Roy, D.P.; Radeloff, V.C.; [et al.]. 2022. Fifty years of Landsat science and impacts. Remote Sensing of Environment. 280: 113195. https://doi.org/10.1016/j.rse.2022.113195

Wulder, M.A.; White, J.C.; Carroll, A.L.; [et al.].. 2009. Challenges for the operational detection of mountain pine beetle green attack with remote sensing. The Forestry Chronicle. 85:32-38. https://doi.org/10.5558/tfc85032-1

Yamaoka, Y.; Swanson, R.H.; Hiratsuka, Y. 1990. Inoculation of lodgepole pine with four blue-stain fungi associated with mountain pine beetle, monitored by a heat pulse velocity (HPV) instrument. Canadian Journal of Forest Research. 20: 31-36. https://doi.org/10.1139/x90-005

Ye, S.; Rogan, J.; Zhu, Z.; Hawbaker, T.J.; [et al.]. 2021. Detecting subtle change from dense Landsat time series: Case studies of mountain pine beetle and spruce beetle disturbance. Remote Sensing of Environment. 263: 112560. https://doi.org/10.1016/j.rse.2021.112560

Yu, R.; Luo, Y.; Zhou, Q.; [et al.]. 2021a. A machine learning algorithm to detect pine wilt disease using UAV-based hyperspectral imagery and LiDAR data at the tree level. International Journal of Applied Earth Observation and Geoinformation. 101: 102363. https://doi.org/10.1016/j.jag.2021.102363

Yu, R.; Ren, L.; Luo, Y. 2021b. Early detection of pine wilt disease in *Pinus tabuliformis* in North China using a field portable spectrometer and UAV-based hyperspectral imagery. Forest Ecosystems. 8: 44. https://doi.org/10.1186/s40663-021-00328-6

Zabihi, K.; Surovy, P.; Trubin, A.; [et al.]. 2021. A review of major factors influencing the accuracy of mapping green-attack stage of bark beetle infestations using satellite imagery: Prospects to avoid data redundancy. Remote Sensing Applications: Society and Environment. 24: 100638. https://doi.org/10.1016/j.rsase.2021.100638

Zhang, N.; Zhang, X.; Yang, G.; [et al.]. 2018. Assessment of defoliation during the Dendrolimus tabulaeformis Tsai et Liu disaster outbreak using UAV-based hyperspectral images. Remote Sensing of Environment. 217: 323-339. https://doi.org/10.1016/j.rse.2018.08.024

Zhang, Y.T.; Woodcock, C.E.; Chen, S.J.; [et al.]. 2022. Mapping causal agents of disturbance in boreal and arctic ecosystems of North America using time series of Landsat data. Remote Sensing of Environment. 272: 112935. https://doi.org/10.1016/j.rse.2022.112935

Zhao, F.; Huang, C.; Zhu, Z. 2015. Use of vegetation change tracker and support vector machine to map disturbance types in Greater Yellowstone Ecosystems in a 1984–2010 Landsat Time Series. IEEE Geoscience and Remote Sensing Letters. 12: 1650-1654. https://doi.org/10.1109/LGRS.2015.2418159

Zhu, Z.; Qiu, S.; Ye, S. 2022. Remote sensing of land change: A multifaceted perspective. Remote Sensing of Environment. 282: 113266. https://doi.org/10.1016/j.rse.2022.113266

Zhu, Z.; Woodcock, C.E. 2014. Continuous change detection and classification of land cover using all available Landsat data. Remote Sensing of Environment. 144: 152-171. https://doi.org/10.1016/j.rse.2014.01.011

Appendix

List of acronyms and explanations

Acronym	Explanation
BWA	balsam woolly adelgid
HWA	hemlock woolly adelgid
MODIS	Moderate Resolution Imaging Spectroradiometer
MPB	mountain pine beetle
MSS	Multispectral Scanner
NAIP	National Agriculture Imagery Program
NIR	near-infrared
RGB	red-green-blue
RMSE	root-mean-squared error
SBW	spruce budworm
SMA	Spectral mixture analysis
SPOT	Satellite Pour l'Observation de la Terre
SWIR	shortwave infrared
TM	Thematic Mapper
UAS	unmanned aerial systems
WSB	western spruce budworm

See table 5 for spectral indices.

Table A.1—Characteristics of examples of forest insects and diseases important in the western United States and associated responses of trees, stands, and landscapes.

Type of disturbance agent	Insect or pathogen/disease	Insect or pathogen/disease characteristics	Tree, stand, and landscape responses	Selected references
Bark beetles	Mountain pine beetle (*Dendroctonus ponderosae*)	• Hosts: Most pine species, particularly lodgepole, ponderosa, whitebark, sugar • Attacks host by burrowing through bark; adults and larvae feed on phloem • Under outbreak conditions, successful attacks result in tree mortality • Introduces xylem-penetrating fungus • Attacks occur in late summer • Typically one generation per year, sometimes one per two years in high/cold locations • Aggressive beetle species: can kill healthy trees • Prefers older, large trees, and trees that are stressed (in dense stands or by drought) • Extensive outbreaks occur in stands and landscapes with large amounts of susceptible hosts	• No visual change in needle color for months after attack • Fungus reduces transpiration within weeks of attack, causing needle temperature to increase • In the late spring/early summer following attack, needles change to deep red or orange-red (depending on tree species) • Needle drop occurs 2–5 years following attack; trees then appear gray • Within a stand, trees can be killed for several years to a decade • Tree mortality can be severe in a stand (>60%) and widespread across a landscape	Hall et al. (2016) Gibson et al. (2009) Wulder et al. (2009)
	Spruce beetle (*Dendroctonus rufipennis*)	As with mountain pine beetle, with following exceptions: • Hosts: Engelmann, white, lutz, Sitka spruce • Attacks are typically in early summer, but can occur through fall • 1–3 years to complete life cycle; two years is typical • Windthrown trees are source for outbreaks	As with mountain pine beetle, with following exception: • Needles remain green for 1–2 years following attack, then turn yellow-green or red (in conterminous US) or orange-red (in Alaska) before dropping within weeks to months	Hall et al. (2016) Holsten et al. (1999)
	Western balsam bark beetle (*Dryocoetes confusus*)	As with mountain pine beetle, with following exceptions: • Primary hosts: subalpine and corkbark fir • Life cycle: two years, perhaps one year in favorable conditions • Less aggressive than other bark beetle species; attacks trees weakened by drought, defoliation, or root diseases • Attacks begin in early summer • Three broods per year can be produced	As with mountain pine beetle, with following exceptions: • Often part of a complex of biotic agents attacking subalpine fir that includes root disease, balsam woolly adelgid, western spruce budworm • Needle color changes to yellow in year following attack, then to brick-red for subsequent two years	Ciesla et al. (2015) McMillin et al. (2017)

Table A.1 continued.

Type of disturbance agent	Insect or pathogen/disease	Insect or pathogen/disease characteristics	Tree, stand, and landscape responses	Selected references
Bark beetles	Fir engraver (*Scolytus ventralis*)	As with mountain pine beetle, with following exceptions: • Hosts: most species of true fir • Attacks occur throughout summer • Life cycle: warmer years lead to 1 generation per year or 1 plus a partial generation, otherwise 2 years per generation • Attacks occur in the crown and throughout the bole • Attacks may not kill trees • Healthy trees are rarely killed; mortality occurs with trees stressed by drought or defoliation • Trees of any size are attacked	As with mountain pine beetle, with following exceptions: • Can cause top-kill, flagging, and dead branches in addition to killing trees • In the 3–6 months following attack, foliage turns first yellow, then red-orange in grand fir or orange in white fir	Ciesla et al. (2015) Ferrell (1986) Randall (2012)
	Douglas-fir beetle (*Dendroctonus pseudotsugae*)	As with mountain pine beetle, with following exceptions: • Host: Douglas-fir • Attacks are primarily by overwintering adults and occur in spring; some parent adults re-emergence to attack later in summer; attacks of adults that overwintered as larvae occur later in summer • Outbreaks initiation in trees disturbed or stressed by other agents, including drought, blowdowns, breakage from snow/ice, or other biotic agents	As with mountain pine beetle, with following exceptions: • Trees can fade within several months of attack, or fading occurs after a year • Needles are dropped within two years of attack	Ciesla et al. (2015) Furniss and Kegley (2014)
	Western pine beetle (*Dendroctonus brevicomis*)	As with mountain pine beetle, with following exceptions: • Hosts: ponderosa pine and Coulter pine • 1–4 generations per year (more generations in warmer locations) • Attacks occur in June and August (colder locations) or March-December (warmer locations) • Outbreaks are initiated by drought	As with mountain pine beetle, with following exception: • Foliage fades within weeks to months of attack (faster in warmer, drier conditions)	Homicz et al. (2022)
	Piñon ips beetle (*Ips confusus*)	As with mountain pine beetle, with following exceptions: • Hosts: piñon pines • Attacks during warmer months (March-October) • 2–6 generations per year	As with mountain pine beetle, with following exceptions: • Detection may be challenging because of low tree cover (density) and bright soil • Needles retained 9 months after dying	Ciesla et al. (2015) Clifford et al. (2008) Negrón and Wilson (2003) Rocky Mountain Region (2010)

Table A.1 continued.

Type of disturbance agent	Insect or pathogen/disease	Insect or pathogen/disease characteristics	Tree, stand, and landscape responses	Selected references
Defoliators	Western spruce budworm (*Choristoneura freemani*)	• Host species: Douglas-fir, true firs, spruces, western larch, among others • Feeds on needles, beginning with upper crown • Defoliation leads to reduced growth and, with repeated years, to top-kill, crown deformities, or mortality • One generation per year; larvae emergence in May-June, feed for several weeks; larvae spin webs that also damage needles • Multilayered, dense stands are most susceptible • Stress and damage can lead to attacks by Douglas-fir beetle or fir engraver	• Webbed needles turn reddish-brown in July • Defoliation most evident in late summer • Outbreaks can last for several years to several decades	Ciesla et al. (2015) Fellin and Dewey (1986) Hall et al. (2016) Rocky Mountain Region (2010) Schultz and Bedard (1987)
	Douglas-fir tussock moth (*Orgyia pseudotsugata*)	As with western spruce budworm, with following exceptions: • Primary host species: Douglas-fir; other hosts include true firs, other conifers	As with western spruce budworm, with following exceptions: • Defoliated trees appear reddish-brown or gray • Silken webs appear at treetops • Outbreaks occur every 5–7 years in the Pacific Northwest; other areas have different periodicities • Outbreaks typically last 1–4 years • Hosts can recover from light or moderate defoliation in a year • Extensive and severe defoliation can occur	Ciesla et al. (2015) Eidson et al. (2021) Pederson et al. (2020)
	Western hemlock looper (*Lambdina fiscellaria lugubrosa*)	As with western spruce budworm, with following exceptions: • Primary host species: western hemlock; hosts include other conifers	As with western spruce budworm, with following exceptions: • Insects partially chew needles, which turn red-brown • Severe defoliation during outbreaks • May cause tree mortality in just one year • Outbreaks last 2–3 years • Outbreaks are not cyclic in nature except in interior British Columbia, where they occur at every 9–11 years • High populations can cover trees with silken webs	Ciesla (2006) Dickinson and Kohler (2020) Furniss and Carolin (1977b) Hall et al. (2016) Hagle et al. (2003)

Table A.1 continued.

Type of disturbance agent	Insect or pathogen/disease	Insect or pathogen/disease characteristics	Tree, stand, and landscape responses	Selected references
Sucking insects	Balsam woolly adelgid (*Adelges piceae*)	• Invasive; in western U.S. since at least 1929 • Host species: true firs • Insects insert stylets into branches, stem • Feeding disrupts water conductance to crown • All sizes of trees attacked, but larger trees more susceptible	• Infestation in one tree can last years, or can result in tree death within 2–3 after attack • Attacked tree responses include crown decline, flagging, fiddle-shape crown, top curl, gouting (stunting of terminal growth with swellings around buds and branch nodes) • Foliage turns yellow on dying tree, then red or brown • Outbreak can last decades within a stand	Ciesla (2006) Ragenovich and Mitchell (2006)
Pathogens	Root diseases: *Armillaria* spp. Annosus root rot (*Heterobasidion annosum*) Schweinitzii root and butt rot (*Phaeolus schweinitzii*) Black stain root disease (*Leptographium wageneri*) Laminated root rot (*Phellinus weirii*)	Common characteristics of root diseases • Hosts: many conifer species • All ages, sizes are infected and killed	Common characteristics of root diseases • Infections can result in reduce growth and associated symptoms; repeated years can lead to mortality • Symptoms: shortened terminal growth, thin crown, branch dieback, foliage yellowing • Crown symptoms common among root diseases, making attribution difficult • Slow progression through stand • Expanding centers of mortality, which contain older gray trees (or no trees) in center, newly infected trees at periphery	Betlejewski et al. (2011) Ciesla (2006) Hagle and Filip (2010), Hessburg et al. (1995) Nelson et al. (1981) Oblinger et al. (2022) Schmitt et al. (2000) Williams et al. (1986)
	Swiss needle cast	• Host species: Douglas-fir • Foliage disease caused by native fungus *Phaeocryptopus gaeumannii* • Fungus found on older needles • One-year lifecycle • Inland locations have more defoliation in lower crown (better microclimate for fungus)	• Needles turn yellow to brown; color change occurs before budburst (in spring) • Needles are lost from infection; more defoliation in parts of crown with higher light exposure • Thin crowns • Reduced growth (diameter and height) • Spatially extensive damage	Ciesla (2006) Mulvey et al. (2013)
	White pine blister rust	Caused by invasive pathogen *Cronartium ribicola*, which was introduced prior to 1900 • Host species: white (5-needle) pines: eastern white, western white, sugar, whitebark, limber	• Tree responses include needle spots, yellow-orange bark, flagging, top- and branch-kill • Can cause widespread and severe mortality	Ciesla et al. (2015) Miller et al. (1959) Rocky Mountain Region (2010)

Table A.2—Summaries of studies that used remote sensing to map outbreaks of defoliating insects in coniferous forests of North America. Most studies are in western North America, with selected examples of studies of conifers in eastern North America).

Defoliator species	Study	Relevant study objective(s)	Study location	Imagery or data used	Method used	Description of tree response (gray, red, etc.)	Reference data set(s)	Findings
Western spruce budworm (WSB) (*Choristoneura freemani*)	Meigs et al. (2011)	Characterize time series trajectories of outbreaks of western spruce budworm and mountain pine beetle	Cascade Mountains, OR	Landsat (30 m) annual time series of Normal-ized Burn Ratio	Disturbance metrics generated using LandTrendr; compare with outbreak areas identified with aerial surveys and field plots	Mixture of responses: time series	Aerial surveys and field measurements	WSB outbreaks were long, slow disturbances, possibly followed by recovery; mountain pine beetle outbreaks exhibited both short- and long-term disturbances
	Meigs et al. (2015)	Map outbreaks of WSB and mountain pine beetle by integrating aerial surveys (for mapping), forest inventories (for basal area), and imagery	OR and WA	Landsat (30 m) annual time series of Normal-ized Burn Ratio	Disturbance metrics generated using LandTrendr; metrics then intersected with aerial surveys and inventories	Mixture of responses: time series	Aerial surveys provided comparison of dynamics	Imagery provided disturbance maps at finer spatial resolution than aerial surveys and also provided information about dead basal area
	Senf et al. (2015)	Map and attribute forest insect outbreaks; separate insect outbreaks from other forest disturbances, and separate WSB from mountain pine beetle	British Columbia, Canada	Landsat (30 m) annual time series of Normal-ized Burn Ratio and Tasseled Cap	Disturbance metrics generated using LandTrendr; random forest models were developed	Mixture of responses: time series	Aerial surveys; host species maps from vegetation database (very high-resolution imagery, photointerpretation)	Insect versus other forest disturbances were mapped with 77% overall accuracy; WSB and mountain pine beetle were mapped with 75% accuracy (mixed host tree species stands) and 88% accuracy (pure host species stands); severity of disturbance more important than duration; WSB class errors were 10–11%

Table A.2 continued.

Defoliator species	Study	Relevant study objective(s)	Study location	Imagery or data used	Method used	Description of tree response (gray, red, etc.)	Reference data set(s)	Findings
Spruce budworm (SBW) (*Choristoneura fumiferana*)	Bhattarai et al. (2020)	Investigate capability of spectral indices from Sentinel-2 imagery for mapping spruce budworm	New Brunswick, Canada	Sentinel-2 imagery (20 m), spectral indices	Change detection from healthy to defoliated forest using either prior month or prior year; compared spectral indices as well as classifications from random forest versus support vector machine; evaluated detection (presence/absence), then classification into severity (nil, light, moderate)	Annual (current year) defoliation	Field data (roadside surveys)	Detection: 83% accuracy; classification: 68% accuracy; better for single-year than multiple-year change detection; random forest slightly higher accuracy than support vector machine
	Coops et al. (2023)	Define characteristics of trajectories of non-stand replacing disturbances, then map for Canada; insects were mountain pine beetle and spruce budworm	Canada's forests	Landsat (30 m) time series	Disturbance metrics generated using Composite2-Change (C2C); developed exemplars of different types of non-stand replacing disturbances	Mixture of responses: time series	For insects, aerial surveys	Cluster analysis produced classes of trajectories that were grouped into 7 exemplar trajectories; mountain pine beetle and SBW had some similarities and some differences in proportion of exemplars within outbreak areas
	Donovan et al. (2021)	Classify current-year defoliation with satellite hyperspectral imagery	Quebec, Canada	Vegeta-tion indices from EO-1 Hyperion (30 m) imagery; change detection using imagery before and after annual defolia-tion in one year	Classification from random forest versus support vector machine; three classes of defoliation (light, moderate, severe)	Annual (current year) defoliation	Field measurements	Most importance vegetation indices came from visible, NIR, and SWIR spectral regions; accuracies of the three defoliation classes were 55–85%, 40–76%, and 40–80%; overall accuracy using random forest was slightly higher than using support vector machine (64% versus 59%)

Table A.2 continued.

Defoliator species	Study	Relevant study objective(s)	Study location	Imagery or data used	Method used	Description of tree response (gray, red, etc.)	Reference data set(s)	Findings
Spruce budworm (SBW) (*Choristoneura fumiferana*)	Franklin et al. (2008)	Evaluate correlations between cumulative defoliation and spectral indices from satellite imagery	Saskatchewan, Canada	Landsat (30 m), including one spectral index computed from two dates, and SPOT (20 m)	Correlations calculated between spectral indices and mean stand-level defoliation	Cumulative defoliation	Field measurements in 35 stands	Correlations (r) were >0.8, slightly higher for SPOT imagery
	Goodbody et al. (2018)	Assess structural and spectral metrics derived from aerial imagery for sensitivity to defoliation using field measurements	Ontario, Canada	Digital aerial photogrammetric data, 25 cm; visible (red, green, blue) and NIR multi-spectral bands; metrics aggre-gated to 20 x 20 m (matching area of field plots)	Evaluation of structural, spectral metrics using field measurements of defoliation and partial least squares analysis	Cumulative defoliation; imagery acquired in May before feeding and red stage of current-year defoliation	Field measurements	Spectral metrics most effective at identifying defoliation (R^2 = 0.79); structural metrics less effective (R^2=0.49)
	Rahimzadeh-Bajgiran et al. (2018)	Classify annual defoliation using Landsat imagery	Quebec and Maine	Quebec: Landsat-5 TM (30 m) 2004–2005 (healthy), 2008-2009 (defoliated) Maine: Landsat MSS (60 m), 1972–73 healthy; 1975, 1982 defoliated	Multidate change detection (four levels of defoliation) using vegetation indices and random forest classifier	Annual (current year) defoliation	Aerial sketch maps	Presence/absence had about 90% overall accuracy; for best model of defoliation level, class accuracies were 52–77%
Jack pine budworm (*Choristoneura pinus*)	Leckie et al. (2005)	Evaluation of airborne imagery for detecting defoliation	Ontario, Canada	Airborne multi-spectral imagery (2.5 m) from two sensors	Correlations assessed between discoloration and bands; Jeffries-Matusita class separability values computed; classifications performed	Current year defoliation (reddened canopy)	Aerial observations, photography, field estimates of classes of discoloration	NIR and red bands were highly correlated with discoloration; red and SWIR bands were best for discriminating all classes of defoliation; classification produced defoliation class accuracies of 73–95%

Table A.2 continued.

Defoliator species	Study	Relevant study objective(s)	Study location	Imagery or data used	Method used	Description of tree response (gray, red, etc.)	Reference data set(s)	Findings
Jack pine budworm (*Choristoneura pinus*)	Radeloff et al. (1999)	Classify jack pine budworm defoliation levels during outbreak.	Wisconsin	Landsat (30 m) from two years (pre- and peak-outbreak)	Spectral mixture analysis was performed using multiple end-members.	Cumulative defoliation	Field observations of budworm populations	High negative correlation between budworm population and green vegetation end-member.
Hemlock looper (*Lambdina fiscellaria fiscellaria*)	Fraser and Latifovic (2005)	Assess using coarse resolution satellite imagery to map outbreaks of hemlock looper.	Quebec, Canada	SPOT VGT (1.15 km)	Change detection; logistic regression models of presence/ absence of defoliation using satellite metrics	Defoliated	Aerial surveys	High correlation of regression model (R^2 = 0.96); overall accuracy compared with aerial surveys was 97%, though with 33% omission error and 60% commission error in the defoliation class.
Multiple Agents	Ahmed et al. (2017)	Assess classification accuracies of forest disturbance types, including harvest, roads, insect outbreaks (spruce budworm, forest tent caterpillar), wildfire, flooding.	Ontario, Canada	Landsat (30 m) time series	Disturbance metrics generated using composite2-change (c2c); random forest classifier.	Mixture of responses: time series	Local forest management plans, forest inventories, fire maps, land cover classifications	Overall accuracy for three stand-replacing classes and one non-stand-replacing class (including insect outbreaks) was 90%; overall accuracy when separating non-stand-replacing classes was 75%; spruce budworm class had 29–36% errors.
	Franklin and Robitaille (2020)	Evaluate using time series to map defoliation of spruce budworm, jack pine budworm, and forest tent caterpillar (outbreaks occurred during different years).	Ontario, Canada	Landsat (30 m) time series	Logistic regression with change detection and texture metrics	Crown thinning, yellowing, tree mortality	Aerial surveys	Mean overall accuracy (for the three different insect species) was 80%.

Table A.2 continued.

Defoliator species	Study	Relevant study objective(s)	Study location	Imagery or data used	Method used	Description of tree response (gray, red, etc.)	Reference data set(s)	Findings
Multiple Agents	Thapa et al. (2022)	Evaluation of multi-temporal imagery to estimate defoliation metrics for three different defoliators, jack pine budworm, spruce budworm, and spongy moth, as well as a combined model.	Minnesota, Wisconsin, Maryland	Landsat (30 m)	Considered three metrics of defoliation: shoot-based defoliation, frass biomass, proportion of foliage loss; used change detection of imagery from winter in regression models of these metrics.	Annual defoliation	Field measurements and biosim modeling	R^2 was 0.08-27 for spruce budworm defoliation, 0.27–75 for jack pine budworm; combined budworm model had r^2=0.35.

Table A.3—Summaries of all studies that used remote sensing to map outbreaks of the major sucking insects in the western U.S., balsam woolly adelgid (two studies; additional studies in eastern North America), and all studies of a related species, hemlock woolly adelgid, in eastern North America.

Sucking insect species	Study	Relevant study objective(s)	Study location	Imagery/data used	Method used	Description of tree response (gray, red, etc.)	Reference data set(s)	Findings
Balsam woolly adelgid (BWA) (*Adelges piceae*)	Campbell et al. (2023)	Compared different approaches to mapping BWA-damaged trees that used satellite, climate, and terrain information	Utah, U.S.	Landsat (30 m) time series, multiple bands, indices, slopes	Random forest to model BWA damage severity	Trees damaged by BWA	Field observations; comparison with aerial surveys	Cross-validation evaluation for spectral-only model had R^2=0.54 and RMSE=0.105 compared with independent observations, worse than climate-only and combined models.
	Cook et al. (2010)	Determine if fine spectral resolution can detect damaged branches	Idaho and Washington, U.S.	Handheld spectroradio-meter	Discriminant analysis to classify branched from infested versus uninfested trees	Trees damaged by BWA	Field observations of trees	Classification accuracy was 93–94%
	Allen and Kupfer (2001)	Assess changes in forests from remote sensing caused by BWA; determine spatial patterns and relate to topography	Fraser fir in Appala-chian Moun-tains, eastern U.S.	Landsat TM (30 m); Tasseled Cap indices	Change vector analysis	Trees damaged by BWA	Photo interpretation of aerial imagery	Relationships with topography, latitude, longitude
	Franklin et al. (1995)	Assess ability of aerial multispectral imagery to detect BWA damage on individual trees	Newfoundland, Canada	Airborne multispectral imager (0,5-1 m)	Detection and designation into multiple severity classes; texture variables used to assess variability	Various levels of damage	Field data	Class accuracy was 40% for six classes and 76% for presence/absence
Hemlock woolly adelgid (HWA) (*Adelges tsugae*)	Atkins et al. (2020)	Assess the capability of using structural variables from lidar to detect various types of moderate disturbance, including HWA	Multiple forests in eastern U.S.; HWA site was Harvard Forest	Terrestrial lidar	Structural metrics derived from lidar; HWA: compared sites with low and moderate damage	HWA site: tree decline and mortality	Field measurements	HWA: more damaged areas were more structurally complex (had more canopy layers, more variable heights); out-of-bag error: 21%

Table A.3 continued.

Sucking insect species	Study	Relevant study objective(s)	Study location	Imagery/data used	Method used	Description of tree response (gray, red, etc.)	Reference data set(s)	Findings
Hemlock woolly adelgid (HWA) (*Adelges tsugae*)	Boucher et al. (2020)	Evaluate airborne, space-based lidar for HWA-caused damage	Harvard Forest, MA	Simulated large-footprint, space-based lidar (25 m) from airborne lidar	Change detection (data four years apart)	Tree mortality	Field measurements of mortality	HWA damage present in mid-canopy; correlation with lidar metrics yielded R^2=0.6
	Pontius et al. (2005)	Use airborne remote sensing to map hemlock and early decline caused by HWA	Catskill Mountains, NY	Airborne hyperspectral imagery (18 m)	Linear regression with one reflectance band and one index	Various stages of decline	Field measurements of hemlock decline, grouped into 11 classes	Early decline predicted with accuracy of 88%
	Hanavan et al. (2015)	Use airborne remote sensing to map decline caused by HWA	Catskill Mountains, NY	Airborne hyperspectral imagery (18 m)	Linear regression	Various stages of decline	Field measurements of hemlock decline, grouped into 11 classes	R^2 of 0.88 (2001 imagery) and 0.57 (2012 imagery)
	Jones et al. (2015)	Use remote sensing to map damage caused by HWA	Eastern U.S.	Landsat TM (30 m), spectral indices	Index differences between two years as well as single-date imagery; linear regression and maxent	Various levels of damage	Field measurements of damage	Maxent model including difference was slightly more accurate than single-date (94% and 91%)
	Kantola et al. (2016)	Map damage from HWA	North Carolina, U.S.	Color-infrared aerial imagery (NAIP) (3 m) and lidar	Decision trees and NAIP/lidar for mapping forest and support vector machines and NAIP for mapping three forest classes (dead, conifer, hardwood)	Dead	Interpretation of NAIP plus 15 cm color aerial imagery	Overall accuracy: 98%
	Royle and Lathrop (1997)	Map damage from HWA	New Jersey, U.S.	Landsat (30 m), simple ratio	Change detection	Levels of damage	Field measurements of damage and classes	SR related to field-measured damage (R^2=0.73); overall accuracy of damage classification was 64–92%, depending on number of classes

Table A.3 continued.

Sucking insect species	Study	Relevant study objective(s)	Study location	Imagery/data used	Method used	Description of tree response (gray, red, etc.)	Reference data set(s)	Findings
Hemlock woolly adelgid (HWA) (*Adelges tsugae*)	Royle and Lathrop (2002)	Map damage from HWA	New Jersey, USA	Landsat (30 m), NDVI	Change detection	Levels of damage	Field measurements of damage and four levels of damage	Overall accuracy of damage classification was 82%, depending on number of classes
	Williams et al. (2016)	Evaluate changes in hemlock foliage physiology and reflectance following HWA infestation	Northeastern U.S.	Laboratory measurements	Compared physiological (e.g., chlorophyll and moisture) and spectral (e.g., NDVI) differences in uninfested and infested foliage	Infested foliage	N/A	Physiology and reflectance were changed in infested foliage
	Williams et al. (2017)	Map low-level HWA infestation	Northeastern U.S.	Landsat (30 m)	Seven classes of probability of infestation using a decision tree	Infestation	Field measurements	Accuracies for presence/ absence of HWA infestation at the regional and property scales were 57% and 73%, respectively

Table A.4—Summaries of studies that used remote sensing to map outbreaks of diseases in coniferous forests of North America (all studies for western North America; selected examples of studies of conifers elsewhere).

Forest disease and/or pathogen	Study	Relevant study objective(s)	Study location	Imagery/data used	Method used	Description of tree response (gray, red, etc.)	Reference data set(s)	Findings
Armillaria root disease	Oblinger et al. (2022)	Use remotely sensed data to map individual tree health	Oregon, USA	Airborne lidar, Red-green-blue (RGB) imagery (5 cm)	Lidar data used to delineate trees; lidar and RGB metrics used in random forest classification	Four classes: asymptomatic; live, infected; recently killed (50% red needles remaining); dead (<50% needles remaining)	Field measurements	Overall accuracy of four classes: 83%; accuracy of live versus dead was 95%
White pine blister rust	Hatala et al. (2010)	Map red trees affected by mountain pine beetle and white pine blister rust	Greater Yellowstone Ecosystem, USA	HyMap satellite hyperspectral imagery (2–4 m)	Mixture-tuned matched-filter (MTMF) algorithm for classification; Mountain pine beetle mortality separated from blister rust damage with spatial analysis	Three classes: healthy, stressed, dead (red needles)	Field measurements	Class accuracies of 82–97%
Laminated root rot	Leckie et al. (2004)	Evaluate capability of remote sensing for detecting, assessing damage by laminated root rot	British Columbia, Canada	Airborne multispectral imagery (60 cm)	Change detection; evaluation of spectral signatures of healthy and damaged trees; classification into eight classes	Crown thinning and health class	Field measurements	High correlations between percent needle loss and some bands and band ratios; average class accuracy for relaxed classification was 82%; higher accuracy for more severely damaged and healthy trees and classes; confusion with other damage agents
Root, butt, stem rot	Allen et al. (2022a)	Detect rot in Norway spruce	Norway	Airborne hyperspectral (30–80 cm); airborne lidar collection for tree delineation	Presence or absence of rot; random forest and support vector machines	Not available	Ground-based observations of rot during harvest	Overall accuracy of 64%; class accuracies of 60–70%

Table A.4 continued.

Forest disease and/or pathogen	Study	Relevant study objective(s)	Study location	Imagery/data used	Method used	Description of tree response (gray, red, etc.)	Reference data set(s)	Findings
Root, butt, stem rot	Allen et al. (2022b)	Detect rot in Norway spruce	Norway	UAS hyperspectral (16 cm)	Presence or absence of rot; support vector machines	Not available	Ground-based observations of rot during harvest	Overall accuracy of 76% (with 490-band imagery) and 60% (29-band imagery)
	Dalponte et al. (2022)	Detect rot in Norway spruce	Norway	Multispectral Dove satellite imagery (3 m); airborne lidar collection for tree delineation	Presence or absence of rot; support vector machines	Not available	Ground-based observations of rot during harvest	Overall accuracy of 56%
Pitch pine canker	Lee and Lee (2019)	Detect pitch pine canker using high-resolution satellite imagery	South Korea	KOMPSAT satellite four-band imagery, (3–4 m)	Change detection using two dates using NDVI	Crown thinning, discoloration	Field measurements	Accuracy: 71%
Lophodermium piceae	Luo et al. (2022)	Map subalpine tree species damaged by pathogen with remote sensing	Sichuan Province, China	Landsat 8 (30 m), NDVI, change detection between two years	Linear regression between classes of field-observed damage and NDVI change (between two dates)	Gray (loss of needles)	Ground surveys	R^2 of linear regression: 0.74
Pine wilt disease	Yu et al. (2021a)	Classify infection stage of individual pines with unmanned aerial vehicle (UAS) imagery	Zhejiang Province, China	UAS hyperspectral imagery and lidar data	Individual trees delineated and classified; hyperspectral and lidar metrics used in a random forest classification	Five stages of crown discoloration: green, yellow, orange, red, grey	Field measurements	Overall accuracies of 67% (hyperspectral), 46% (lidar), and 74% (hyperspectral and lidar)

Table A.5—Summaries of all attribution studies of forest disturbances that included insect outbreaks.

Study type	Study	Location	Insect species or guild	Attribution classes and number (n)	Imagery, ancillary data sets	Methods	Insect class error
1: Lumps insects with other disturbance types	Hermosilla et al. (2015)	Saskatchewan, Canada	Not available	Fire, harvest, road, non-stand-replacing (phenology, insects, stress) n=4	Landsat	Trend analysis of time series (composite2change, c2c) used together with random forest to classify disturbance types	Non-stand-replacing class: omission error = 10% commission error = 11%
	Hermosilla et al. (2016)	Canada	Not available	Fire, harvest, road, non-stand-replacing (phenology, insects, stress) n=4	Landsat	Methods from Hermosilla et al. (2015)	Non-stand-replacing class: omission error = 4% commission error = 14%
	Huo et al. (2019)	Continental U.S.	Not available	Stress (insects, disease, drought), fire, stem removal (harvest) n=3	Landsat	Trend analysis of time series used together with random forest to classify disturbance types	Stress class: omission error = 20% commission error = 32%
	Kennedy et al. (2015)	Puget Sound area, U.S. and Canada	Not available	Urbanization, forest management, riparian change, other natural change (fire, insects, landslides, windthrow) n=5	Landsat, topography	LandTrendr time series algorithm used together with random forest to classify disturbance types	Natural change class: omission error = 63% commission error = 22%
	Moisen et al. (2016)	Northern Colorado, USA	Not available	Fire, harvest, stable, stress (insects, disease, drought) n=4	Landsat	Time series algorithm used together with statistical shape fitting to classify disturbance types	Stress class: omission error = 49% commission error = 34%
	Schleeweis et al. (2020)	Continental U.S.	Not available	No event (stable), removal (harvest), fire, stress (insects, drought, diseases), land use conversion, and wind n=5	Landsat, topography, forest and vegetation types	Outputs from two time series change detection algorithms and a burned area database used together with ancillary data were used in random forest classification	Stress class: omission error = 80% commission error = 40%
	Schroeder et al. (2017)	10 Landsat scenes across the contiguous US	Not available	Conversion, fire, harvest, stress (insects, diseases, drought, acid rain), wind, stable n=5	Landsat, topography, forest type maps, burn perimeters	Time series algorithm outputs used together with random forest classification	Stress class: omission errors = 40–90% (depending on Landsat scene) commission errors = 30-70%
	Senf and Seidel (2021)	Europe	Not available	Storm, fire, other (harvest, biotic agents, etc.) n=3	Landsat	LandTrendr time series algorithm used together with random forest to classify disturbance types	Other class: omission error = 4% commission error = 8%

Table A.5 continued.

Study type	Study	Location	Insect species or guild	Attribution classes and number (n)	Imagery, ancillary data sets	Methods	Insect class error
1: Lumps insects with other disturbance types	Zhao et al. (2015)	Greater Yellowstone Ecosystem, MT, ID, WY U.S.	Not available	Fires, harvest, other (insects, diseases, abiotic disturbances) n=3	Landsat	Outputs from time series change detection algorithm (vegetation change tracker) used in support vector machines classification	Other class: omission error = 18% commission error = 27%
2: Attributes one insect guild/ species class	Havašová et al. (2017)	Slovakia/ Poland	European spruce bark beetle (*Ips typographus*)	clearcut, beetle-induced mortality, windthrow, fire n=4	Landsat	Maximum likelihood classification of time series	Beetle class: omission errors = 14-18% (depending on year) commission errors = 12-25%
	Neigh et al. (2014a)	Wisconsin and Minnesota, USA	Multiple insect species	No change, logging, insect (one class that included all insects), salvage logging, unknown n=5	Landsat	Time series outputs used in classification	Insect class: omission error = 68% commission error = 44%
	Neigh et al. (2014b)	Oregon and California, USA	Multiple insect species	No change, logging, insect (one class that included all insects), salvage logging, unknown n=5	Landsat	Time series outputs used in classification	Insect class: omission error = 79% commission error = 62%
	Oeser et al. (2017)	Central Europe	European spruce bark beetle (*Ips typographus*)	Windthrow, cleared windthrow, bark beetles, other harvest n=4	Landsat, topography, storm dates	Time series outputs used in random forest classification	Beetle class: omission errors = 4–20% (depending on site) all-site model = 11% commission errors = 6–23% all-site model = 14%
	Pouliot and Latifovic (2016)	Alberta and Saskatchewan, Canada	Insect damage	Fire, forest harvest, insect damage, flood, surface mining, other disturbance (4), wetland variability, no disturbance n=12	Landsat	Time series outputs used in expert-rule-based classification	Insect class: omission error = 12% commission error = 25%
	Sebald et al. (2021)	Austria	Bark beetles	Wind, bark beetles, harvest n=3	Landsat, topography	Landsat indices, topography used to identify disturbances; these variables plus spatio-temporal information about disturbance patches used in attribution	Beetle class: omission error = 85% commission error = 69%

Table A.5 continued.

Study type	Study	Location	Insect species or guild	Attribution classes and number (n)	Imagery, ancillary data sets	Methods	Insect class error
2: Attributes one insect guild/ species class	Zhang et al. (2022)	Northwestern North American	Insect damage	Fires, logging, insect damage n=3	Landsat	Landsat time series analyzed with Continuous Change Detection and Classification (CCDC) algorithm	Insect class: omission error = 78% commission error = 37%
3: Attributes more than one insect guild/ species class	Ahmed et al. (2017)	Ontario, Canada	Spruce budworm (*Choristoneura griseicoma*), forest tent caterpillar (*Malacosoma disstria*)	Stand-replacing: fire, harvest, roads; non-stand-replacing: spruce budworm, forest tent caterpillar, flooding in wetlands, other n=7	Landsat	Trend analysis of time series (Composite2Change, C2C) used with random forest to classify disturbance types; first, stand-replacing disturbances separated from non-stand-replacing disturbances, then non-stand-replacing disturbances separated	Spruce budworm class: omission error = 29% commission error = 36% Forest tent caterpillar class: omission error = 27% commission error = 26%
	Senf et al. (2015)	British Columbia, Canada	Mountain pine beetle (MPB) (*Dendroctonus ponderosae*), Western spruce budworm (*Choristoneura freemani*)	Step 1: insects, harvest, wildfire, undisturbed Step 2: western spruce budworm, mountain pine beetle n=4	Landsat	LandTrendr time series algorithm used with random forests to separate insects from harvest and wildfire, then separate the two insects	Western spruce budworm class: omission error = 29%, commission error = 8% Mountain pine beetle class: omission error = 15%, commission error = 44% (higher accuracies achieved in pure host stands)